Characterization of a transgenic mouse overexpressing SRP-35 in their skeletal muscle.

Inauguraldissertation

Zur

Erlangung der Würde eines Doktors der Philosophie

Vorgelegt der Philosophisch-Naturwissenschaftlichen Fakultät

Der Universität Basel

Von

Alexis Jesus Ruiz Velez

Aus Catia La mar, Venezuela.

Basel, 2018

Genehmigt von der Philosophisch-Naturwissenschaftlichen

Fakultät auf Antrag von:

Prof. Dr. Susan Treves

Prof. Dr. Ivan Martin

Basel, den 27. März 2018.

Prof. Dr. Martin Spiess.

Dekan

ACKNOWLEDGMENT

I am very happy to thank all the people in the Perioperative Patient Safety Group, which have been in multiples ways a positive impulse in this stage of my life. I would like to thank Prof. Susan Treves and Prof. Francesco Zorzato, for their constant and always appropriate positive contribution to this project. I am always going to be very thankful to them for their encouragement and help over the years. Also, a special thanks to Prof. Albert Urwyler and Prof. Thierry Girard for their kindness and support.

I would also like to thank the old (Ruben, Ori, Maja, Antonio, Asensio, Anne-Sylvie and Martine) and relatively new (Jan, Christoph, Moran and Sven) members of lab 408 for all their support and help in these years of work.

I was also very lucky to find very interesting and nice people outside of the lab that were an important part of this journey and that I would like to thank. Thanks to: Ruben, Ana Catarina, Lina, Antonio, Kay, Elise, Basti, Lea, Carol, Sabine, Sara, Emma, Eliane, Nathalie and Flurina.

I would like to give a special thanks to my family for all the good and important values that they taught me and the support to all my decisions.

Finally, I would like to thank to Prof. Ivan Martin and Prof. Christoph Handschin for accepting to be members of this committee.

TABLE OF CONTENTS

ABSTRACT

Skeletal muscle is the largest body organ comprising approximately 40% of total body weight under normal conditions; it is not only important for movement and posture but also for thermogenesis and metabolism. In fact this organ is also responsible for 70–75% of the insulin stimulated glucose uptake; part of the energy obtained from glucose is used to fuel muscles and the remaining is stored as glycogen. The effect of vitamin A metabolites including all trans retinoic acid (atRA), have been shown to be involved not only in skeletal muscle differentiation, but also in the skeletal muscle metabolism, enhancing glucose uptake, increasing lipid oxidation capacity and activating of PI3K-AKT pathway. However, the specific signaling pathway involved in retinoic acid signaling is still not completely understood.

SRP-35 is a short-chain dehydrogenase/reductase belonging to the DHRS7C dehydrogenase/ reductase family 7, which use retinol as substrate to produce all-trans-retinaldehyde. In my thesis I will show that the over-expression of SRP-35 enzyme in mouse skeletal muscles enhances muscle performance *in vivo*; this effect is not related to alterations in excitation-contraction coupling but rather is linked to enhanced glucose metabolism. Over-expression of this enzyme causes increased phosphorylation of AKT_{S473}, triggering translocation of Glut4 to the sarcolemma and higher glucose uptake into the muscles. I will also demonstrate that pharmacological application of atRA, a downstream product of the enzymatic activity of SRP-35, to intact muscles from WT mice, mimics the stimulation of AKT_{S473} phosphorylation observed in SRP35TG muscles, while inhibitors of the Retinoic Acid Receptor (RAR) α and RARγ nuclear receptors inhibit AKT_{S473} phosphorylation in muscles from WT mice treated with pharmacological concentrations of atRA. These results indicate that SRP-35 signaling involves non-genomic effects of RARα and RARγ. My results also demonstrate that RA

signaling affects the activation of PI3K. Skeletal muscles from SRP35TG mice showed a 14 fold increase of PIP3 content, indicating the evolvement of Phosphoinositide 3-kinase (PI3K) and Mammalian target of rapamycin complex 2 (mTORC2). Additionally, the skeletal muscles obtained from SRP35TG mice kept under Low vitamin A diet (LVAD) for two generations show higher fatigue resistance and larger glycogen stores compared to those of WT littermates fed with the same diet. These results indicate that SRP-35 affects skeletal muscle metabolism and fatigue performance, which may represent an important target for the treatment of metabolic diseases.

LIST OF ABBREVIATIONS.

Ach	Acetylcholine
ADHs	Alcohol dehydrogenases
AKT	Protein kinase B
AMP	Adenosine monophosphate
AMPK	AMP-activated protein kinase
ATP	Adenosine triphosphate
β-CTD	β-subunit C-terminal domain
Ca^{2+}	Cacium ions
CaMKK	Ca^{2+}/calmodulin-dependent protein kinase kinase
CASQ	Calsequestrin
CBS	Cystathionine β-synthase
CNS	Central nervous system
CRBPI	RA-binding protein 1
CICR	Ca^{2+}-induced Ca^{2+} release
Deptor	DEP-domain-containing mTOR-interacting protein
DHPR	Dihydropyridine receptors
ECC	Excitation-contraction
ER	Endoplasmic reticulum
Erk	Signal-regulated kinases
FABP5	Fatty acid-binding protein 5
FKBP	FK506-binding proteins
FKBP12	FK506-binding protein of 12 kDa

Glut	Glucose transporter
HDAC	Histone deacetylase protein,
Hsl	Hormone lipase
IGF-1	Insulin-like growth factor 1
IP3	Inositol 1,4,5-trisphosphate
IR	Insulin receptor
IRS	Insulin receptor substrate
JAK	Janus kinases
JP-45	Junctional SR protein 45
MFS	Major facilitator superfamily
mLST8	Mammalian lethal with Sec13 protein 8
mTOR	Mammalian target of rapamycin
MSK1	Mitogen- and stress-activated kinase 1
MyHC	Myosin heavy chain isoforms
NCX	Na^{+}/Ca^{2+} exchanger
p38MAP	p38 mitogen-activated kinase
PP2A	Protein phosphatase 2A
PPAR	Peroxisome proliferator-activated receptor
PDK1	3-phosphoinositide-dependent kinase 1
PI3K	Phosphatidylinositol 3-kinase
PIP3	Phosphatidylinositol-3,4,5-trisphosphate
PKC	Protein kinase C
PRAS40	Proline-richAKT substrate of 40 kDa
RA	Retinoic acid
RAR	Retinoic Acid Receptors
RALDH	Retinaldehyde dehydrogenases

RBP	Retinol binds to retinol-binding proteins
Rictor	Rapamycin insensitive companion of mTOR
RXR	Retinoid X receptor
RyR	Ryanodine receptors
S6K1	Protein S6 kinase 1
SERCA	SR Ca^{2+} ATPase pump
SGK	Serum glucose kinase
SR	Sarcoplasmic reticulum
SRP-27	Sarcoplasmic reticulum protein 27
SRP-35	Sarcoplasmic reticulum protein 35
STRA6	Stimulated by retinoic acid gene 6 protein
T2DM	Type 2 diabetes mellitus
TBC1D1/AS160	Tre-2/BUB2/cdc 1 domain family 1/ AKT substrate of 160 kDa
TSC	Tuberous sclerosis complex
Ucp1	Uncoupling protein 1
UDP	Uridine 5′-diphosphate

CHAPTER 1- INTRODUCTION

1.1 Skeletal muscle.

1.1.1 Skeletal muscle structure and function.

The skeletal muscle represents the principal organ of the locomotor system. It is able to contract longitudinally producing tension that helps the partial or complete mobility of the organism. The movement of this organ is mostly under voluntary control (but some skeletal muscles are involuntarily controlled, such as the diaphragm and extraocular muscles), while the activation and speed of contraction is highly regulated and is controlled by electrical stimuli originating in the somatic nervous system. Aside muscle fibres, additional components make up the skeletal muscle tissue including blood vessels, nerve fibres and connective tissue that all work together to facilitate coordinated movements that convey locomotion and stability to the whole body. An important function of skeletal muscle is also its contribution to the maintenance of body temperature and metabolic homeostasis, by generating heat and regulating glucose metabolism. The heat generated by active muscle is the result of the breakdown of ATP molecules during physical activity and is essential to maintain a stable body temperature, for example by promoting shivering-dependent thermogenesis. On the other hand about 80% of insulin-stimulated glucose metabolism is under control of skeletal muscles. The glucose that is not readily metabolized is stored as glycogen, principally in skeletal muscles, making this organ the largest glycogen store of mammalian organisms (DeFronzo et al., 1981; Hopkins, 2006; Frontera and Ochala, 2015; Drum et al., 2016).

The skeletal muscle is generally attached to bones by tendons and cartilage or through direct contact and is also defined as striated for its typical striped microscopic appearance. The

striations are a consequence of the ordered and regular arrangement of the sub-cellular contractile elements (Drum et al., 2016).

The skeletal muscle is made up of several specialized layers, structured in fascicles, muscle fibres, myofibrils and sarcomeres, as is shown in the figure 1.1. Specifically, the fascicle is defined as a bundle of muscle fibres bound together and surrounded by a layer of connective tissue (known as perimysium). The muscle fibres on the other hand, are multinucleated cells, able to contract once they receive an electrochemical stimulus in the neuromuscular junction, released by neurons belonging to the central nervous system. The diameter and length of fibres can vary enormously depending on the muscle location and animal species. In mouse, the soleus muscle fibres present a diameter of 47 μm and a length of 8.1 mm, while in humans the sartorius muscle fibres can have a diameter of 100 μm and a length up to 200 mm. The plasma membrane that protects the muscle fibre is calls sarcolemma and a layer of connective tissue composed of collagen and reticular fibres (endomysium) surrounds this membrane. The cytoplasm (sarcoplasm or myoplasm) of muscle fibres contains a specialized endoplasmic reticulum called sarcoplasmic reticulum (SR), which is involved in the storage, release and reuptake of calcium ions (Ca^{2+}) during the excitation-contraction (ECC) coupling process. The myofibrils are the internal muscle fibre structures that make muscle contraction possible. There are hundreds of thousands of myofibrils in a single muscle fibre, and when the myofibrils contract the whole muscle fibre contracts. Myofibrils present an elongated shape that runs the length of the fibre, only connected to the sarcomere at the extremes of the fibre (see figure 1.1). Each myofibril is composed of thousands of sarcomeres, each having a length of 2 μm. These small structures (sarcomeres) have been defined as the basic functional contractile unit, made up by two principal proteins, actin and myosin. The actin proteins are attached to the border of the sarcomere in a structure called Z-discs and due to their elongated shape and thinner diameter (compared to myosin) are call thin filaments. The actin filaments

are located from the Z disc to the center of the sarcomere, where the myosin filaments (thick filaments) are located. These two proteins (actin and myosin) are the principal players involved in muscle contraction, presenting both an elongated shape and longitudinal arrangement that facilitate the sliding past one another that causes the contraction of the sarcomere. Specifically, in resting conditions the tropomyosin I protein blocks the binding of myosin to actin, inhibiting the two filamentous proteins from sliding past one another and therefore impeding sarcomere contraction. When Ca^{2+} is released to the myoplasm during an ECC event, this ion binds the troponin in its Ca^{2+} binding site, inducing its conformational

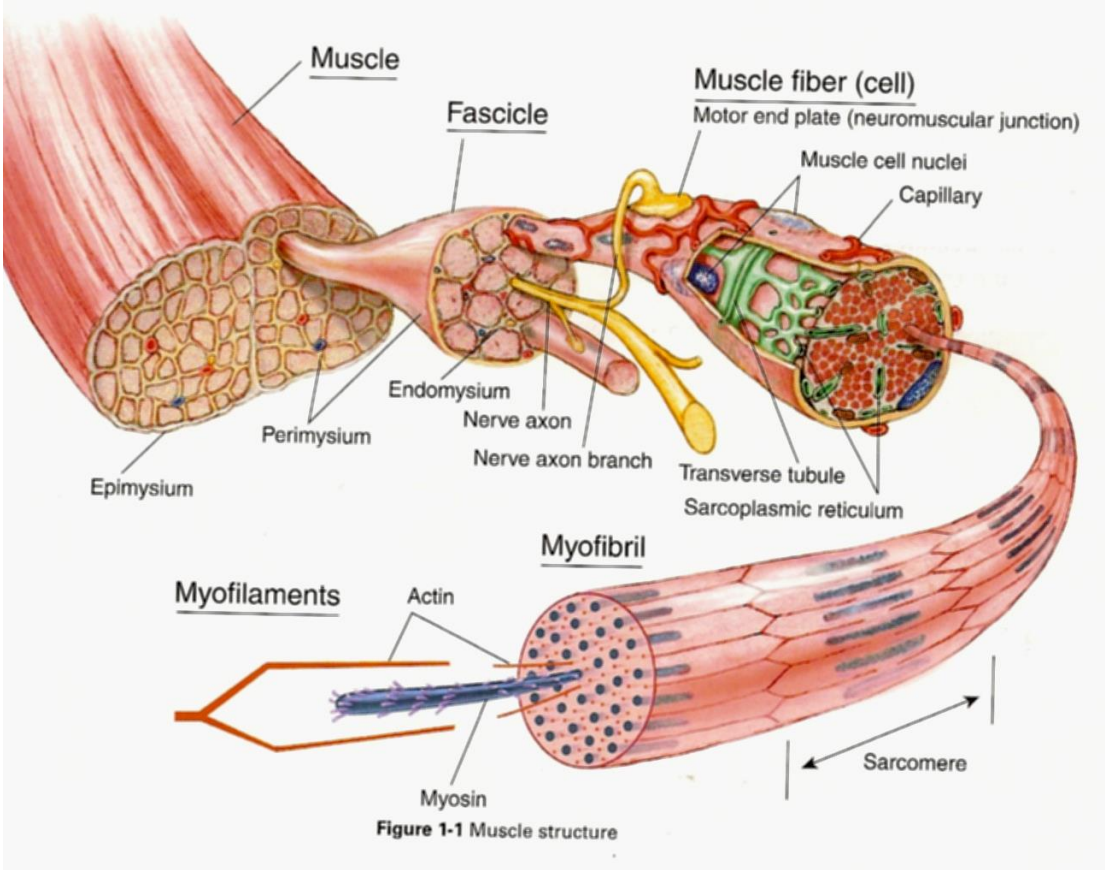

Figure 1.1 Schematic representation of the structure of skeletal muscle showing its internal components. The figure shows internal structures of the skeletal muscles including, fasicles, muscle fibre sarcomeres and myofilaments. (June, 2007, retrieved from https://humananatomy-libs.com/gross-anatomy-of-the-skeletal-muscles2/)

ECC event, this ion binds the troponin in its Ca^{2+} binding site, inducing its conformational change that shifts the position of tropomyosin and moves it away from the myosin-actin binding sites. Once the inhibition of the tropomyosin on the actin-myosin proteins is removed, the actin and the globular heads of myosin come into contact, forming a cross-bridge between the two proteins. Myosin hydrolyze ATP molecules and obtain the energy to move the head groups along the actin filaments and slide the thin and tick filaments past one another, causing the contraction of the sarcomere and of the whole muscle fibre (See figure 1.1 and figure 1.3) (Hegarty and Hooper, 1971; Burkholder et al., 1994; Harris et al., 2005; Treves et al 2009; Marini and Veicsteinas, 2010; Frontera and Ochala, 2015; MacIntosh et al., 2015).

1.1.2 Skeletal muscle and fibre type composition.

The skeletal muscle is a very plastic tissue, responding to the different needs of the organism, for example it allows the body to have explosive fast movements for short periods of time (like in the 100 m sprint race) or slow and long lasting movements (like in a marathon race). One of the principal keys underlying this plasticity is the presence of different types of myosin heavy chain isoforms (MyHC), giving different metabolic characteristics, contractile speed and cellular Ca^{2+} handling characteristics to the muscle fibres (Westerblad et al., 2010). Based on these important characteristics, skeletal muscle fibres are classified according their MyHC isoforms as type I, IIa, IIx and IIb. The principal characteristic of these different fibre types is their speed of contraction, with MyHC type I being the slowest, type IIa of intermediate speed and type IIx and IIb being the most rapid. A secondary but just as important characteristic observed in different fibre types is their expression of proteins related to metabolism and Ca^{2+} homeostasis. In fast type II fibres, where the rate of cross-bridged cycling and ATP consumption is higher, the expression of the SR Ca^{2+} ATPase pump SERCA 1 isoform (a major ATP consuming Ca^{2+} pump) is observed at a high density, on the other

hand in slow type I fibres, the SERCA isoform that is expressed is type 2 and is found at a lower density (Bottinelli and Reggiani, 2000). Furthermore, parvalbumin an important protein involved in Ca^{2+} homeostasis is almost exclusively expressed in fast fibres and almost not at all in slow fibres (Füchtbauer et al., 1991) whereas fast fibres express exclusively the low affinity high capacity calcium binding protein isoform calsequestrin 1, For their part, slow fibres express in addition to calsequestrin 1 also calsequestrin 2, the isoform which is also expressed in cardiac cells (Biral et al., 1992; Mosca et al., 2016). These findings can thus explain why the Ca^{2+} transient kinetics between different fibres types is so different, with the Ca^{2+} kinetics of type I and IIa fibres being slower, with a wider Ca^{2+} transient of smaller amplitude compared to that exhibited by fast type IIx and IIb fibres (Calderon et al., 2009; Calderon et al., 2014).

The different types of fibres also exhibit important metabolic adaptations in response to the energy consumption requirements. Fast type II fibres (with a higher ATP consumption) are endowed with a higher anaerobic metabolism and lower oxidative capacity that allows them to have short explosive movements, but with a low resistance to fatigue. These fibres thus have few mitochondria and are typically more white in appearance. The slow type I fibres present a high content of mitochondria and rely heavily on aerobic metabolism and oxidative phosphorylation, and contain a high density of capillaries increasing their resistance to fatigue (Westerblad et al., 2010; Argilés et al., 2016).

1.2 Excitation contraction coupling and calcium homeostasis in skeletal muscle.

Excitation contraction coupling (ECC) is the underlying mechanism linking plasma membrane depolarization to muscle contraction and represents a fast communication between

electrical events that occur at the plasmalemma and Ca^{2+} release from the sarcoplasmic reticulum, SR. In eukaryotic cells, other mechanisms link membrane receptor activation to Ca^{2+} release from the endoplasmic reticulum (ER) stores to the cytosol, but unlike ECC, the latter events are mediated by the ubiquitous second messenger inositol 1,4,5-trisphosphate (IP3) via activation of the IP3 receptors which are calcium channels located on the ER membrane. This second mechanism that involves Ca^{2+} channels sensitive to IP3 is not involved in the ECC mechanism in skeletal muscle but may be involved in transcriptional activation (Treves et al., 2009; Taylor et al., 2014).

In twitch skeletal muscle fibres the sequence of events known as ECC involves: (**i)** initiation and propagation of an action potential along the sarcolemma, (**ii)** radial distribution of the change in membrane potential along the transverse tubule system (T-tubule system) which invaginates deep into the muscle fibres, (**iii)** sensing of the change in membrane potential by the dihydropyridine receptors (DHPR) which are L-type Ca^{2+} channels, (**iv)** mechanical interaction between the DHPR and the ryanodine receptor 1 (RyR1) Ca^{2+} release channels, which are activated to release Ca^{2+} from the SR into the myoplasm, (**v)** binding of Ca^{2+} to the contractile apparatus leading to fibre contraction, (**vi)** Ca^{2+} clearance: reuptake into the SR mediated by the sarcoplasmatic reticulum Ca^{2+} transport ATPase (SERCA) pumps and, to a lesser extent, removal to the extracellular medium by activation of the Na^{+}/Ca^{2+} exchanger (NCX) and activation of the plasma membrane Ca^{2+} ATPase (Rios and Pizarro, 1991; Baylor and Hollingworth., 2011; Calderon et al., 2014).

1.2.1 Ca^{2+} release mechanism.

Ca^{2+} release from the SR is the result of multiple different processes, the first one being sensing the electric signal coming from the nervous system, which is translated into a chemical signal for the motor neurons in contact with the muscle fibres, releasing

acetylcholine (ACh) into the neuromuscular junction. These small neurotransmitter molecules (ACh) bind to their receptors on the sarcolemma and cause a change in the permeability of the sodium (Na^+) and potassium (K^+) channels leading to a change in the membrane potential from a resting potential of -85 mV up to 100 mV. The depolarization travels along the sarcolemma and enters the transverse tubules (t-tubules), which as mentioned previously are invaginations of the plasma membrane that reach deep into the muscle fibre and constitute the triad. The triad is the intracellular structure containing the ECC machinery; it is composed of the two membrane compartments, T-tubules containing the voltage sensor L-type calcium channel (DHPR) channel and the terminal cisternae on which RyR1 channels are located together with additional ECC-related proteins including JP-45, triadin and junctin (see figure 1.2 and figure 1.3; Horowicz, 1961; Zorzato et al., 2000; Apostol et al., 2009; Treves et al., 2009; Calderón et al. 2014). Once the depolarization of the sarcolemma reaches the DHPRs in the T-tubules, the latter undergo a conformational change that sends a signal to the RyR1, located on the membrane of the SR (Rios and Pizarro, 1991, Mosca et al., 2013). The DHPR is a macromolecular complex made up of 5 subunits including the alfa I (α1) or Cav1.1 which contains the pore forming unit of the complex, α2-δ1, β1a, and γ are auxiliary subunits located on the extracellular, intracellular, and transmembrane space, respectively (Catterall et al. 2011; Treves et al. 2017). More detailed characteristic of these two proteins (DHPR and RyR) are presented later in this chapter in section 1.2.3. In skeletal muscle the Cav1.1/DHPR channels are arranged in groups of four (tetrads) and face the RyR1 channels in a special spatial organization having a checkerboard appearance (Franzini-Armstrong, 1999). The short distance between these two macromolecular complexes makes the transmission of an electro-mechanical signal between them possible, triggering conformational changes in the RyRs that open the channels allowing the Ca^{2+} to be released into the myoplasm (Hill et al., 2009; Reyes y Zarain, 2006). Ca^{2+} is

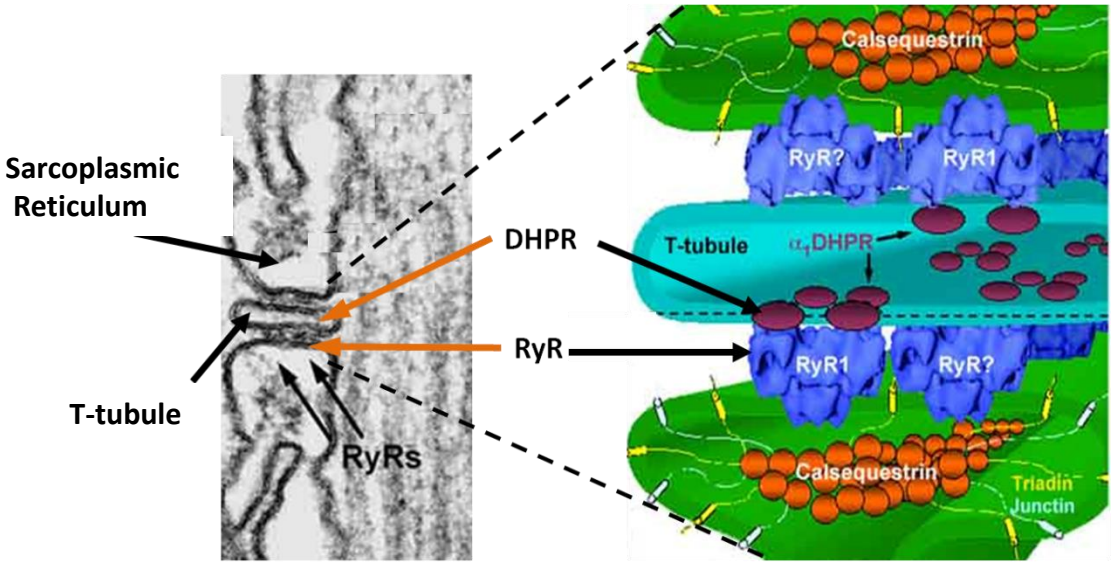

Figure 1.2. Structure of a triad. Triads are composed by a T -tubule and the sarcoplasmic reticulum terminal cisternae. The image on the left shows an electron micrograph of a transversal section of a triad, (left). The image on the right shows a schematic representation of a triad, showing the spatial distribution of the RyR and DHPR (image on the left taken from ….; image on the right, modified from Protasi, 2002).

released from the SR at a rate of 200 µmol/ms, changing the cytosolic Ca^{2+} concentration from 100 nM (resting condition; Williams et al., 1990) up to 20 µM (Baylor and Hollingworth, 2003). The Ca^{2+} in the myoplasm interacts with troponin C removing the inhibition of the troponin I leading to muscle contraction, see Figure 1.3 (Treves et al 2009; Calderon et al., 2014; MacIntosh et al., 2015).

1.2.2 Ca^{2+} removal mechanism.

After contraction of the muscle fibre has occurred, the Ca^{2+} removal machinery is activated, removing the majority of the Ca^{2+} from the myoplasm at a rate of 50 µmol/ms, and brining the resting Ca^{2+} concentration back to its original level (100 nM); the latter event will then lead to muscle relaxation. In fast fibres, two main components are involved in reducing the free Ca^{2+}

concentration: the first component of the relaxation process is almost completely due to the action of parvalbumin and the second component involves the action of the SERCA pumps (Gillis et al., 1982; Hasselbach and Makinose, 1961) and the Na^{+}/Ca^{2+} exchanger (NCX) (Balnave and Allen, 1998; Calderón et al. 2014).

In the first milliseconds following Ca^{2+} release from the SR, the parbalbumin proteins are saturated with Mg^{2+}, blocking their potential interaction with Ca^{2+} and allowing Ca^{2+} ions to interact with troponin C leading to muscle fibre contraction. However, due to the higher affinity of parvalbumin for Ca^{2+} compared to Mg^{2+}, it then releases Mg^{2+} and rapidly binds the free cytosolic Ca^{2+}. This rapidly reduces the concentration of Ca^{2+} in the myoplasm, but without lowering it to its original basal line since the parvalbumin proteins become saturated with Ca^{2+}. Once the Ca^{2+} concentration has been lowered, the Mg^{2+} (now present in a higher concentration) is able to replace the calcium ions on the parvalbumin (Klaus 1990; MacIntosh et al.2006).

The other components involved in the Ca^{2+} removal process (SERCA and NCX) work together to lower the myoplasmic Ca^{2+} concentration to its resting level and re-fill the SR calcium stores so that the muscle fibre is then ready for another round of activation (MacIntosh et al.2006; Treves et al 2009).

The SERCA pumps are enriched in the longitudinal sarcoplasmic reticulum membranes where they constitute almost 80% of the proteins by mass. They are endowed with a slower activity and thus it takes longer to remove the remaining free Ca^{2+} from the myoplasm compared to the speed of parvalbumin, but the activity of the SERCA pump is considered the principal factor in the reuptake of Ca^{2+} into the SR (Méme et al 1998). SERCA is an ATP-dependent protein that transports 2 molecules of Ca^{2+} per hydrolyzed ATP. SERCA proteins can adopt two conformational states, E1 and E2. E1 represents the structural conformation where two

Ca^{2+}-binding sides show high affinity and are facing the myoplasm while in the E2 conformation the two Ca^{2+}-binding sides present a low affinity and face the luminal side of the SR. The pumping process starts when two Ca^{2+} ions and one ATP molecule bind to the SERCA E1 conformational state; using the energy released from the hydrolysis of ATP, the pump undergoes a conformational change to its E2 state. Once the two Ca^{2+} ions are released into the SR, the SERCA undergoes once again a conformational change and regains its E1 conformational state, which is thermodinamically more favorable (Green et al., 1986, Wuytack et al., 2002). The SERCA pumps represent the main mechanism responsible for re-filling the SR with Ca^{2+} following ECC and are the main players involved in muscle fibre

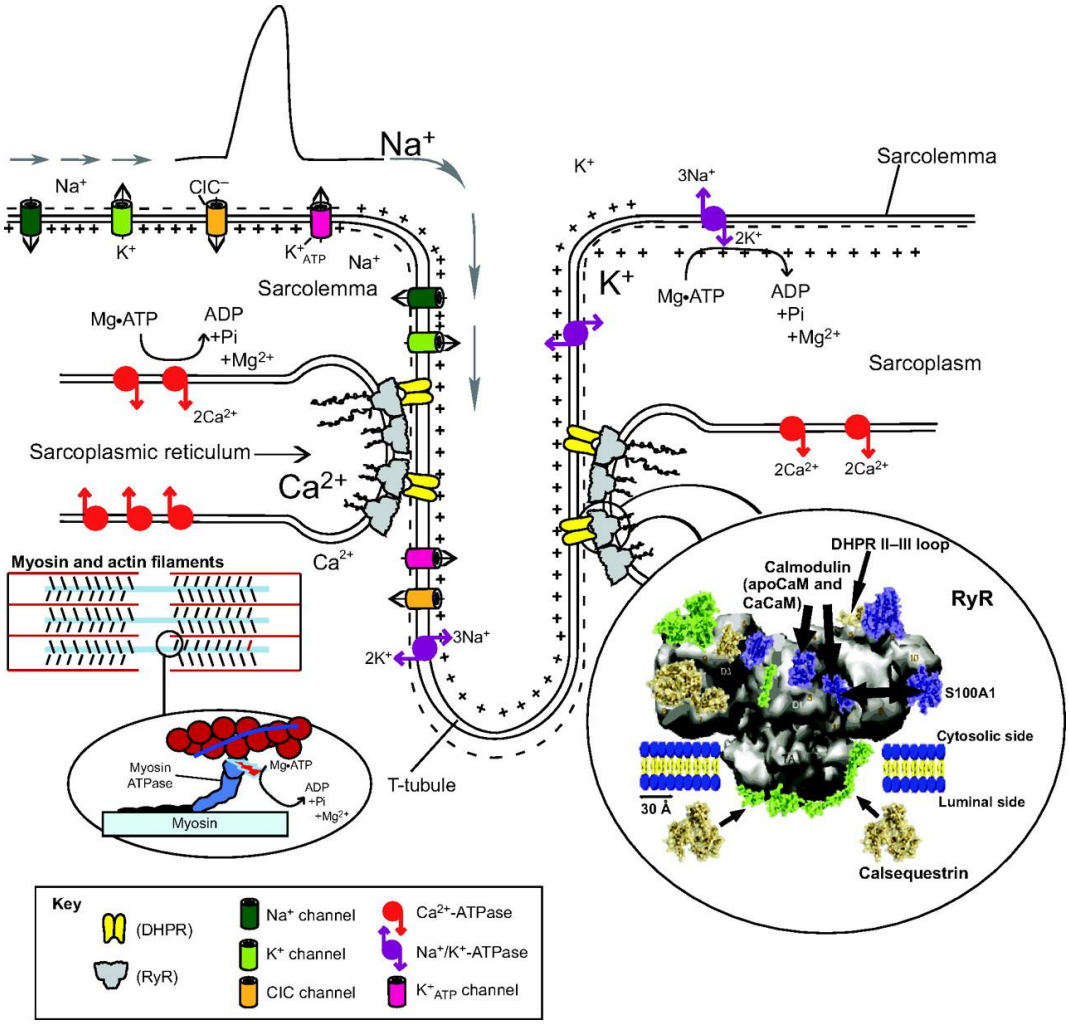

Figure 1.3. Excitation-contraction coupling mechanism. Proteins involved in the release and uptake of calcium in skeletal muscle (Image taken from MacIntosh et al., 2015).

relaxation. Several proteins including phospholamban, sarcoplipin and the micropeptide myoregulin are involved in the fine regulation of SERCA activity (see section 1.2.3 for a more detailed explanation (Periasamy et al., 2017; Treves et al., 2017).

The Na^+/Ca^{2+} exchanger, NCX, is a transmembrane protein found in the sarcolemma of cardiac and skeletal muscle and is able to transport 3 sodium ions inside for each calcium ion transported outside the muscle cell. Under physiological conditions, when the Na^+ concentration is higher outside of the cell (due to the Na^+ gradient created by the Na^+/K^+ ATPase), the NCX uses the energy generated by the entry of 3 Na^+ to remove 1 Ca^{2+} against its concentration gradient. Under specific physiological conditions however, the NCX can also operate in reverse mode, bringing Ca^{2+} in from the extracellular environment in exchange for Na+. This transporter plays a greater role in cardiac muscle than in the skeletal muscle, where its participation in Ca^{2+} clearing is relatively minor (Balnave and Allen, 1998; Iwamoto et al., 2007).

1.2.3 Components of ECC in skeletal muscle.

The proteins involved in the release and uptake of Ca^{2+} during the ECC process have been the topic of studies for many years. The main players of ECC are the two calcium channels RyR1 and DHPR/Cav.1.1, but many additional proteins play an important role in regulating this process and participate in Ca^{2+} homeostasis.

Ryanodine receptors (RyR).

RyR Ca^{2+} release channels take their name from the fact that they bind the alkaloid ryanodine with high affinity. The functional calcium release channel is a homotetramer of around 2 MDa (each subunit of 565 kDa (Zorzato et al., 1990) that plays a crucial role in the mobilization of Ca^{2+} from the SR during ECC in muscle cells. RyRs were first identified in the SR of skeletal

and cardiac muscles, but have also been identified in the endoplasmic reticulum of non-muscle cells, where they play a role in Ca^{2+} homeostasis (Treves et al., 2017). RyRs are a family of proteins which exist as three different isoforms, RyR1, RyR2 and RyR3, sharing an overall sequence homology of 65%, and being encoded by three different genes, *RYR1*, *RYR2* and *RYR3* (Lanner et al., 2010; Ozawa, 2015). RyR1 is principally expressed in skeletal muscle and to a lesser extent in smooth muscle cells, some immune cells such as dendritic cells and B-lymphocytes, some areas of the CNS and in neurons. As mentioned in the previous section, in skeletal muscle its activation occurs via an electro-mechanical process due to its coupling to the DHPR channels (Block et al. 1988; Zorzato et al., 1990; Ottini et al., 1996; Ozawa et al., 2009). On the other hand, RyR2 is mainly expressed in cardiac muscles where it is not coupled to DHPR/Cav1.2 channels but is activated by a mechanism initiated by depolarization-induced Ca^{2+} influx through DHPR/Cav1.2. This mechanism that activates RyR2 and induces Ca^{2+} release from the SR is referred to as Ca^{2+}-induced Ca^{2+} release (CICR) (Otsu et al 1990, Treves et al., 1993; Franzini-Armstrong, 1999). Finally RyR3 is ubiquitously expressed, principally in brain, as well as other tissues such as skeletal, smooth and eye muscles, lung, kidney, ileum, uterus, bladder and esophagus. In skeletal muscle the expression of RyR3 appears to be developmentally regulated.. RyR3s, as RyR2, are not coupled to DHPR/Cav1.1 channels, a fact that suggests their indirect activation by CICR. (Giannini et al., 1995; Lanner et al., 2010; Sekulic-Jablanovic et al., 2015)

RyR1

The RyR1 was originally identified, cloned and sequenced from rabbit skeletal muscle (Taheshima et al. 1990.; Zorzato et al. 1990) In humans the gene encoding RyR1 (RYR1) is located on chromosome 19q13.2. The structure of this channel is homotetrameric, see figure 1.4, with each subunit having a molecular mass of 565 KDa. The topology of each subunit consists of a pore region formed by six transmembrane helices located within the C-terminal

region, representing almost 20% of the protein. On the other hand, the N-terminal region is made up by a large cytoplasmic region that represents 80% of the total protein (known as the foot region). In skeletal muscle two different special organization models have been observed between the RyR1 and the DHPR/Cav1.1 channels. In the first one, each DHPR/Cav1.1 channel belonging to a tetrads (groups of 4 DHPR/Cav1.1) located on the T-tubule membrane, are under each foot of the RyR1s, matching all the "feet" of the RyR1 and the DHPR/Cav1.1

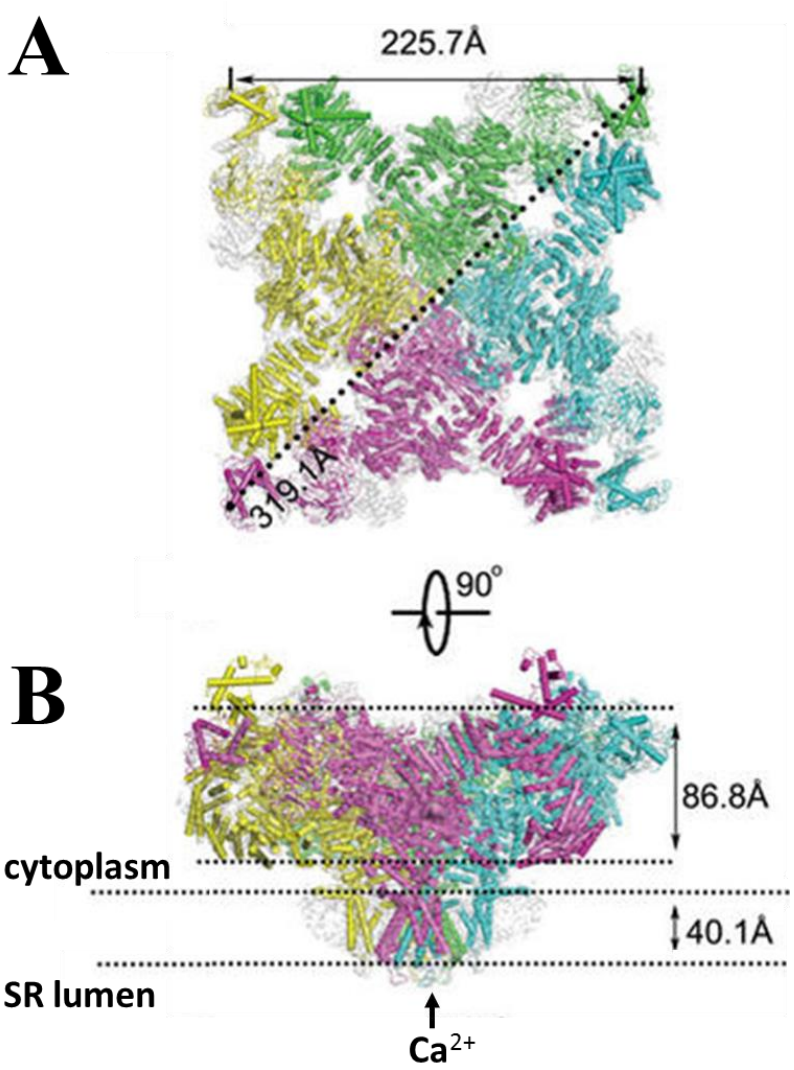

Figure 1.4 Near atomic structure of a **Ryanodine receptor**. **A)** Shows the top view of the 3D model of the RyR, presenting the side and diagonal dimensions of this protein. **B)** Shows the side views of the 3D model of RyR, presenting the dimension in the cytoplasmic assembly and the transmembrane region (modified from Wei et al., 2016).

channels (as is shown in the figure 1.2). In the second model the RyR1 and DHPR/Cav1.1 are not associated, and there are in fact uncoupled RyR1. In mature skeletal muscles half of the RyR1 are coupled and the other half is uncoupled (Franzini-Armstrong and Nunzi, 1983; Zorzato et al., 1990; Franzini-Armstrong et al., 1998).

Physiological activation of Ca^{2+} release from RyR1s occurs via an electro-mechanical coupling to the DHPR/Cav1.1 channel. But additionally RyR1s can also be activated by Ca^{2+} as well as pharmacologically, with caffeine, 4-chloro-m-cresol and low concentration of ryanodine (<10 μM). RyR1 are inhibited by Mg^{2+}, higher concentrations of ryanodine (≥100 μM) and ruthenium red (Meissner et al. 1986; Lai et al. 1989; Lanner et al., 2010). The activity of the calcium channel is also modulated by the interaction with calmodulin (CaM), S100, calsequestrin (CASQ), FK506-binding proteins (FKBPs) triadin and junctin. Mutations in the *RYR1*, the gene encoding RyR1, have been associated with several human diseases including the pharmacogenetic disorder malignant hyperthermia, the congenital myopathies central core disease, multimini core disease, centronuclear myopathy, congenital fibre type disproportion, heat/exercise induced exertional rhabdomyolysis and atypical periodic paralyses (Priori and Napolitano, 2005; Lanner et al., 2010; Treves et al., 2017).

DHPR/Cav1.1

The DHPRs present a molecular mass of 190-250 KDa and belong to the family of L-type high-voltage-activated Ca^{2+} channels; they are made up of 5 subunits of which the pore-containing calcium channel subunit is called alfa 1 or Cav. Mammalian cells express at least 4 Cav isoforms (Cav1.1–1.4) (Catterall). Cav1.1 and Cav1.2, are known as dihydropyridine receptors (DHPR), and are located principally in the skeletal and cardiac muscles, respectively. The α1 subunit is both the voltage sensing and the pore forming subunit, whereas the α2δ, β and γ are auxiliary subunits located in the extracellular, intracellular, and

transmembrane space, respectively (See figure 1.5). The latter subunits modulate, the activation and inactivation kinetics, gating properties and membrane trafficking of the α1-subunit (Bers, 2002; Lanner et al., 2010; Treves et al., 2017).

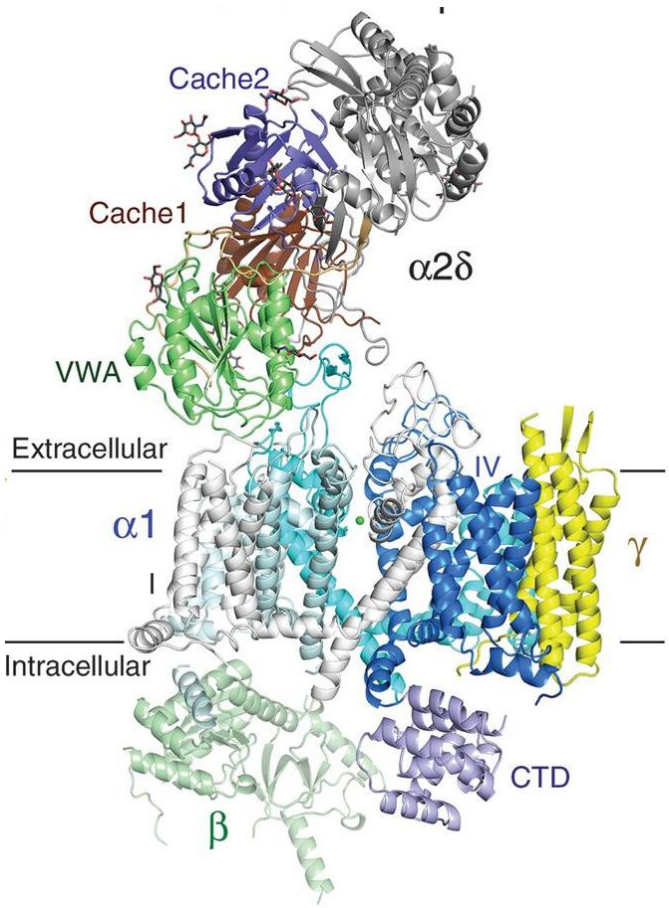

Figure 1.5 Structure of the voltage-gated Ca2+ channel Cav1.1. The cryo-EM structure of the Cav1.1 complex at a nominal resolution of 4.2 Å, showing the four Cav1.1 subunits (α1, α2δ, β and γ) with colored domains (image taken from Wu et al., 2015).

The Cav1.1 subunit of is encoded by *CACNA1S* gene, mutations in this gene have been shown to have negative effects on skeletal muscle Ca^{2+} homeostasis.. Specifically, the presence of the *CACNA1S* p.R174W mutation induces RyR1 leak due to the alteration of the regulation of Cav1.1 over RyR1. The RyR1 leak causes negative effect in the muscle fibres, increasing resting cytosolic Ca^{2+} and partial depletion of SR Ca^{2+} stores (Treves et al., 2017). Another

significant aspect that was recently identified is the role of DHPR as Ca^{2+} channels. In the skeletal muscle the voltage-induced conformational changes of DHPRs is transmitted to RyR1s, which subsequently open and release Ca^{2+} to the sarcoplasm, as previously explained. However DHPRs are also able to transport a Ca^{2+} current, whose role in ECC is still not completely clear (Rios and Brum., 1987; Bannister and Beam, 2013). To clarify if DHPRs play important or just a vestigial role in ECC, Grabner`s group (University of Innsbruck, Austria) designed a DHPR pore-blocked channel, based on the non-Ca^{2+}-conducting DHPRs from euteleost fish, to block the DHPR Ca^{2+} current in the skeletal muscle of mice (Dayal et al., 2017). Evaluation of muscle fibres, isolated mucle force and whole body muscle force (in vivo experiments) of DHPR knock-in-mice revealed no difference in SR Ca^{2+} release, locomotor activity, muscle strength and fatigue resistance compared to wild-type mice (Dayal et al., 2017).

Calsequestrin

The Ca^{+} sequestering protein calsequestrin (CASQ), is an SR Ca^{2+} binding/storage protein concentrated in the terminal cisternae of the SR. This protein was first isolated from the SR of rabbit; in mammalian cells CASQ is present in two isoform (1 and 2), CASQ 1 is present in slow and fast skeletal muscle fibres while CASQ 2 is expressed predominantly in cardiac muscles and to a lesser extent in slow-twitch skeletal muscle fibres (D'Adamo et al., 2016). CASQ1 migrates as a protein with an apparent mol weight of 60 kDa, but the cDNA sequence encodes a protein of 367 residues plus a 28 residue amino-terminal signal sequence (MacLennan and Wong, 1971; Zarain-Herzber et al., 1988). In the SR CASQ buffers a large amount of Ca^{2+} due to its low-affinity (Kd $\sim 10^{3}\ _{M}^{-1}$) and high Ca^{2+} binding capacity (40 mol Ca^{2+}/mol protein at pH 7.5; Sanchez et al., 2012). When millimolar Ca^{2+} is present in the lumen of the SR (resting conditions), CASQ polymerizes forming long polymeric tendrils (also known as calcium wires) in an area adjacent to the RyR1 where it acts as the principal

SR Ca^{2+} storage protein (MacLennan and Wong., 1971; Treves et al., 2017). Recent in vivo experiments have demonstrated that CASQ is partially depolymerized when the SR Ca^{2+} concentration decreases (conditions produced by fatigue stimulation, long-lasting depolarization or low drug concentrations) and is fully depolymerized when Ca^{2+} depletion is maximal, a condition which is achieved when the SR is treated with calcium channel opening drugs (Manno et al., 2017).

SERCA

The sarcoendoplasmic reticulum Ca^{2+} ATPase (SERCA) is a single polypeptide of 110 kDa, localized in the longitudinal SR membrane. This protein is widespread in both eukaryotic and prokaryotic cells, revealing it as a versatile and evolutionarily conserved protein (Periasamy and Kalyanasundara, 2007) SERCA presents a big variability in vertebrates, where three distinct genes encoding SERCA 1, 2, and 3, that produce 10 different isoforms through alternative splicing can be found. The expression of each isoform is also variable depending on the organ and tissue where it is expressed. *SERCA1* is expressed in fast-twitch skeletal muscle and is alternatively spliced to encode SERCA1a (adult) and 1b (fetal). On the other hand *SERCA2* encodes SERCA2a, which is present predominantly in cardiac and slow-twitch skeletal muscle; SERCA2b is ubiquitously expressed but in low levels. Finally, *SERCA3* isoform are expressed in non-muscle tissues.

SERCA belongs to the family of P-type ATPases that includes plasma membrane Ca^{2+}+ ATPase (PMCA), Na+/K+ ATPase, and H+, K+ ATPase. As mentioned in the previous section this pump utilizes the energy derived from ATP hydrolysis to transport 2 Ca^{2+} ions across the membrane; its activity is regulated by the small-molecular-weight proteins phospholamban and sarcolipin, in a tissue-specific manner. The lack of SERCA has been

linked to human diseases and several animal models have been generated. In Brody's disease, it was demonstrated that both copies of the SERCA1 gene contain inactivating mutations; such patients show a skeletal muscle disorder characterized by impaired muscle relaxation, stiffness, and cramps (Odermatt et al., 1996). The SERCA1 KO animal models, demonstrated that the lack of SERCA1 causes severe impairment of the respiratory muscles with the mice becoming cyanotic and finally dying shortly after birth (Pan et al. 2003). SERCA2 null mice do not survive birth due to the principal role of this protein in cardiac and slow-twitch skeletal muscle (Prasad et al., 2004; Maclennan, 2004; Periasamy and Kalyanasundaram, 2007; Periasamy et al., 2017).

JP-45

JP-45 is a 45 KDa protein transmembrane protein of the SR junctional face membrane of skeletal muscle (Zorzato et al., 2000). Its expression is developmentally regulated, reaching maximal levels during the second month of post-natal development. This protein is phosphorylated by PKA and interacts with CASQ in the SR lumen through its luminal short carboxy-terminal domain. Different experiments have shown that it also interacts through its amino terminus with a region within the I–II loop (referred to as AID) of the Cav1.1 The interaction of JP-45 with CASQ and Cav1.1 hints towards the possible functional role of this protein (JP-45) in a signalling pathway linking CASQ and the DHPR. Over-expression and ablation of JP-45 affect the functional expression of Cav1.1 inducing a decrease of voltage-dependent Ca^{2+} release. Young JP-45 KO mice, show a skeletal muscle phenotype similar to that observed in aged mice, with a lower membrane density of the voltage sensor (Cav1.1; Zorzato et al., 2000; Anderson et al. 2003; Rossi and Dirken, 2006; Treves et al., 2013; Mosca et al., 2016).

Triadin

Triadin is a 95 kDa protein, specifically localized in the triad of skeletal muscle. Triadins are a family of multiple proteins, of different isoforms produced by the alternative splicing of a single *TRDN* gene. Expression of three different triadin isoforms has been observed in rat skeletal muscle (Trisk 95, Trisk 51 and Trisk 32 (Vassilopoulos et al., 2005). These isoforms present a common structure, only differentiated by the length of their luminal segment and their unique C-terminal domain. Trisk 95 and Trisk 51, are exclusively expressed in skeletal muscle, associated with RyR1 and CASQ1. Functional in vivo studies have shown that triadin is able to regulate the activity of the RyR1 channel either directly or via its interaction with CASQ (in vivo). Trisk 32, is mainly expressed in cardiac muscle and to a lesser extent in skeletal muscle (Marty et al., 2009).. Studies on triadin KO mice model, showed that the mice have a moderate but clear skeletal muscle weakness, associated with reduction in the amplitude of calcium releass, and cardiac muscle abnormalities, showing arrhythmia following isoproterenol administration (Treves et al. 2009; Marty, 2015).

Junctin

Junctin is a structural protein present in cardiac and skeletal muscle junctional SR membranes, with a molecular weight of 26 KDa. Studies in skeletal muscle show that junctin belongs to the family of single membrane-spanning proteins (along with aspartyl β-hydroxylase and junctate) that result from alternative splicing events of the same gene located in human chromosome 8. Junctin binds to the Ca^{2+} binding protein calsequestrin and the transmembrane protein triadin forming a complex in the lumen of the SR capable of associating and communicating with the RyR1. Studies have demonstrated that this quaternary complex, junctin, triadin, calsequestrin and RyR1, may be important for Ca^{2+}

release during the ECC event in skeletal and cardiac muscles (Zhang et al., 1997; Treves et al., 2000; Treves et al., 2009)

Parvalbumin

Parvalbumin is a low molecular weight soluble protein of 12 KDa belonging to the large family of EF-hand Ca^{2+}-binding proteins (Raymackers et al., 2000). It is present principally in fast skeletal muscle and specific nerve cells. In lower vertebrates, five parvalbumin isoforms have been identified, whereas in adult rodents a single isoform is expressed. Fast skeletal muscles from lower vertebrates and from small mammals contain high concentrations (0.5 mM) of parvalbumin. This protein is exclusively found in the SR, presenting a high selectivity for Ca^{2+} over Mg^{2+} ions. It has been estimated that, under resting conditions parvalbumin is essentially in the Mg-parvalbumin complex form, but during an ECC event, it binds myoplasmic Ca^{2+}, reducing the Ca^{2+} concentration and enhancing relaxation. Experiments using parvalbumin (PV −/−), knockout mice show that in skeletal muscle the decay of intracellular Ca^{2+} concentration after 20 ms stimulation was slower compared to WT mice. The longer extension of the half-relaxation time in these PV −/− mice induced an increased in the intracellular Ca^{2+} concentration that caused a greater force (40 %) compared to that of WT mice (Schwaller et al., 1999; Raymackers et al., 2000; Racay et al., 2006).

SRP-27

Sarcoplasmic reticulum protein of 27 kDa (SRP-27) also known as mitsugumin-33 or TRIC-A trimeric intracellular cation-selective channel (TRIC-A) is expressed in skeletal muscle, heart and brain. Specifically, it is highly expressed in fast twitch skeletal muscle fibers and to a lesser extent in slow twitch fibres and its peak expression level occurs during the first month of post-natal development. This protein is composed by four transmembrane-spanning alpha helices and its C-terminal domain faces the cytoplasmic side of the endo(sarco)plasmic

reticulum. Three-dimensional reconstruction studies of the native protein suggest that it acquires a pyramidal elongated structure and experimental data have shown that it is a cation channel, with a selectivity of K^+ over Na^+, presenting a permeability ratio of PK/PNa= 1.5. SRP-27 KO mice are viable and do not present a critical change in their phenotypes, nevertheless they had a reduced K^+ permeability accompanying thapsigargin-induced Ca^{2+} efflux (Bleunven et al., 2008; Yazawa et al., 2007; Treves et al 2009).

1.3 Skeletal muscle metabolism.

As important as skeletal muscle is for movement, using energy to produce contraction, it also plays an important role in metabolism and specific carrier molecules bring energy into the muscle in the form of glucose. Thus skeletal muscle is considered one of the main players in whole body metabolic homeostasis. This tissue is able to take up glucose in response to insulin signaling or after muscle contraction.

1.3.1 Insulin

Insulin is an anabolic polypeptide hormone, considered the most potent physiological anabolic agent known. It plays an important role in the storage and synthesis of lipids, protein, and carbohydrates, regulating their breakdown and release into the circulation. In humans the insulin gene is located on the short arm of chromosome 11 in the region p13. The atomic resolution structural analysis revealed that this hormone is a quaternary macromolecule, composed of two polypeptide chains, A and B, which are cross-linked by two disulphide bonds, as shown in figure 1.6 . The stability of insulin can be affected by different factors such as its concentration, pH and the presence of ions (principally zinc). Insulin can form aggregates that reduce drastically its biological activity and block the delivery routes of this

hormone. Such an effect could cause severe problem for patients under insulin treatment, due to the possible blocking effect caused by aggregates of artificial drug delivery systems (Bunner et al. 2014). At low insulin concentrations this polypeptide hormone exists as monomers and can undergo protein unfolding. The insulin peptides that lose their native 3-dimensional structure interact with each other to form aggregates known as fibrils, reducing the activity of insulin. On the contrary, at high insulin concentrations (>5 mg/ml) and pH 7.4 the insulin monomers form dimers or hexamers through their hydrophobic interaction. Additionally, the presence of zinc ions in a pH range 4–8, induce the assembly of insulin hexamers (see figure 1.6), which avoids insulin denaturation and maintains prolonged insulin activity (Owerbach et al., 1981; Zhang et al., 2004; Bunner et al., 2014)

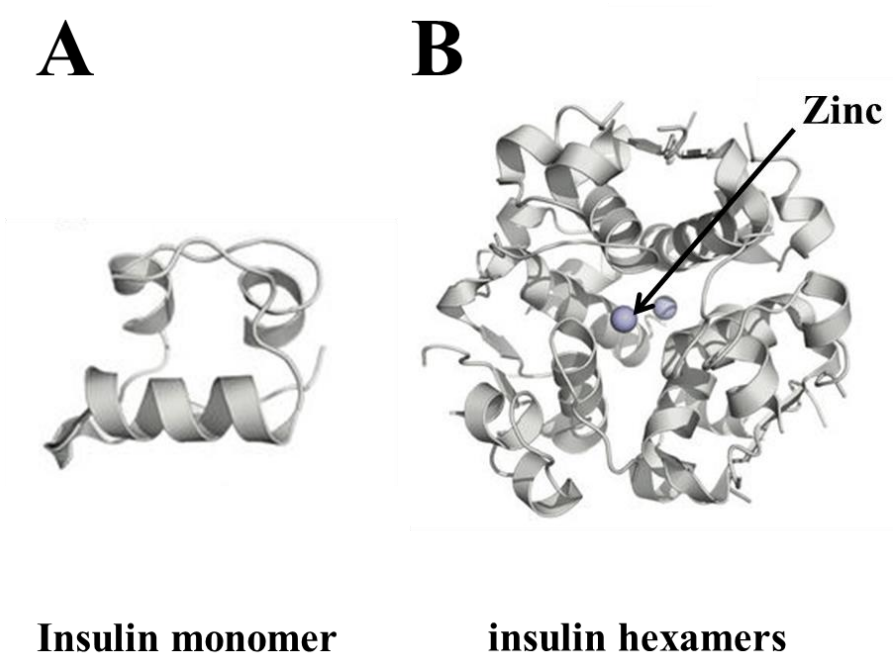

Figure 1.6 Insulin structure. A) 3D model of the insulin monomeric structure. **B)** 3D model of the insulin hexameric structure showing the zinc ion in the center of the hexamer (image modified from Nedumpully-Govindan and Feng Ding, 2015).

Insulin induces a big effect on the whole organism, but its bigger effects are on the liver, brain, adipose tissue and skeletal muscle. After insulin is released into the blood stream,

different organs respond in a specific manner: the brain inhibits both hepatic glycogenolysis and lipolysis and decrease the appetite through lepting regulation; the liver increase its glycogen synthesis and lipogenesis and decrease the gluconeogenesis and glucose release; the adipose tissue increases its glucose uptake and storage, and also affects its lipid breakdown pathway, increasing lipogenesis and decreasing the lipolysis; finally, the skeletal muscle increases its glucose uptake and glycogen synthesis. Beside the strong metabolic effects of insulin on the organism, this hormone has also an important role in different cellular processes, which include protein synthesis, mitochondrial biogenesis, growth, autophagy, proliferation, differentiation, and migration (Filippi et al., 2013; Bunner et al., 2014).

Insulin pathway in skeletal muscle.

The body presents a complicated and sophisticated mechanism that regulates the glucose levels in the organism. After a meal, insulin that is produced by the beta cells of the pancreas as result of the processing of the molecular precursor proinsulin, is released into the blood stream, where it travels to different tissues and organs including adipose tissue, liver, skeletal muscle and nervous system. Skeletal muscle plays a very important role in glucose homeostasis, being responsible for about 80-90% of insulin-stimulated glucose uptake (Leto and Saltiel, 2012).

Because of metabolic syndrome disorders and the increase in worldwide type 2 diabetes, the insulin pathway has become the focus of many research laboratories and its mode of action in muscle has been investigated in detail. After the binding of insulin to the α-subunit of the insulin receptor (IR), a heterotetrameric bifunctional complex composed by 2 extracellular α subunits and 2 transmembrane β subunits with tyrosine kinase activity, this complex (IR) becomes activated and one of its β subunit is trans-phosphorylated. This in turn increases the kinase catalytic activity of the (IR) β subunit which phosphorylates and activates the insulin

receptor substrates 1 and 2 (IRS1, IRS2). These phosphorylated IRS proteins interact with phosphatidylinositol 3-kinase (PI3K), an important regulator of glucose homeostasis. Phosphatidylinositol-3,4,5-trisphosphate (PIP3) is produced by PI3K at the cytoplasmic face of the plasma membrane and induces the activation of 3-phosphoinositide-dependent kinase 1 (PDK1) that phosphorylates AKT on threonine 308 (T308). For the full activation of AKT, phosphorylation of serine 473 (S473) is also necessary and this phosphorylation is mediated by the mTORC2 complex activated by PIP3. Active AKT also phosphorylates the tre-2/BUB2/cdc 1 domain family (TBC1D1, also known as AKT substrate of 160 kDa, AS160) and triggers the translocation of the Glucose transporter 4 (Glut4) to the plasma membrane, as shown in figure 1.7 (Leney and Tavare, 2009; Dibble and Cantley, 2015; Cartee, 2015).

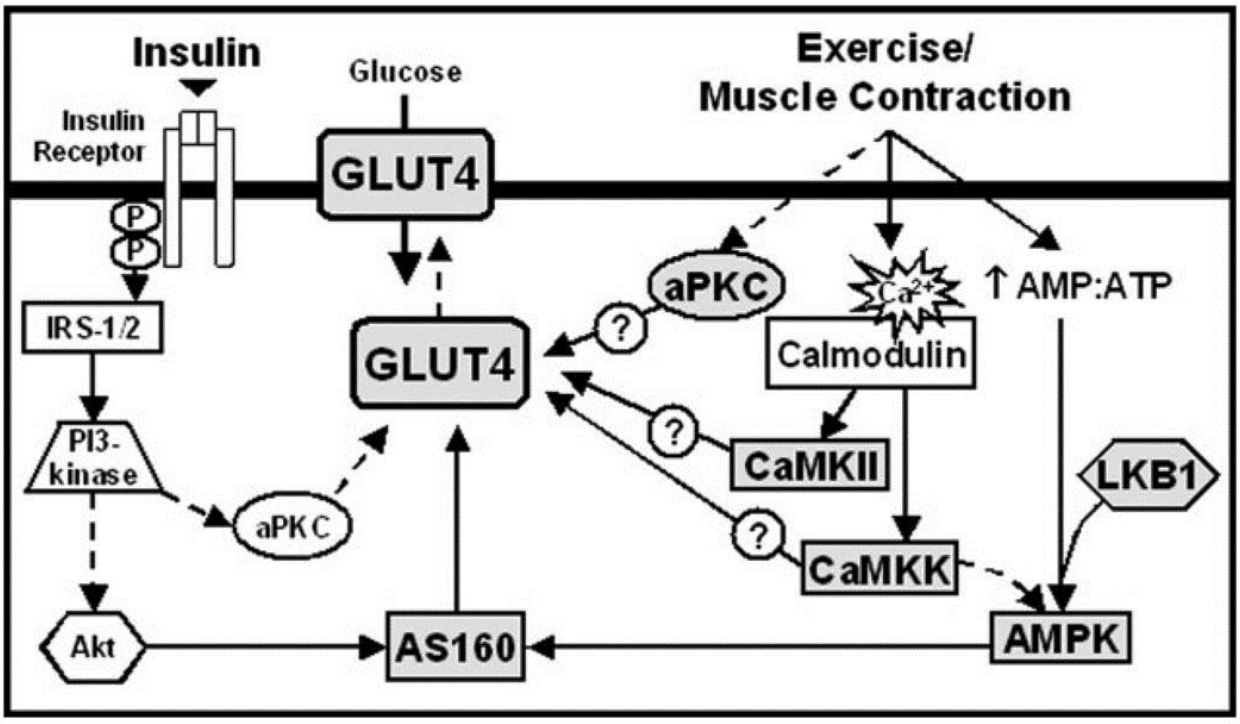

Figure 1.7. Insulin and muscle contraction pathways. Insulin and muscle contraction pathways share both AKT and AMPK, dependent phosphorylation, respectively. Both proteins activatedAS160 and induce the translocation of Glut4 to the sarcolemma (image from Röckl et al. 2008).

Experiments in animal models where the disruption of insulin signaling in liver, skeletal muscle or adipose tissue was induced using different experimental approaches, including genetic, pharmacological, surgical, and dietary inductions, showed severe hyperinsulinemia and in general leaded to the development of diabetes in these animals. Specifically, mice lacking whole body insulin receptors (IR) show that insulin is important for postnatal fuel homeostasis but not for prenatal growth and metabolic control. IR-KO newborn mice exhibited a slight growth retardation, but no metabolic abnormalities. After birth fast metabolic changes were observed, with glucose levels increasing drastically upon feeding, and insulin levels rising up to 1000 fold above normal. After a few days β-cell failure occurred and finally the animals died of diabetic ketoacidosis. On the other hand, when less severe approaches were taken such as mice lacking insulin receptors in specific cell types, different phenotypes were observed, with mice developing only mild metabolic and reproductive abnormalities (Kitamura et al., 2003; Zhang et al., 2004. Bunner et al., 2014).

1.4.2 AMPK

The AMP-activated protein kinase (AMPK) is considered one of the crucial cellular energy sensor proteins. The AMPK structure, as determined by X-ray crystallography, shows a heterotrimeric complex comprising an α-catalytic subunit and two regulatory subunits (β and γ), (see figure 1.8). Interestingly, genes encoding AMPK subunits are found in essentially all eukaryotes; in humans there are two α-subunits, α1 and α2, encoded by the genes *PRKAA1* and *PRKAA2*, two β-subunits, β1 and β2, encoded by *PRKAB1* and *PRKAB2* and three γ-subunits, γ1, γ2 and γ3, encoded by *PRKAG1*, *PRKAG2* and *PRKAG3* genes, respectively (Hardi et al., 2012). All possible combinations between these different subunits can occur, opening the possibility of forming 12 potential AMPK complexes. In detail, the α-subunit is generally structured with a conventional kinase domain at its N terminus which is

immediately followed by an auto-inhibitory domain (AID) and subsequently by an extended 'linker peptide' that connects the AID to the α-subunit carboxy-terminal domain (α-CTD), see figure 1.8. It is important to mention that threonine residue 172 (Thr172), is located on the segment of the amino-terminal kinase domain of the α-subunit, and its phosphorylation induces AMPK activation increasing the activity of this enzyme several-hundred-fold. The β-subunit contains a carbohydrate-binding module (CBM) which allows AMPK to associate with glycogen particles (the exact mechanism of this module remains uncertain, but possibly is may allow the co-localization of AMPK and glycogen particles). Following the CBM there is the β-subunit C-terminal domain (β-CTD), which interacts with the α and γ subunits. Finally the γ subunit, is made up of four tandem repeats of a sequence motif named after cystathionine β-synthase (CBS), see figure 1.8 (Xiao et al., 2011; Herzig and Shaw, 2017).

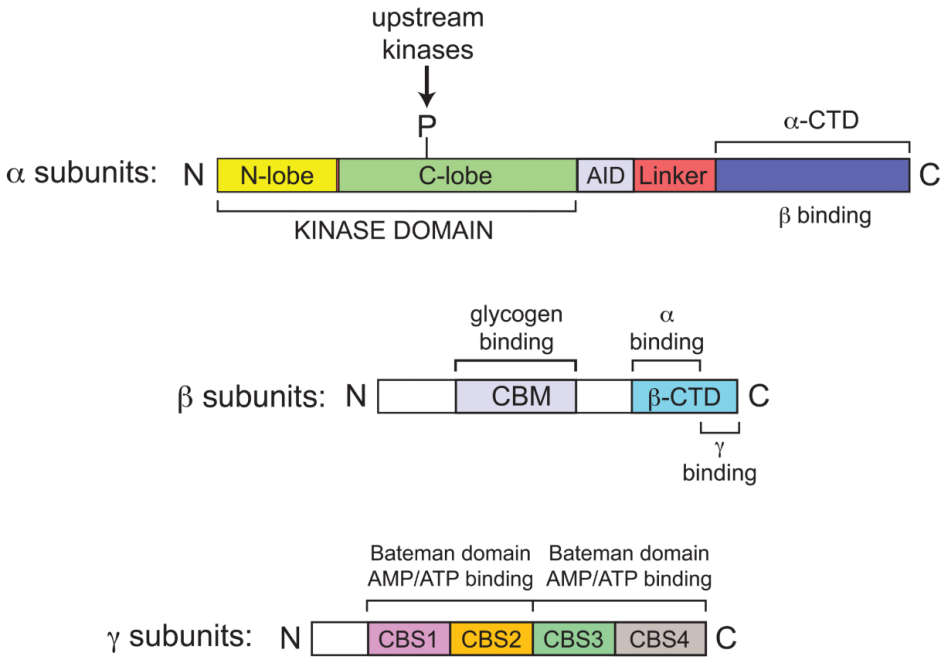

Figure 1.8 Domain map of typical mammalian AMPK. Composition of the heterotrimer AMPK enzyme with its α, β and γ subunits and their domain components (image from Hardi et al., 2012).

AMPK animal model have been very useful to understand the role of the different subunits that make up the AMPK protein. Mice lacking the AMPK α subunit 1 KO (AMPKα1−/−) in their skeletal muscles did not present any significant irregularity in glucose homeostasis, confirmed by glucose tolerance test. Conversely, AMPKα2−/− mice exhibited a clear change in the glucose metabolism (Viollet et al. 2003b). These mice exhibited high plasma glucose levels and reduced insulin sensitivity. On the other hand, studies in mice carrying single mutations in *PRKAB1* and *PRKAB2* or deletions of muscle β1 or β2 subunit, did not show apparent metabolic problems. Nevertheless, when both AMPK β1 and β2 isoforms where deleted in the skeletal muscle of mice (AMPK β1& β2−/) the animals showed physical inactivity and had a drastic diminished capacity for treadmill running. These problems have been associated with a reductions in skeletal muscle mitochondrial content and reduction in the contraction-stimulated glucose uptake (Viollet et al., 2003a; O'Neill, 2011). Lastly, mice with skeletal muscle-specific mutations in the AMPK γ1 subunit showed higher AMPK activation and higher muscle glycogen content (Barrét al., 2007). Moreover, transgenic mice with chronic γ2 AMPK activation exhibited ghrelin signaling-dependent hyperphagia, obesity, and impaired pancreatic islet insulin secretion. For their part, AMPK γ3 knock-out mice revealed that this subunit protect the skeletal muscle against excessive triglyceride accumulation and insulin resistance, forming heterotrimers with α2 and β2 isoforms in glycolytic (fast-twitch type II) skeletal muscle fibres (Barnes et al., 2004; Kim et al., 2014; Willows et al 2017; Yavari et al., 2017).

Muscle contraction and AMPK

Exercise (muscle contraction) presents two different effects on the organism's balance of glucose homeostasis. The first occurs a few hours after exercise when an insulin-dependent

pathway is activated and induces the translocation of Glut4 onto the sarcolemma promoting a higher glucose uptake into the skeletal muscle. This pathway is mediated by AMPK, a protein that as AKT is able to activate the TBC1D1/AS160 protein. The second pathway, unlike the first, takes place up to 48 hours after exercise has stopped and consists in the improvement of whole-body insulin sensitivity (Mikines et al., 1988; Koopman et al., 2005; Jensen and O'Rahilly, 2017). It is thought that the absence of these two effects mediated by exercise are linked to different chronic conditions such as hypertension, coronary heart disease, metabolic syndrome, obesity, type 2 diabetes mellitus (T2DM), and age-related muscle wasting (sarcopenia) and can be prevented and treated with regular physical activity (Juleen and Zierath, 2013).

During exercise the body regulates the rate of energy production, blood flow, and substrate utilization in response to high or low locomotion intensity. The liver releases up to 80 % of the glucose present in the blood in response to exercise-induced changes in glucagon (a polypeptide hormone released by pancreatic alfa cells, that actives liver glycogenolysis) and AMP levels. Adenosine triphosphate (ATP) is considered the "energy currency" of cells, since its hydrolysis provides the energy required by most biological processes; its hydrolysis produces adenosine diphosphate (ADP) and adenosine monophosphate (AMP), which are lower energy molecules. The ATP/ADP or ATP/AMP ratios are used by organisms to determine their energy levels, and AMPK is the protein that senses the changes in these ratios. Under low energy level conditions AMPK is able to switch off ATP consuming pathways such as fatty acid and cholesterol biosynthesis and switches on ATP generating processes mediated by glucose uptake and fatty acid oxidation (Pencek et al. 2005; O'Neill, 2013).

Once the ATP/ADP ratio level decreases a signal is released within the cell signaling that more ATP is required. An allosteric mechanism triggered by the binding of ADP and AMP to the γ-subunit of AMPK stimulates its kinase activity, inducing the phosphorylation of Thr172

and also protecting this residue from being dephosphorylated by phosphatases. Upstream kinases LKB1 and Ca^{2+}/calmodulin-dependent protein kinase kinase (CaMKK) also phosphorylate AMPK Thr172 stimulating its activity by an additional 100 times. LKB1 is activated as a result of low ATP/ADP and ATP/AMP ratios and CaMKK activation is due to elevated intracellular Ca^{2+}, but even if both induce the phosphorylation of AMPK, recent studies have shown that LKB1 plays the major role in AMPK phosphorylation and in translocation of Glut4 to the plasma membrane. See Figure 1.7 for a detailed scheme (O'Neill, 2013; Herzig and Shaw, 2017).

1.4.3 Glucose transporters

The requirement of mammalian cells for energy is supplied by sugar molecules. The transport of sugar is made facilitated by sugar transport proteins belonging to the family of integral membrane proteins called Gluts, which in turn are part of the major facilitator superfamily (MFS) of membrane transporters (Carruthers et al., 2009). Glut proteins catalyze unidirectional sugar uptake and release based on the sugar concentration gradient, from a high to lower sugar concentration. This "facilitated diffusion" is several orders of magnitude faster than sugar diffusion across artificial lipid bilayers (Carruthers et al., 2009). The Glut transporters present strong specificity for d-stereoisomers of pentose and hexose monosaccharides, including, d-glucose, d-galactose, among others. These transporters are encoded by the gene *SLC2A* and are composed of ~500 amino acids. They are predicted to possess 12 transmembrane-spanning alpha helices and a single N-linked oligosaccharide and depending on their sequence similarities, can be grouped into three different Glut family classes (Thorens and Mueckler, 2010). Class I includes the transporters Glut1 to Glut4, which are characterized by their specific glucose transporter function and their characteristic tissue specific distribution (Glut1, erythrocytes, brain microvessels; Glut2, liver, pancreatic islets;

Glut3, neuronal cells; Glut4, muscle, adipose tissue). Class II is composed by the fructose-specific transporter Glut5 and three related proteins, Glut7, Glut9, and Glut11. Finally, class III is composed of Glut6, Glut8, Glut 10, Glut12 and HMIT1, presenting as principal characteristic the lack of a glycosylation site in the first extracellular linker domain and by the presence of such a site in loop 9 (Joost et al., 2002; Carruthers et al., 2009; Thorens and Mueckler, 2010).

Glut1

Glut1 was the first glucose transporter isoform to be identified, purified and cloned; subsequent to its identification it was discovered that this transported can also carry galactose and ascorbic acid. In humans the gene encoding Glut1 is located on chromosome 1 (1p35-31.3; Carruthers et al., 2009). Unlike Glut4, Glut1 is always present on the plasma membrane and is activated by a non-insulin-sensitive pathway, even if present on the plasma membrane of insulin-responsive tissues. Glut1 plays an important role in insulin-non-responsive tissues by mediating glucose transport down its concentration gradient, mostly from the blood into cells (except in the intestine where glucose flows from the lumen of the cells to the extracellular environment). This transporter is highly expressed on the plasma membranes of proliferating cells forming the early developing embryo, in cells forming the blood-tissue barriers, in human erythrocytes and astrocytes, brain and cardiac muscle (Mann et al., 2003; Carruthers et al 2009) and it is cytochalasin B (IC50 = 0.44 μM), HgCl2 (IC50 = 3.5 μM), phloretin (IC50 = 49 μM), and phlorizin (IC50 = 355 μM) (Helgerson and Carruthers., 1987; Agustin, 2010). Under physiological conditions in the brain Glut1 provides the necessary glucose required by neurons to function and indeed glucose is the main energy source of the central nervous system (CNS). In human red blood cells Glut1 plays an important role as demonstrated by the fact that it is the only Glut isoform present and by the fact that it comprises 10-20 % of the integral membrane protein content. Competitive inhibition studies

of the substrate specificity of the Glut1 transporter have shown that hydroxyl (OH) groups at C1 and C3 of d-glucose serve as hydrogen bond acceptors when d-glucose is seated in the Glut1 sugar uptake site (heilig et al., 2003; Carruthers et al 2009; Wang et al., 2017). In skeletal muscle Glut1 expression is usually higher in young mice (4 weeks) and decrease in older mice (22 and 44 weeks). This higher expression of Glut1 in early developmental stages has been explained as a mechanism to ensure insulin-independent glucose transport to sustain the high energetic demands required during the early stages of life (Dos Santos et al. 2012).

Glu1-deficient mice present different metabolic and non-metabolic related effects. Heterozygous and homozygouss Glut1-deficient mice exhibited a 50 and 95 % reduction of the glucose uptake rate, respectively, with the homozygous genotype being lethal for mice during gestation. Developmental problems were also noted in these mice, including intrauterine growth retardation, caudal regression, anencephaly with absence of the head, microphthalmia, micrognathia, and reduced body weight (embryos, ~30 % reduction in body weight). These developmental problems have been related to hyperglycemia of maternal diabetes (where glucose uptake is reduced and apoptosis is activated) caused by the exclusion of Glut1 during the embryonic period (Heilig et al., 2003).

Glut4

Glucose transporter 4, has molecular weight of 50 KDa and belongs to the 13 sugar transporter proteins responsible for importing glucose into the cells through a facilitated diffusion (ATP-independent) mechanism (Leney and Tavare, 2009). This transporter is almost exclusively expressed in skeletal and cardiac muscles (Kraegen et al., 1993) and brown and white adipose tissue, where it is responsible for most of the insulin-stimulated glucose uptake. The affinity of Glut4 for glucose is similar to that of (K_m~5mM) and it is inhibited by

cytochalasin B (IC50 = 0.2 µM), Phloretin (IC50 = 10 µM), and phlorizin (IC50 = 140 µM) (Leney and Tavare, 2009; Agusting, 2010).

In non-stimulated muscle fibres Glut4 is mostly stored in distinct intracellular compartments as Golgi complex, trans-Golgi network, lysosomes, late endosomes and recycling endosomes (Ralston and Ploug, 1996; Leney and Tavare, 2009) and just 5 % of this protein is present on the sarcolemma, but once the signal from insulin (though AKT) or muscle contraction (through AMPK) induces Glut4 activation, around 50 % of the total Glut4 is translocated onto the sarcolemma. Defects of this translocation system together with defects in insulin secretion and cell insulin recognition system result in a disruption of the whole organism's metabolism, giving rise to type 2 diabetes mellitus (Zisman et al., 2000; Leney and Tavare, 2009).

Heterozygous Glut4 knockout mice show yperglycemia and hyperinsulinemia associated with reduced muscle glucose uptake, hypertension and morphological alterations of the heart and liver. Fifty percent of the mice develop diabetes by the age of 6 moths (Stenbit et al., 1997). Glut4 tissue-specific expression is apparently interconnected with the metabolic response of other tissues. Indeed, muscle-specific Glut4 deficiency in mice leads to a lower insulin response of adipose tissue and liver (Zisman et al., 2000); adipose-tissue specific Glut4 depletion in mice leads to muscle and liver insulin resistance (Abel et al., 2001); moreover, the phenotype from muscle-specific Glut4 deficient mice with glucose intolerance and diabetes can be rescued by selective overexpression of Glut4 in the adipose tissue of these mice (Carvalho et al., 2005; Huang and Czech, 2007).

1.4.4 Skeletal muscle glycogen.

As all cells, skeletal muscles need ATP to sustain muscle contraction, and ATP is not stored and becomes rapidly depleted in less than a second of intense exercise (Hultman and

Greenhaff, 1991), therefore other pathways leading to ATP production need to be activated. Glucose is an important molecule in muscle metabolism providing ATP through two different pathways, anaerobic and aerobic. After a meal under resting conditions an organism stores the ingested carbohydrates in the kidney (10 %), liver (25-35 %) and muscle (40 %) as glycogen. This stored glycogen acts as a stored energy source allowing the muscle to respond rapidly to any environmental signal when glucose is not available, making this tissue an important player for whole body metabolism (Argilés et al., 2016). Glycogen is a branched polymer of glucose presenting also small amounts of glucosamine. The branches can reach a size of 10-44 nm and accumulate up to 55.000 glucose residues. Glycogen synthesis (glycogenesis) is coordinated by several enzymes, and a schematic diagram of this mechanism is shown in figure 1.9; firstly glucose enters the cells through the glucose transporter and becomes phosphorylated to glucose 6-phosphate by hexokinase isoenzymes; next, phosphoglucomutase-1 isomerize glucose 6-phosphate to produce glucose 1-phosphate; at this point, uridine 5′-diphosphate (UDP)-glucose pyrophosphorylase catalyzes the formation of UDP-glucose from glucose 1-phosphate. The next step is the initial synthesis of glycogen by glycogenin, when this enzyme autoglycosylates and transports glucose from UDP-glucose to itself and forming a short linear chain of about 10–20 glucose moieties. The elongation of this small glycogen sequence is performed by glycogen synthase, which transfers a glycosyl moiety from UDP-glucose to the growing glycogen strand, providing the α-1,4-glycosidic linkages between glucose residues. The last part is completed by the glycogen branching enzyme, creating α-1,6 glycosidic bonds at regular intervals that allow the introduction of branch points in the glycogen particle (Adeva-Andany et al., 2016; Röder et al., 2016).

Glycogen breakdown (glycogenolysis) principally takes place in the cytoplasm (and to a lesser extent in lysosomes). In the cytoplasm, glycogen phosphorylase releases glucose 1-phosphate by untangling the α-1,4-glycosidic linkages, and secondly glycogen debranching

enzymes unfasten the branch points releasing free glucose; a scheme of this mechanism is shown in figure 1.9. In lysosomes, glycogen is degraded to glucose by the enzyme acid α-1,4-glucosidase, hydrolyzing the 1,4-linked α-glucose polymers of the glycogen (Adeva-Andany et al., 2016).

Glycogenolysis is tightly regulated by different hormones, insulin, epinephrine and glucagon. Epinephrine (also known as adrenaline) is released from the adrenal medulla during physical activity (muscle contraction) or its anticipation and induces glycogen breakdown in muscle and to a lesser extent in liver (Chasiotis, 1983). On the other hand, the polypeptide hormone glucagon is secreted by the α cells of the pancreas when the blood-sugar levels are low and, similarly to epinephrine also induces glycogen breakdown (Röder et al., 2016). When insulin is released to the blood stream, this hormone stimulates the translocation of Glut4 to the membrane, increasing the glucose uptake into the muscle and activating glycogen synthase, which promotes glycogen synthesis (Halse et al., 2005).

The ECC machinery that allows muscle contraction largely depends on the energy obtained from ATP hydrolysis. The ATP stores in skeletal muscle are relatively small (~8 mmol/kg wet weight of muscle). Therefore the muscle relies on an ATP generation mechanism, which is based on complex store and energy sources such as glycogen (glucose) and triacylglycerols (Baker et al., 2010). Glucose oxidation occurs in the cytosol and continues under aerobic conditions in the mitochondria, producing 36 molecules of ATP for each molecule of oxidized glucose. On the other hand, the anaerobic cytoplasmic pathway only produces 2 molecules of ATP per molecule of glucose, but the rate at which ATP is produced is much faster than that occurring in mitochondria through the Kreb's cycle. During low intensity aerobic exercise, carbohydrate oxidation accounts for 10–15% of total energy production (Holloszy et al., 1998; Jensen and Richter 2012); the majority of this glucose originates from glucose uptake

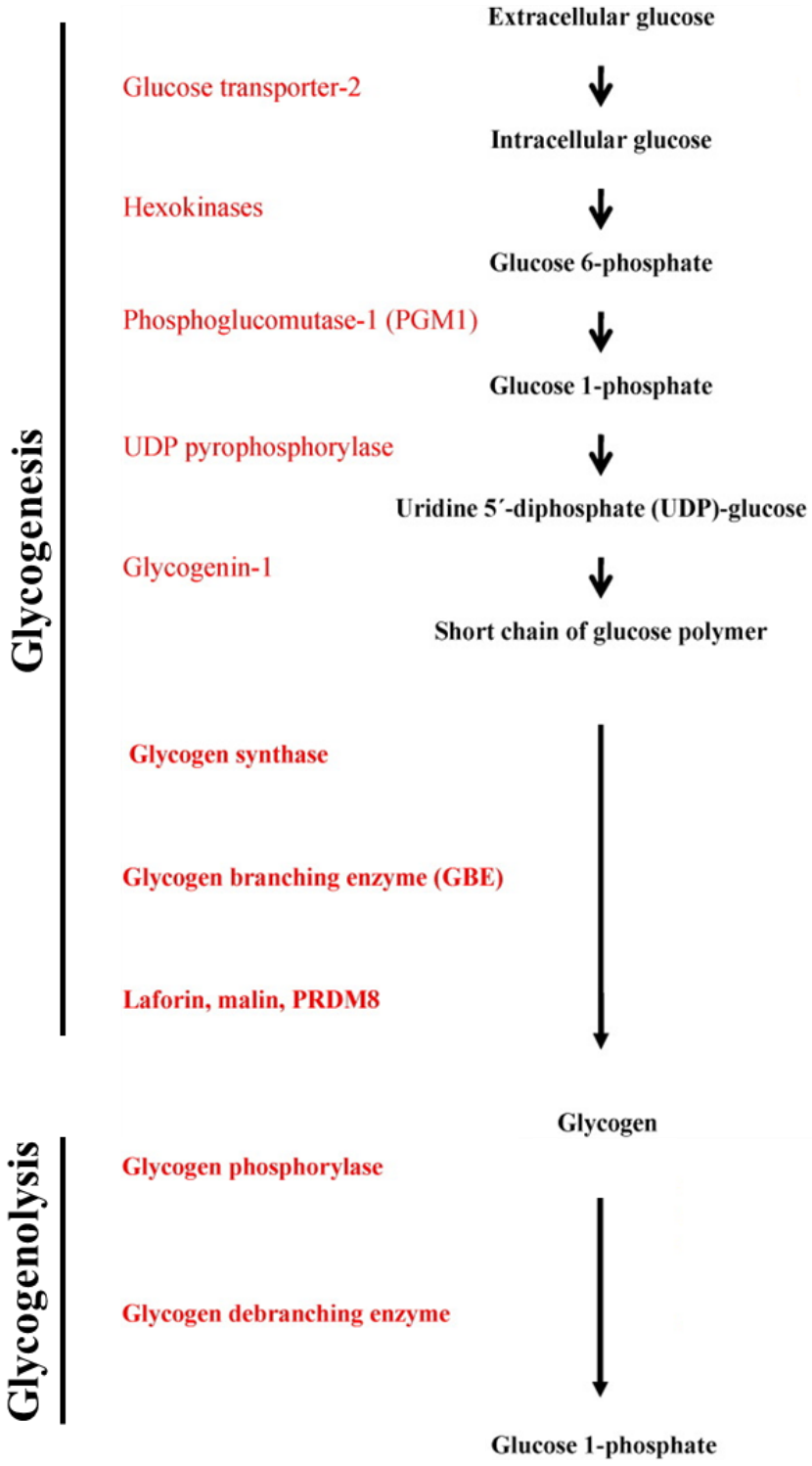

Figure 1.9 Glycogen synthesis (glycogenesis) and Glycogen degradation (glycogenolysis) models. Overview of the participial enzymes and the products involved in the glycogenesis and glycogenolysis, which take place in the cytoplasm (image modified from Adeva-Andany et al., 2016).

(plasma glucose) and only a small portion from glycogen stores. But during higher exercise intensity carbohydrate oxidation accounts for 70-80 % of total energy production and glycogen-breakdown becomes the predominant glucose source (Jensen and Richter 2012). For this reason high carbohydrate-diets are often used by elite athletes during training to increase muscle glycogen levels and increase the muscle's fatigue resistance (Jensen and Richter 2012). Another important mechanism that produces ATP is the phosphagen system. During low intensity exercise the majority of ATP is generated by the conversion of phosphocreatine, protons (H^+) and ADP to ATP and creatine. This reaction is catalyzed by creatine kinase and induces a slightly alkalinization of the muscle due to the H^+ consumption. On the other hand, during high intensity exercise the stores of phosphorcreatine decrease and the production of ATP by phosphagen system is reduced rapidly. For instance, after 10 seconds of maximal exercise the phosphocreatine stores are depleted and almost all the ATP generation is comes from glycolysis. This means that the limiting step of phosphagen is the concentration of phosphocreatinine in the muscle (Baker et al., 2010).

1.4 Mammalian target of rapamycin (mTOR).

Mammalian target of rapamycin (mTOR) is a 289 kDa serine/threonine kinase that is the target of the immunosuppressant drug rapamycin. This kinase belongs to the phosphoinositide 3-kinase (PI3K)-related kinase family and is key component of the cell survival pathways that regulates cell growth and proliferation through monitoring the availability of nutrients, mitogenic signals, cellular energy and oxygen levels (Zarogoulidis et al., 2014). Disturbances of the mTOR signaling pathway have been associated with a variety of human diseases including diabetes, neurodegeneration and cancer. mTOR inhibitor (initially rapamycin and more recently rapamycin analogs) have been used to treat different

pathological cases as solid tumors, organ transplantation, coronary restenosis and rheumatoid arthritis (Zarogoulidis et al., 2014; Kim et al., 2017). Molecular analysis of the anti-proliferative and cytostatic effect of rapamycin showed that this drug blocks some but not all mTOR activities. More detailed investigations have revealed that mTOR acts in two functionally distinct multiprotein complexes (Sarbassov et al., 2004; Kim et al., 2012): mTOR complex 1 and 2 (mTORC1 and mTORC2, respectively). mTORC1 is characterized by the presence of a regulatory associated protein of mTOR called Raptor and Proline Rich AKT Substrate of 40 kDa (PRAS40), but also shares some proteins with mTORC2 such as mTOR, mammalian Lethal with Sec13 protein 8 (mLST8) and DEP-domain-containing mTOR-interacting protein (Deptor). mTORC2 is recognized by the presence of Mammalian lethal with Sec13 protein 8 (mSin1) and Rapamycin insensitive companion of mTOR (Rictor) as show in the figure 1.10 (Laplante and Sabatini 2009).

1.4.1 mTORC1

The principal characteristic of mTORC1 is that it is rapamycin sensitive. Rapamycin binds to FK506-binding protein of 12 kDa (FKBP12) and interacts with the FKBP12 rapamycin binding domain (FRB) of mTOR, blocking it. Each component of the mTORC1 macromolecular complex presents a different role in the activity of this complex, contributing to substrate specificity, subcellular localization and complex specific regulation; mTOR, is the central catalytic component; mLST8 works as scaffolding protein; DEPTOR is important for mTOR complex assembly and stability; Raptor is a scaffolding protein important in the assembly, stability, substrate specificity and regulation; and PRAS40, is a factor that blocks mTORC1 activity until growth factor receptor signaling relieves the inhibition, figure 1.10 shows a scheme of the composition of the mTORC1 complex (Kim et al., 2017). mTORC1 is

affiliated with the endosomal and lysosomal membranes, where it interacts with its effectors 4E-binding protein 1 and S6 kinase 1 (S6K1) (Laplante and Sabatini., 2009)

mTORC1 signaling

The study of mTORC1 signaling has been a complicated task due to the multiples pathways related to this protein complex (see figure 1.10). The most common first step leading to its stimulation is the activation of PI3K in response to growth factor signaling. This leads to the increase in production of the second messenger phosphatidylinositol (3,4,5)-triphosphate (PIP3), directly activating Protein kinase B (AKT) by phosphorylating residue Thr308 and indirectly by PDK1 (Laplante and Sabatini., 2009).

AKT has two strong effects on mTORC1, the first is the phosphorylation of PRAS40 (mTORC1 inhibitor) causing PRAS40 to dissociate from Raptor and allowing mTORC1 activation; the second is indirect, by phosphorylating tuberous sclerosis complex 2 (TSC2), which brakes the TSC1-TSC2 complex, a negative regulator of the mTORC1 activator RHEB, (see figure 1.10). An additional similar pathway that induces the activation of mTORC1 involves Ras/Raf/MEK/ERK and RSK proteins. Where ERK and RSK proteins also phosphorylate TSC2 and PRAS40 proteins, breaking their inhibitory effects on mTORC1, which is an effect similar to that of AKT on mTORC1. On the other hand when the ATP/AMP ratio in the cell is low (meaning low cell energy), AMPK is activated and indirectly inhibits mTORC1 activity, by promoting TSC1/2 complex formation, as show in Figure 1.10 (Inoki et al., 2003; Kim et al. 2017). Downstream changes accompanying mTORC1activation include the phosphorylation of different substrates, such as eukaryotic translation initiation factor 4E-binding protein 1 (4EBP1) and ribosomal protein S6 kinase 1 (S6K1), which increases cell size and proliferation (Dowling et al., 2010).

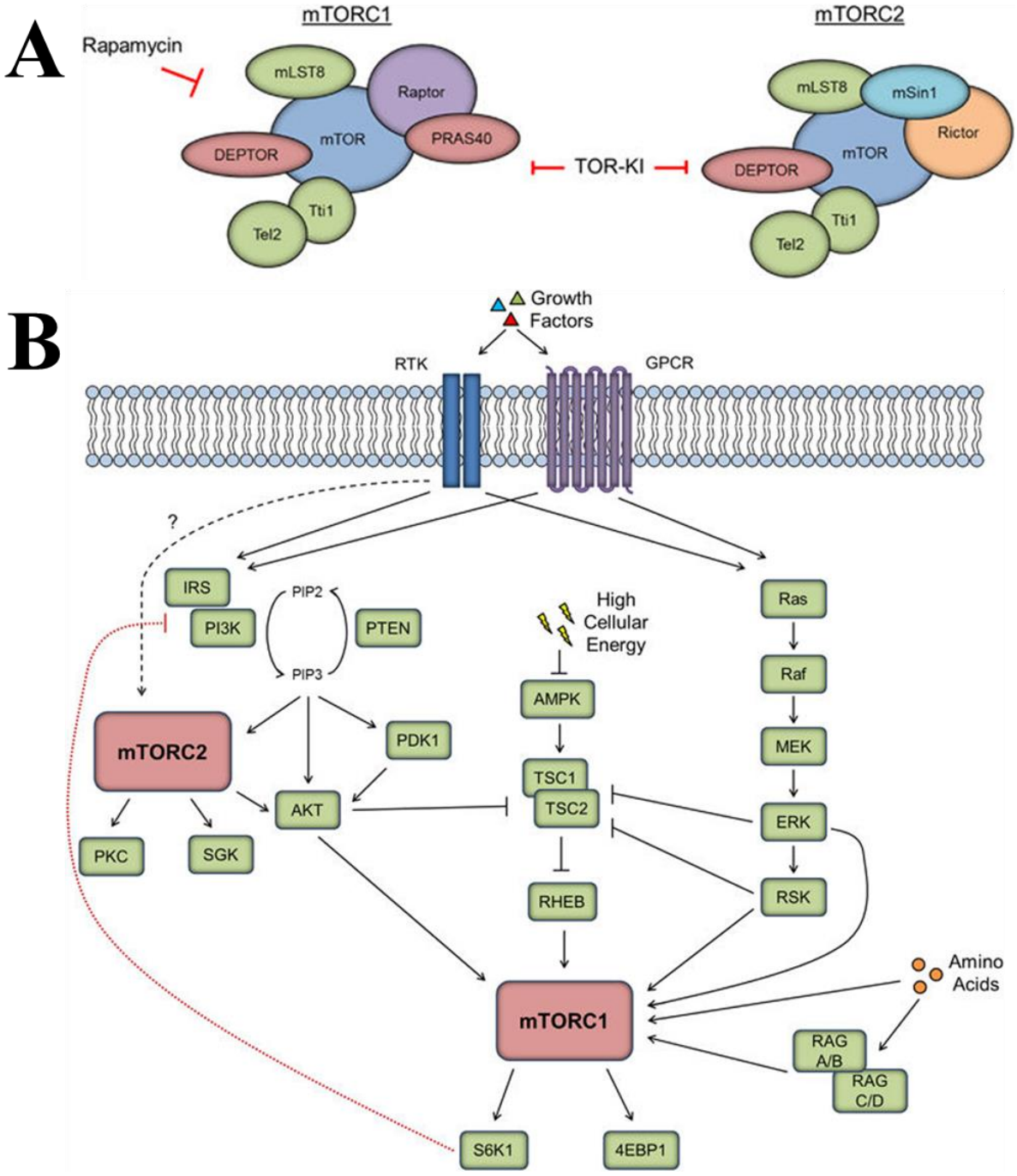

Figure 1.10 Composition and signaling pathways of mTORC1 and mTORC2. A) Schematic representation of mTOR1 and mTORC1 complexes with their protein components. **B)** Overview of the mTORC1 and mTORC2 signaling pathway, showing the most important proteins and molecules involved in the activation and inhibition of these two complexes (image modified from Kim et al., 2017).

translation initiation factor 4E-binding protein 1 (4EBP1) and ribosomal protein S6 kinase 1 (S6K1), which increases cell size and proliferation (Dowling et al., 2010).

1.4.2 mTORC2

One of the principal characteristics of mTORC2 is its insensitivity to the effect of rapamycin..In mTORC1 FKBP12 inhibits mTOR in the FKBP12-rapamycin complex binding domain, but in mTORC2 FKBP12 cannot interact physically most probabll because Rictor blocks the FKBP12-rapamycin complex binding site in mTOR (Jacinto et al., 2004; Sarbassov et al., 2004). Aside the three proteins (mTOR, mLST8, Deptor) that mTORC2 shares with mTORC1, mTORC2 also contains Rictor, which is important in the assembly, stability, substrate identification and subcellular localization of this complex to the appropriate sites of action. Furthermore, mSin1, is also part of the mTORC2 complex and is necessary for the subcellular localization of mTORC2 to the plasma membrane as shown in figure 1.10 (Kim et al., 2017). mTORC2 was found to be associated with the plasma membrane and ribosomal membranes, where it interacts with its key substrates, the AGC kinases including AKT1-3, serum glucose kinase (SGK) isoforms and protein kinase C (PKC) family members (Sarbassov et al. 2005; Zinzalla et al. 2014).

mTORC2 signaling

Even though cofactors such as insulin and IGF-1 are able to activate mTORC1 and mTORC2, the difference in protein composition of the two complexes can induce completely different responses but studies aimed at elucidating the biological role of mTORC2 have been complicated by the fact that there are no specific pharmacological inhibitors for mTORC2. Because of this, genetically modified animals have been created, such as muscle-specific

rictor knockout mice, to determine the role of mTORC2 in skeletal muscle function (Bentzinger et al 2008; Sarbassov et al. 2004).

mTORC2 is activated by growth factor and ribosome association (Sarbassov et al. 2004; Zinzalla et al., 2011). The second messenger PIP3, which is produced by PI3K, recruits and activates mTORC2 (figure 1.10 presents a schematic representation of mTORC2 pathway). At this point mTORC2 is located close to the cell membrane in close proximity to its three substrates, AKT, SGK, and PKC. mTORC2 is the only complex that phosphorylates AKT at serine 473 under physiological conditions (Vadlakonda et al. 2013) and recent studies show that a positive feedback loop between mTORC2 and AKT ser473 exist. AKT phosphorylates mSin1 at T86 enhancing mTORC2 kinase activity and mTORC2 phosphorylates AKT ser473, catalyzing the full activation of AKT. The physiological consequences of AKT activation are very broad, including effects on metabolism, cell growth, proliferation, cell survival and motility (Yang et al 2015; Kim et al., 2017). SGK activation by mTORC2 induces the activation of NDRG1 and FoxO family transcription factors. These two factors are able to promote cell survival signals in response of oxygen or nutrient deprivation (Bakker et al 2007). On the other hand, the effect of PKC activation by mTORC2 is still not very clear. It is known that PKC is involved in different cellular functions as proliferation, apoptosis, differentiation, motility, and inflammation, but the responses induced by activation or overexpression of PKC highly depending on the types of cell and and physiological conditions (Nakashima et al., 2002; Kim et al., 2017).

1.5 Retinoic acid and Vitamin A

For the production of retinoic acid, vertebrates including humans, need to consume vitamin A (retinol) with the diet (it is present in plant carotenoids and to a lesser extent in meat), since they are unable to synthesize this vitamin. Deficiency of this vitamin in newborns causes

neonatal growth retardation and different congenital malformation (vitamin A deficiency syndrome), and importantly retinol and its derivatives (retinoids) play an important role in spermatogenesis, fertilization, pregnancy maintenance, morphogenesis, organogenesis and general fetal and perinatal growth. In adults, retinol and retinoids regulate a wide spectrum of physiological processes involved in maintaining the proper functions of skin, lung, bone marrow, liver, and neuronal system and are also associated with regulation of reproduction, immunity, vision and metabolism (Zhang et al., 2015). atRA has been also shown to work as a potent therapeutic compound in multiples diseases due to its anti-proliferative, anti-oxidative, pro-apoptotic, and differentiation-inducing effects (Persaud et al., 2016). For instance, pharmacological administration of vitamin A (or retinoids) has shown important results in the treatment of acne and myelocytic leukemia. Acne is a consequence of abnormalities in the proliferation, adhesion and differentiation of keratinocytes, which no longer separate from each other, and obstruct the sebaceous duct located in the infrainfundibulum. Retinoids (all-trans-retinoic acid, atRA and 13-cis-retinoic acid) act against acne inducing the differentiation and proliferation of keratinocytes. Furthermore these vitamin A derivatives are able to regulate the activity of the adhesion molecules that ensure the normal cohesion of keratinocytes (Chivot, 2005). On the other hand, retinoids (especially atRA) have been very useful to induce differentiation of blast cells in patients with myelocytic leukemia. Using differentiation markers (cell surface myeloid antigens CD11b, CD15, CD14, and CD33) to monitor blast differentiation Sartorelly`s group (Rise et al., 2004) observed that atRA is able to produce changes in at least one surface antigen differentiation marker in 89% of patient blasts. In presence of lithium chloride atRA was able to induce the differentiation of leukemic blasts in up to 94% of patients. These myelocytic leukemia progenitors cells exposed to atRA in vitro or during clinical treatment continued their differentiation program into neutrophils which eventually resulted in their senesce (Rise et al., 2004; Su et al., 2015).

1.5.1 Vitamin A signaling

Once ingested, vitamin A is taken up by the intestinal epithelial cells in the small intestine and is stored in the liver or sent through the blood circulation to different tissues. The retinols bind to retinol-binding proteins (RBP) and such complexes interact with the RBP receptor (STRA6), which is specifically expressed on target cells. Once inside the cell, the retinol can be used to produce retinyl esters such as palmitate or be hydrolyzed by alcohol dehydrogenases (ADHs) to

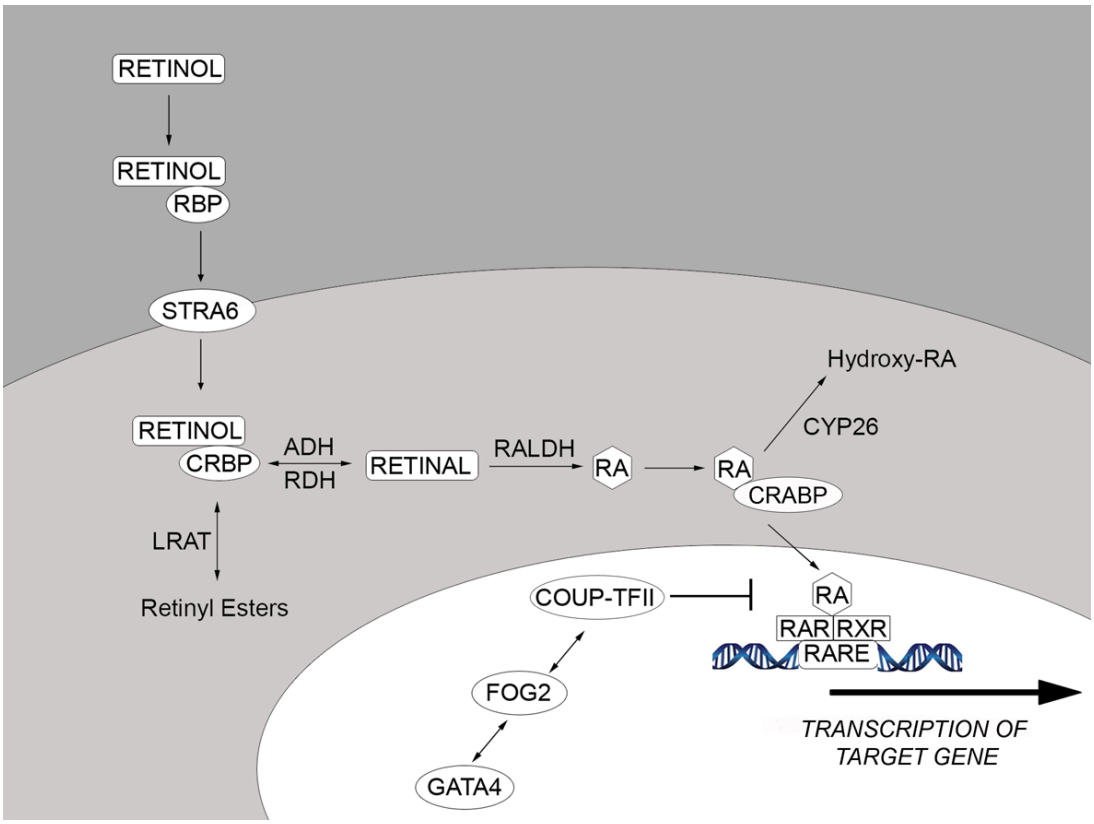

Figure 1.11. Retinol (vitamin A) pathway. Retinol enters the cell through STRA6 and is converted to RA (atRA) by different enzymes, to be subsequently transported into the nucleus and interact with RAR, inducing the transcription of several target genes (Carretero et al 2013).

retinaldehyde (retinal) in a reversible way, as shown in figure 1.11. The formation of retinoic acid (RA) represents the irreversible step, taking place when retinaldehyde dehydrogenases (RALDHs) hydrolyzes retinal to RA. Depending on the cell's energy levels, the RA can bind to the RA-binding protein 1 (CRBPI) and be targeted for degradation or it could bind to CRABPII and be transported into the nucleus where it interact with the Retinoic Acid Receptors (RAR), a family of ligand-dependent regulators of transcription. There are three separate RAR genes encoding nuclear receptor, RARα, RARβ and RARγ, which will be discussed in more detail in section 1.6.1. RARs can heterodimerize with retinoic X receptors (RXR), inducing the transcription of different RA target genes connected to cell growth, differentiation, development, and tissue homeostasis (Huang et al. 2014; Larange and Cheroutre, 2016).

The effect of RA on organisms is still a dynamic topic, with classical experiments showing that in some cells atRA interacts with the RAR and induces the expression of genes involved in apoptosis, cell growth inhibition, cell cycle arrest and anti-carcinogenic activities in different tissues and cancer cells (Altucci et al., 2001; Donato and Noy, 2005; Schug et al., 2007). But contradictorily results have been obtained by other groups showing that atRA can promote cell proliferation..atRA is critical for neuronal survival, induces skin tumor formation and stimulates dermal repair by causing the expression of target genes related to mitogenisis and antiapoptotic responses (Verma et al., 1982; Jacobs et al., 2006; Schug et al, 2007). These opposite effects have been explained by the participation of two different proteins, cellular RA-binding protein II (CRABP-II) and fatty acid-binding protein 5 (FABP5). Depending on the CRABP-II/FABP5 ratio, RA will bind to CRBP-II (when the ratio is high) or to FABP5 (when the ratio is low). Once atRA binds to CRBP-II this is mobilized to the nucleus where it interacts with the RAR (as explained in the section above); on the other hand

when RA binds to FABP5, it is mobilized to the nucleus, and associates with peroxisome proliferation-activated receptor β/δ (PPARβ/δ) (Schug et al, 2007; Berry, and Noy, 2009).

1.6 Genomic effects of atRA. RAR and RXR.

Retinoic Acid Receptors and Retinoic X Receptors, are ligand-transcription factors that can function as heterodimers, regulating gene networks involved with different physiological functions, including cell proliferation, differentiation, senescence and apoptosis. RAR-RXR is an important heterodimer that control multiple physiological phenomena through the modulation of transcriptionof different gene; additionally each nuclear receptor (RAR and RXR) can respond in a specific manner to specific physiological conditions. For instance, RXR is able to form heterodimers with a large number of nuclear receptor family members (PPARs, LXRs, PXR, VDR, TR), activating multiple cellular pathways in response to RXR-selective ligands (Le Maire et al,. 2012).

1.6.1 Retinoic acid receptor.

RA and its isomer 9-cis RA bind to RARs, regulating the expression of over 500 genes. In the absence of ligands RAR actively repress transcription by establishing a co-repressor (CoR) complex with HDACs, and other repressive factors (Le Maire et al., 2012). RAR is present in 3 different isoforms, RARα, RARβ, and RARγ and each of these receptors is encoded by genes located on different chromosomes that use different promoters giving rise to alternatively spliced variants following a spatial and temporal specific pattern during embryonic development and adulthood (Dollé et al., 1989, Theodosiou et al., 2010).

RARα represent a ubiquitously expressed receptor and RARα null mice show decreased viability, growth deficiency, male infertility and congenital malformations that could be reversed by RA treatment (Mark et al., 2009; Theodosiou et al., 2010). During mouse

embryogenesis RARβ is specifically distributed in tracheobronchi, lungs, the genital tract and intestinal epithelial cells (Dollé et al., 1989; Desaia et al., 2006) and during adulthood in the brain (Krezel et al 1999). RARβ null mice present locomotor defects and selective loss of striosomal compartmentalization in the rostral striatum. The RARγ is also tissue specific and is found in skeletal muscle. RARγ null mice present growth deficiency, early lethality and male sterility (similar effects observed in vitamin A deficient mice), and the phenotype could be rescued with RA treatment (Lohnes et al., 1993).

Metabolic related effects of RAR have been shown when adult mice overexpressing a dominant-negative RARα mutant that induces a hypomorphic RAR in β cells caused a decrease of β cell mass and glucose-stimulated insulin secretion. These results indicate that RARs is also involved in maintaining the function and mass of pancreatic β cells (Brun et al., 2015). RAR have also been connected with the regulation of RA-inhibited adipocyte differentiation by controlling adipogenesis-related gene expression. RAR can also induce the activation of uncoupling protein 1 (Ucp1) and hormone lipase (Hsl), genes involved in energy expenditure (Berry and Noy. 2009) and such as Gck and insulin-like growth factor-binding protein 1 (Igfbp1) (Scribner et al 2007).

1.6.2 Retinoic X receptor

RXR are unable to interact directly with RA, but as mentioned above, can complex with RAR and also have a high affinity for 9-cis RA. RXR produce homodimers and heterodimers with RXR and other nuclear receptors (NR), respectively and their transcriptional activation depends highly on the nature of their partner. In the case of RAR/RXR heterodimers the ligand-bound RXR is not active until RAR interact with its ligand.

The RXR, RXRβ and RXRγ are three different isoform of RXR. They are encoded by different genes and are also expressed in specific patterns during development. RXRα and RXRβ are amply distributed for example in the eye, cardiac muscle, liver, epidermis, prostate gland, etc.. While RXRγ is highly tissue specific, mainly expressed in skeletal muscle and to a lower extent in sensory epithelia of visual and auditory systems and in the central nervous system. RXRα/RAR, and the different combinations of RXRα/RARα, RXRα/RARβ, and RXRα/RARγ heterodimers are involved in developmental processes. Studies with mutant RXRs genes indicate a critical role of these heterodimers since mutant mice embryos die in mid-gestation due to congenital heart, metabolic and behavioral defects (Krezel et al., 1996). Tissue specific conditional knockout mice show that RXRα plays an essential role in multiple pathways including glutathione homeostasis and detoxification of xenobiotics, regenerative capacity of hepatocytes, proliferation and differentiation of epidermal keratinocytes, and development of prostatic intraepithelial neoplasia (Li et al 2000; Wu et al., 2004; Chan und Wells, 2009). Fifty percent of the RXR β knockout mice (RXRβ-/-) mice die before or at birth. The other 50 % that survive showed physiological deficiencies including sterility of male mice due to oligo-astheno-teratozoospermia. The sertoli cells of these surviving mice presented a progressive accumulation of lipids (triglycerides) indicainge the interaction of RXRβ with the peroxisomal proliferator-activated receptor signaling pathway (Kastner et al 1996; Krezel et al., 1996). Lastly, RXRϒ knockout mice were indistinguishable from their wild-type littermates with respect to growth, fertility, viability and behavior (Krezel et al., 1996).

1.6.3 Non genomic effects of atRA.

The genomic effect of steroid hormones occurs after a time lag of several hours, altering target gene expression for an extended period of time. On the other hand, non-genomic steroid

actions occur much faster, with a duration of minutes to seconds, and affecting multiple signaling pathways (Persaud et al., 2016).

The role of atRA in the regulation of gene transcription is well known but in recent years a different kind of RA effect has been observed. RA has been associated with extranuclear-related and non-transcriptional dependent activities, that transiently activate several kinase cascades (Tanoury et al 2013). In different cell types such as fibroblast, mammary breast and leukemia cells, atRA activates the p38 mitogen-activated kinase (p38MAP). In myeloid leukemia and breast cancer cell lines atRA is able to activate protein kinase C δ (Zhang et al., 2015) and in other cells types such as neuronal, Sertoli and embryonic stem cells, RA triggers the activation of p42/p44 extracellular signal-regulated kinases (Erk) and finally activation of MAPKs proteins (Cheung et al., 2009; Lösel and Wehling, 2003; Zhang et al., 2015).

Non genomic effect mechanism.

Even if there is strong evidence for the non-genomic effects of atRA on different cell types, the intracellular signaling pathway of this molecule is poorly understood. Different experiments exposed two main pathways, through RARs or cellular retinoic acid binding protein 1 (CRABP1) (Tanoury et al., 2013; Persaud et al., 2016). The atRA non-genomic effect through RARs activation acts in different ways depending of the cell type and RARs involved (see figure 1.12). Firstly, RA activates Gαq protein in fibroblasts, embryo carcinoma cells, mammary breast tumor cells, and leukemia cells, inducing the activation of downstream proteins such as GTPases, p38 mitogen-activated protein kinase (p38MAPK) and Mitogen- and stress-activated kinase 1 (MSK1), as shown in figure 1.12. The activation of MSK1 triggers the phosphorylation of CREB and Histone H3, which regulate a specific subset of immediate early genes (Bruck et al., 2009; Reyskens and Arthur 2016). On the other hand in Sertoli cells and embryonic stem cells treated with atRA activation of p42/p44 extracellular

signal-regulated kinases (Erks) has been observed. Possible upstream activators, of these signaling pathways include the Src-family protein kinases/RARγ or phosphoinositide 3-kinase (PI3K)/protein kinase B (PKB/AKT) (Figure 1.12) (Masia et al., 2007; Tanoury et al., 2013). Additionally experimental results also demonstrate that retinol directly activates Signal transducer and activator of transcription 5 (STAT5) by association with Retinol-binding protein (RBP) through the activation of Janus kinases (JAK), see figure 1.12 (Berry et al., 2011; Tanoury et al., 2013).

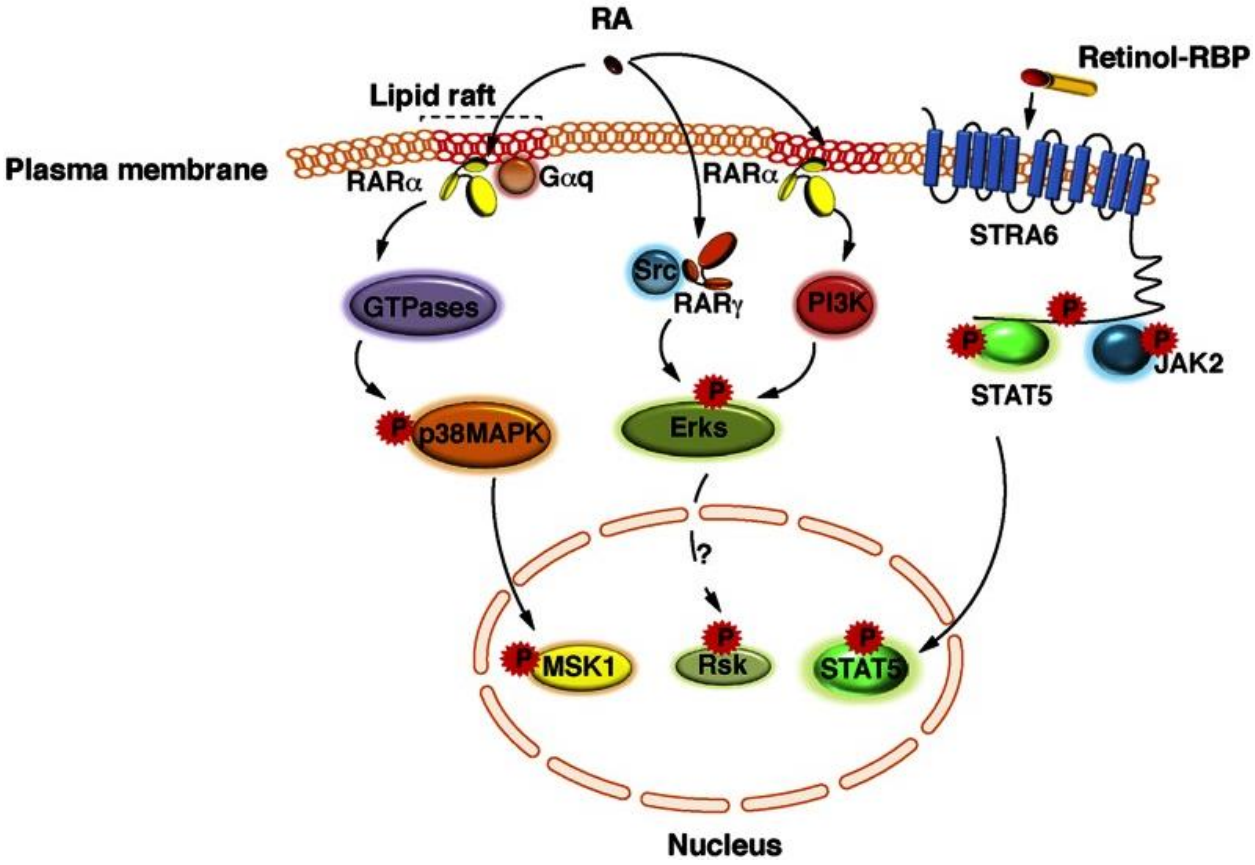

Figure 1.12. Extranuclear and non-transcriptional effects of RA and retinol. RAR and retinol activating transitorily RARα, RARϒ and Retinol-RBP, inducing the activation of MSK1, Rsk and STAT5 downstream proteins of these signaling pathways (image from Tanoury et al., 2013).

Another recently proposed mechanism in which atRA acts through a non-genomic effect is based on the activation of cellular retinoic acid binding protein 1 (CRABP1), in an RAR-independent manner (Persaud et al., 2016). This pathway implicates the activation of the extracellular signal regulated kinase 1/2 (ERK1/2) in embryonic stem cells (ESC), in a manner similar to non-genomic RAR. Activation of ERK1/2, triggers the activation of protein phosphatase 2A (PP2A) regulating cell cycle progression and induction of apoptosis. This (CRABP1) pathway represents an important target since it is independent of RAR activation. Treatment of cancer patients with atRA has resulted in negative toxici side effect, which are mainly attributed to retinoids' canonical, genomic actions through binding to RARs. Additional negative effects of this pharmacological treatment of cancer patients, is that at therapeutic doses atRA loses efficacy due to the development of RA resistance (RAR related). For these reasons it is important to find new drugs that specifically bind to Crabp1 to elicit activity mimicking atRA's non-genomic (RAR-independent) activity (Persaud et al., 2016).

CHAPTER 2- RESULTS

2.1. Publication

Scientific Reports volume 8, Article number: 636 (2018). doi:10.1038/s41598-017-18844-3

Over-expression of a retinol dehydrogenase (SRP35/DHRS7C) in skeletal muscle activates mTORC2, enhances glucose metabolism and muscle performance.

[1]Alexis Ruiz, [2]Erez Dror, [3]Christoph Handschin [3]Regula Furrer, [3]Joaquin Perez-Schindler, [1]Christoph Bachmann, [1,4#]Susan Treves and [1,4*]Francesco Zorzato

[1]Departments of Anesthesia and of Biomedicine, Basel University Hospital, Hebelstrasse 20, 4031 Basel, Switzerland; [2]Max Planck Institute of Immunobiology and Epigenetics, 79108 Freiburg, Germany; [3]Biozentrum, University of Basel, CH-4056 Basel, Switzerland; [4]Department of Life Sciences, General Pathology section, University of Ferrara, Via Borsari 46, 44100 Ferrara, Italy. (

Running Title: *SRP35TG mice reveal novel non-genomic effects of retinoic acid in skeletal muscle*

*Corresponding Author: zor@unife.it, fzorzato@uhbs.ch

ABSTRACT:

SRP-35 is a short-chain dehydrogenase/reductase belonging to the DHRS7C dehydrogenase/ reductase family 7. Here we show that its over-expression in mouse skeletal muscles induces enhanced muscle performance *in vivo*, which is not related to alterations in excitation-contraction coupling but rather linked to enhanced glucose metabolism. Over-expression of SRP-35 causes increased phosphorylation of AKT_{S473}, triggering plasmalemmal targeting of GLUT4 and higher glucose uptake into muscles. SRP-35 signaling involves RARα and RARγ (non-genomic effect), PI3K and mTORC2. We also demonstrate that all-trans retinoic acid, a downstream product of the enzymatic activity of SRP-35, mimics the effect of SRP-35 in skeletal muscle, inducing a synergistic effect with insulin on AKT_{s473} phosphorylation. These results indicate that SRP-35 affects skeletal muscle metabolism and may represent an important target for the treatment of metabolic diseases.

Key Words: SRP-35, glucose, metabolism, retinoic acid, mTORC2, AKT phosphorylation, skeletal muscle.

INTRODUCTION

Skeletal muscle is the largest body organ comprising approximately 40% of total body weight under normal conditions, it is important not only important for movement and posture but also for metabolism and thermogenesis (1, 2). Furthermore, skeletal muscle adapts to different environmental conditions and load requirements by modifying its fiber type composition and glycolytic or oxidative characteristics (3, 4). Muscle fiber type composition is determined mainly by the expression of specific myosin heavy chain isoforms: MyHC I in slow fibres, MyHC type IIa in fast oxidative fibres and MyHC IIx/b in fast glycolytic fibres (4, 5). The differences in contractile properties between slow and fast fibers also depends on the higher density of sarco/endoplasmic reticulum Ca^{2+}-ATPase (SERCA), expression of Ca^{2+}- binding proteins such as parvalbumin, calsequestrin 1 and calsequestrin 2, and a higher mitochondrial content in slow type I fibers compared to fast type II fibers (4, 6, 7).

Skeletal muscle is responsible for 70-75 % of the insulin stimulated glucose uptake (8); part of the energy obtained from glucose is used to fuel muscles and the remaining is stored as glycogen (9). Two glucose transporters are expressed in skeletal muscle: GLUT4 and GLUT1 which are insulin-sensitive and insulin-insensitive, respectively (10-12). Insulin receptor stimulation activates a number of downstream signaling proteins including phosphoinositide 3-kinase (PI3K) and protein kinase B (PKB or AKT) which induce GLUT4 translocation to the plasma membrane where it facilitates blood glucose clearance and glucose uptake into muscles (9, 13).

In the past years our laboratory has discovered novel proteins of the skeletal muscle sarcoplasmic reticulum (SR) (14). One such protein we identified at the molecular level is SRP-35, a 35 kDa membrane bound protein enriched in sarcotubular membranes. The NH_2-terminus of SRP35 encompasses a short hydrophobic sequence associated to SR membranes, whereas its C-terminal domain faces the myoplasm. Sequence comparison and functional *in*

vitro experiments established that SRP-35 is a short-chain dehydrogenase/ reductase belonging to the DHRS7C [dehydrogenase/reductase (short-chain dehydrogenase/reductase family) member 7C] subfamily (15, 16), using retinol (Vit. A) as its substrate and leading to the formation of *all*-trans-retinaldehyde (17). The latter is the substrate for an irreversible oxidative reaction generating *all*- trans retinoic acid (atRA). Retinoic acid (RA) acts as a ligand for nuclear receptors of the RAR and RXR family, mediating the transcriptional effect of RA on genes involved in tissue development and cell differentiation (18). Recent studies have also revealed that atRA influences cell metabolism (19, 20), by modulating, the (i) phosphorylation state of AMPK and AKT (21) and (ii) rate of glucose uptake by L6 myotubes (22).

Because of the important metabolic role of RA, we generated a transgenic mouse line overexpressing SRP-35 in skeletal muscle. Our results show that these transgenic mice (SRP35TG) exhibit enhanced running capacity, enhanced glucose uptake leading to larger glycogen stores. Furthermore, the presence of the transgene induces a stronger activation of PI3K and of mammalian target of rapamycin complex 2 (mTORC2) signaling pathways, triggering the phosphorylation of AKT_{S473} which account for GLUT4 translocation onto the plasma membrane. The metabolic changes observed in SRP35TG mice could be mimicked by treating skeletal muscles of wild type mice with atRA.

RESULTS

Impact of SRP-35 over-expression on the expression of SR ECC proteins and on muscle function

We generated TG mice encoding mouse SRP-35 under the skeletal muscle specific creatine kinase promoter (Supplementary Figure 1A). The presence of the transgene was confirmed by polymerase chain reaction (PCR) (Supplementary Figure 1B), Coomassie Blue staining on a total SR extract of skeletal muscle from WT and SRP35TG mice (Supplementary Fig.1C asterisk) and Western blotting. We obtained three mouse lines expressing the TG to different extents: line 4, 5 and 6 over-expressing SRP-35 by 28%, 61 % and 23%, respectively (Supplementary Fig. 1D). In this study, we performed most of the experiments on muscles from line 5 and their respective wild-type (WT) littermates but similar results were obtained on the other TG lines. We first investigated *in vivo* and *in vitro* muscle function using the voluntary running wheel and electrically stimulated force generation, respectively. Figure 1 shows that after 21 days young (7 months, Fig.1A left panel) and old (14 months, Fig. 1A right panel) SRP35TG male mice (closed circles) ran approximately 50 Km more (n=16 $p<0.001$, Mann Whitney test) compared to their age matched WT littermates (Fig. 1A, open circles). The higher running capacity of the SRP35TG mice between day 15 and day 20 is also paralleled by a remarkable increase in the number of 10 s high speed events (>2.5 km/hr) occurring during the dark phase (Fig. 1B). The enhanced running capacity is not linked to changes in fiber type composition since we found an equal distribution of MyHC I and MyHC II positive fibers in *extensor digitorum longus* (EDL) and soleus muscles in WT and SRP35TG mice (Fig. 1C). However, over-expression of SRP-35 caused a small (10%) but significant ($p<0.05$ Student's *t* test) increase of the minimal Feret's diameter of MyHC type I and MyHC type II fibers (Fig. 1D and Fig1 E) in soleus. The mechanical properties of WT and SRP35TG mice are similar (Fig. 1F and Supplementary Table 1) indicating that the

enhanced running is not due to a gain of function of the excitation-contraction coupling (ECC) mechanism. This conclusion is also consistent with the absence of changes in the content of RyR1, $Ca_v1.1$ and calsequestrin, the main proteins constituting the ECC macromolecular complex (Fig. 1G). On the other hand, SRP-35 over-expression was accompanied by a significant reduction of the ER(SR) calcium binding protein calreticulin ($n=6$, $p<0.01$, Student's t test) and of the β1a subunit of the dihydropyridine receptor ($n=6$ $p<0.01$, Student's *t* test). SRP35TG muscles also display a 40% increase of glycogen phosphorylase content (GP; Fig. 1G; $n=6$ $p<0.01$, Student's t test), a key enzyme involved in glucose metabolism activation during muscle contraction (23). Because of this increase of glycogen phosphorylase we hypothesized that the enhanced running capacity was the result of an effect on glucose metabolism.

SRP35TG mice show enhanced glucose metabolism.

In vivo glucose clearance was performed by the intraperitoneal glucose tolerance test (ipGTT) in young and old (7 and 16 months old, respectively) mice. Both age groups of SRP35TG mice showed a two-fold reduction in serum glucose levels 60 min after the glucose challenge compared to their WT littermates (Fig. 2A; $n=8$ $p<0.05$, Student's *t* test). Additionally, there was a significant difference in glucose clearing kinetics between young and old WT mice at 90 and 120 min. Interestingly in SRP35TG mice the glucose clearance curves of young and old mice were similar, with no delay in clearance, suggesting a protective effect of SRP-35 over-expression in age-related glucose uptake processes (23). The enhanced glucose clearance was not related to altered levels of insulin release, as blood insulin levels were similar in WT and SRP35TG mice (Fig. 2B).

Skeletal muscles express two main types of glucose transporters, GLUT1 which is insulin insensitive and GLUT4 which is exocytosed onto the plasma membrane in response to insulin. GLUT1 expression levels in total muscle homogenates and in the R1 fraction

enriched in transverse tubules and plasma membrane (25), was similar in WT and SRP35TG mice (Supplementary Fig. 2A and 2B). On the other hand GLUT4 expression in SRP35TG mice was approximately 50% higher (n=7 $p<0.01$, Student's *t* test) compared to WT littermates (Fig. 2C). The total amount of GLUT4 in the total muscle homogenates from both EDL and soleus was unchanged (Fig. 2D), indicating that SRP35TG mice constitutively activate or activate more efficiently the signal(s) responsible for GLUT4 translocation onto the plasma membrane and that the increased membrane expression of GLUT4 is not caused by enhanced synthesis of this transporter.

The increased running capacity of SRP35TG mice may thus be related to the enhanced capacity of their skeletal muscles to remove circulating glucose and store it. We verified this directly (i) by monitoring the capacity of isolated muscles to take up glucose and (ii) by monitoring muscle glycogen stores. EDL and soleus muscles were assessed for their capacity to take up 2-deoxy-D-glucose-[^{3}H]) by three different protocols, namely (i) no stimulation, (ii) after challenge with insulin (100 nM for 10 min), and (iii) by a train of action potentials delivered at 80 Hz for 5 min (Fig 3A). Under basal conditions, 2-DG-[^{3}H] uptake in muscles from SRP35TG (7 months old) male mice was significantly increased compared to WT littermates (Fig. 3A n=8; $p<0.05$ Student's *t* test). This difference in glucose uptake was further increased either by insulin treatment or electrical stimulation. Insulin promoted more glucose uptake by EDL and soleus muscles of SRP35TG mice (Fig.3A filled bars n=6; $p<0.05$ Student's *t* test) compared to WT littermates (Fig. 3A, empty bars). Muscles from SRP3TG mice accumulated more 2DG-[^{3}H] compared to those from WT littermates also after electrical field stimulation (Fig. 3A n=6; $p<0.05$ unpaired *t* test). Altogether our data demonstrates that both fast and slow muscles isolated from SRP35TG mice show significant higher glucose uptake compared to WT littermates, and that the highest increase in glucose uptake was observed after insulin stimulation. Glucose taken up by muscles is stored as glycogen, a

glucose polymer acting as a readily available energy store for muscle activity. Thus the higher glucose uptake by SRP35TG muscles should result in larger glycogen stores and this was directly verified by assessing glycogen content by an enzyme coupled assay. Figure 3 B shows that the glycogen content in muscles from 7 months old SRP35TG male mice was around 30 % higher compared to that in WT littermates (n= 6; $p<0.05$ Student's *t* test). Since muscle glycogen content is an important factor determining the respiratory exchange rate (RER), we also assessed basic metabolism using a CLAMS apparatus. Fig. 3C shows cumulative RER of WT (empty circles) and SRP35TG (filled circles) littermates. Each data point represents the average of RER from 7 months old male mice and shows a high degree of variability. There were no significant differences in the RER during the dark phase. However, 10 out 23 RER data points of the light phase acquired on the last day of measurements were significantly increased in SRP35TG mice compared to WT (n= 8; $p<0.05$ Student's t test). These events likely result from an increase of voluntary motor activity because we observed a parallel significant increase of the infrared beam breaks data points (Fig. 3D).

Overexpression of SRP-35 affects AKT and AMPK phosphorylation

GLUT4 membrane translocation and glucose uptake in skeletal muscle result from the activation of two major pathways, namely AKT and AMP-activated protein kinase (AMPK). AKT activation is linked to the stimulation of the insulin receptor, while AMPK activation may occur via multiple mechanisms, including muscle contraction (26). To assess the involvement of these signaling pathways we performed quantitative western blot analysis and determined the degree of phosphorylation of AKT (Ser473 and Thr308) and AMPK (Thr172) in total muscle homogenates. Our results show that in muscles from SRP35TG and WT (7 months old) male mice the absolute content of AKT and AMPK in EDL and soleus at rest, after electrical stimulation or after the addition of insulin are similar (Fig. 4). Under resting conditions in soleus muscles the level of phosphorylation of $AMPK_{Thr172}$ was similar in

SRP35TG and WT littermates (Fig. 4A and Fig. 4B), whereas EDLs from SRP35TG show a significant increase (n=6; $p<0.05$, Student's t test) of $AMPK_{T172}$ phosphorylation compared to WT littermates (Fig. 4A and 4B). Upon delivery of a repetitive train of action potentials the phosphorylation level of $AMPK_{T172}$ in EDL from SRP35TG mice was further increased from resting levels by 49.3% (Fig. 4C and Fig. 4D, $p<0.05$ Student's t test), whereas in soleus the increase was not statistically significant (Fig. 4C and Fig. 4D). As to the phosphorylation level of AKT, we found different effects concerning Thr 308 and Ser 473, namely overexpression of SRP-35 only increases the phosphorylation of Ser 473 in both EDL and soleus (results for AKT_{t308} are not shown). Under resting conditions we observed an increase of the AKT_{S473} phosphorylation level in EDL and in soleus, respectively (286.1±132% and 251±137%, mean ±S.D., n=7, $p<0.05$, Student's t test; Fig. 4A and Fig. 4B). Insulin caused a further increase of the resting phosphorylation level of AKT_{S473} in EDL and soleus muscles by 58 and 40%, respectively (n=7, $p<0.05$, Student's t test Fig. 4E and Fig. 4F).

atRA causes AKT_{S473} phosphorylation

Although the exact mechanism by which SRP-35 affects AKT phosphorylation is not know, it might be due to the formation of RA resulting from the oxidation of *all*-trans-retinaldehyde, the precursor of RA generated by the up-regulation of the SRP-35 dehydrogenase activity (17) in muscles of SRP35TG mice. We tested this by assessing whether the phosphorylation of AKT_{S473} could be mimicked by treatment of muscles from WT mice with pharmacological concentrations of atRA (27). Treatment of intact EDL and soleus muscles for 30 and 60 min with 10 μM atRA alone did not cause significant changes in the total amount of AKT and AMPK protein content (see Supplementary Fig. 2C) and had no effect on the phosphorylation status of AKT_{S473}, AKT_{T308}, and $AMPK_{T172}$ (Fig. 5A and Fig. 5C). However, atRA may synergize with activators of the AKT and AMPK signaling pathways (28). Indeed incubation of intact EDL and soleus muscles with atRA in the presence of insulin significantly stimulates

the phosphorylation of AKT_{S473} by 166.6±24% and 173.6±44%, respectively (mean±S.D., n=6, $p<0.05$, Student's *t* test). This increase occurred after 30 min and subsequently declined to control values by 60 min. The effect of atRA in the presence of insulin was specific for AKT_{S473} since we did not observed an increase in the phosphorylation of either AKT_{T308} or $AMPK_{T172}$ (Fig. 5B and Fig. 5D). The fast time course of atRA-induced AKT_{S473} is consistent with a non-genomic action and this was further investigated by testing the effect of Retinoic acid Receptor (RaR) RARα, RARβ and RARγ inhibitors on AKT_{S473} phosphorylation. Fig. 5E and Fig. 5F show that phosphorylation of AKT_{S473} induced by atRA in the presence of insulin was abolished by RARα and RARγ inhibitors and was insensitive to the RARβ inhibitor

atRA stimulation of AKT phosphorylation is mediated by mTOR complex 2

The higher extent of phosphorylation of AKT_{S473} in SRP35TG mice and the *in vitro* experiments with atRA may result from the activation of the Rictor/mTORC2 complex (29-31). In order to verify this we performed control experiments on muscles isolated from muscle specific Rictor knock-out (RImKO) mice (32), a mouse model exhibiting down-regulation of the mTORC2. EDL and soleus muscles from (3 months old) male RImKO mice were treated with 100 nM insulin in the presence or absence of 10 μM atRA. Under these conditions the RImKO mice failed to show significant changes in AKT_{S473} phosphorylation (Fig.6 A and Fig. 6B). This effect is specific since under identical experimental conditions phosphorylation of AKT_{S473} occurred in EDL and soleus muscles from WT littermates.

PIP_3 content in total muscle homogenates from WT and SRP35TG mice.

The data obtained with RImKO mice demonstrate that atRA synergizes with physiological activators in triggering the enzymatic activity of mTORC2. PIP_3, a product of the PI3K signaling pathway, is a physiological activator of the kinase activity of mTORC2 (33, 34). We

next measured PIP_3 content in EDL and soleus muscles from SRP35TG and WT mice. Fig. 6C and 6D shows that both EDL soleus muscles from (4 months old) male SRP35TG mice have a significant increase of PIP_3 content ($p<0.05$, Mann-Whitney test). The intracellular level of atRA is influenced by the content of Vitamin A in the diet and a reduction of Vitamin A from 14 to 4 IU/g in the mouse chow was reported to induce a decrease in atRA content in various mouse tissues (35). We assume that at any given intracellular retinol concentration the muscle fibres over-expressing SRP-35 would generate greater amounts of *all*-trans-retinaldehyde the precursor of the irreversible oxidation reaction leading to atRA formation. Thus one would expect that if mice were fed a low Vitamin A diet, the SRP35TG mice would generate more atRA compared to WT littermates and that the higher atRA levels would be associated with enhanced PI3K activity. We found that in (4 months old) male mice that had been fed for two generations with a low vitamin A (4 IU/g) diet, the PIP_3 content in EDL and soleus muscles from WT mice under resting conditions was below the detection limit of the method (EDL) or barely detectable (soleus), whereas in EDL muscles from SRP35TG littermates the level is approximately 10% of that measured in EDL muscles of mice fed a standard chow (Fig. 6C lower panel) and in soleus muscles the levels is approximately 70% of that measured in soleus muscles of mice fed a standard chow diet. The higher PI3K activity in muscles from SRP35TG kept on a low vitamin A diet should enhance mTORC2/AKT signaling which in turn may lead to higher glucose uptake and increased glycogen stores. If this were the case, one would expect better muscle performance. We tested this by investigating the *in vitro* resistance to fatigue by measuring the force developed after repeated stimulation of EDL (tetanic stimulation with a frequency of 70Hz, 300msec duration) and soleus muscles (tetanic stimulation with a frequency of 50Hz, 600msec duration) isolated from mice kept on a low vitamin A diet for two generations. In the presence of insulin, soleus muscles from SRP35TG showed a significant increase of about about 50% ($p< 0.05$, n= 5 WT and 5 SRP35TG) of the force remaining after tetanic stimulation (Fig. 6F). EDL muscles also

showed a significant resistance to fatigue, though the difference between WT and SRP35TG mice was not as pronounced (Fig. 6E) The resistance to fatigue is likely due, at least in part, by the size of the glycine stores. Indeed, after the fatigue protocol the glycogen content of EDL (Fig. 6G) and soleus (Fig. 6H) muscles from SRP35TG mice kept on a low vitamin A diet was significantly higher than that of muscles from WT mice kept on a low vitamin A diet. It should also be pointed out that the glycogen stores in EDL and soleus muscles were smaller after the fatigue protocol compared to the glycogen stores present in unstimulated muscles (compare Fig.3B to Fig. 6G and H)).

DISCUSSION

The present study demonstrates that the skeletal muscle protein SRP-35, a retinol dehydrogenase, is directly involved in skeletal muscle metabolism, since its over-expression results in higher glucose uptake and increased glycogen storage. In addition, SRP-35 over-expression improves muscle performance *in vivo*, an effect which occurs in the absence of changes in the ECC machinery. We also provide compelling evidence as to the mechanism by which SRP-35 leads to the increased glucose uptake in skeletal muscle. In particular we show that SRP35TG mice have an up-regulation of the signaling pathway involving AKT_{S473} phosphorylation via activation of mTORC2. Pharmacological application of atRA to intact muscles from WT mice mimics the stimulation of AKT_{S473} phosphorylation observed in SRP35TG muscles, while inhibitors of the RARα and RARγ nuclear receptors inhibit AKT_{S473} phosphorylation in WT muscle treated with pharmacological concentrations of atRA. On the basis of these results we believe that AKT_{S473} phosphorylation in skeletal muscles of SRP35TG mice is linked to the enzymatic activity of SRP-35 which produces locally within the muscle, *all*-trans-retinaldehyde, the precursor of the irreversible oxidation reaction leading to atRA formation. Altogether these data support a role for retinoic acid as the biological mediator of the metabolic response responsible for the enhanced muscle function of SRP35TG mice. Figure 7 shows a schematic representation based on the results of the present investigation, of the cellular pathways involving SRP-35 and retinoic acid metabolism in skeletal muscle.

Overexpression of SRP-35 and atRA increase AKT_{S473} phosphorylation.

Activation of AKT is due to phosphorylation of Thr308 and Ser473 by phosphinositide-dependent protein kinase 1 (PDK1) and mTORC2, respectively (29, 31, 36). Overexpression of SRP-35 in skeletal muscle selectively increases the phosphorylation of the mTORC2-

dependent AKT phosphorylation site AKT_{S473} and this occurred both in isolated EDL and soleus muscles from SRP35TG in the presence and absence of insulin. This implies that: (i) chronic over-expression of SRP35 in skeletal muscle increases the basal AKT_{S473} phosphorylation level, and (ii) the atRA generated by the irreversible oxidation *all*-trans-retinaldehyde, acts as a co-activator of the insulin signaling pathway leading to AKT_{S473} phosphorylation. This conclusion is also supported by a separate set of data showing that atRA mimics the effect of SRP-35 overexpression. Indeed, treatment of EDL muscles from WT mice with pharmacological concentrations of atRA enhanced insulin-induced AKT_{S473} phosphorylation levels. At variance with what was observed in EDL muscles isolated from SRP35TG mice however, incubation of EDL from WT mice with atRA in the absence of insulin did not result in AKT_{S473} phosphorylation. Our results differ from those showing that in a variety of cells types including A549, F9 and HL-60 cells, atRA alone is able to induce AKT phosphorylation (37-39). These apparent discrepancies may be due to: (i) different experimental models, cofactors and proteins present in the cell culture medium (40); (ii) the lack in the EDL from WT mice of the adaptive changes induced by SRP-35 over-expression leading to an alteration of the atRA level within a subdomain of the muscle fibre. Nevertheless the present study demonstrates that atRA plays a newly identified role in the modulation of cellular functions downstream AKT_{S473} phosphorylation, including glucose metabolism.

SRP-35 and atRA activate mTORC2 signaling

Under physiological conditions mTORC2 is the major kinase responsible for the phosphorylation of AKT_{S473} (29). In the presence of DNA damage AKT can also be phosphorylated at Ser473 by DNA-dependent protein kinase (DNA-PK) (41). Skeletal muscle fibres from SRP35TG mice do not show evidence of nuclear damage (not shown) and thus we exclude the possibility that AKT_{S473} phosphorylation is mediated by DNA-PK. In fact our

results on RImKO mice strongly support the participation of mTORC2 in the SRP-35/atRA signaling pathway. In the present study we show that atRA is unable to reverse the inhibitory effect of Rictor ablation on the phosphorylation levels of AKT_{S47} in insulin stimulated skeletal muscles (32). This result provides unambiguous evidence that mTORC2 activation is a key component of SRP-35/atRA signaling.

atRA: an enhancer of insulin signaling.

atRA acts as an enhancer of insulin signaling since it enhances AKT_{S473} phosphorylation beyond that caused by the activation of the insulin receptor. The latter is coupled to the stimulation of PI3K activity which in turn leads to an increase of PIP_3 on the plasma membrane, a crucial step for the recruitment of AKT onto the plasma membrane where it is phosphorylated by PDK1 and mTORC2. AKT phosphorylation mediates the metabolic effects of insulin, leading to the translocation of GLUT4 onto the plasma membrane and stimulating glucose uptake. Both atRA and SRP-35 over-expression synergize with insulin on the insulin dependent AKT_{S473} phosphorylation. The RA resulting from the oxidation of *all*-trans-retinaldehyde, the precursor of retinoic acid generated by the up-regulation of the SRP-35 dehydrogenase activity could synergize with insulin at different steps of the insulin signaling pathway. The data presented in this study provides insight as to one such possible mechanism. In particular, we found that: (i) skeletal muscles from SRP35TG mice have a 14 fold increase of the PIP_3 content and (ii) manipulation of the myoplasmic concentration of atRA with a low Vitamin A diet affects the PIP_3 content of skeletal muscle. Previous work has shown that inhibitors of RAR nuclear receptors down-regulate PI3K activity, the enzyme responsible for the synthesis of PIP_3. On the basis of these data and on our own results demonstrating that the AKT_{S473} phosphorylation is prevented by RARα and RARγ inhibitors, we believe that the increase of PIP_3 content in skeletal muscle from SRP35TG results from a non-genomic effect of atRA on PI3K activity (42, 43). Accumulation of PIP_3 in skeletal muscle membranes

results in the recruitment and activation of mTORC2 kinase leading to the phosphorylation of AKT_{S473}.

SRP-35 improves muscle performance by increasing glucose uptake and glycogen store.

Over-expression of SRP-35 in skeletal muscle leads to a remarkable improvement of the *in vivo* muscle performance, both in young and old (7 and 14 months old, respectively) mice. This effect could be due to a (i) gain of function of the ECC mechanism, (ii) fast to slow fibre-type switching, (iii) adaptive metabolic changes, or (iv) a combination of two or more of these mechanisms. Our results exclude the first possibility because we did not observe changes of the mechanical properties of EDL and soleus muscles. Additionally, the enhanced muscle performance is not linked to changes in the fibre type composition because there was no evidence of fibre type switching in either EDL or soleus. Both type I and type II fibres is soleus muscle from SRP35TG mice undergo a 10 % increase of the minima Ferret's diameter. The increase of AKT_{S473} phosphorylation may account for this small hypertrophy (44) of soleus muscles in SRP35TG mice and this is also consistent with the enhanced running capacity (45). Nevertheless, such a modest hypertrophy cannot fully account for the enhanced running capacity observed in SRP35TG mice. In fact our results indicate that the enhanced muscle performance is linked to glucose metabolism. Under basal conditions, skeletal muscles from SRP35TG mice display a specific increment in GLUT4 translocation onto the sarcolemma and T tubules and this is accompanied by higher glucose uptake even in the absence of insulin. Expression and activation of GLUT4 depends on a variety of stimuli, including RA. Indeed treatment of the L6 muscle cell lines with atRA enhanced insulin-stimulated glucose uptake and increased GLUT4 expression to plasma membrane (22). Activation of the insulin receptor stimulates PI3K activity which ultimately leads to GLUT4 translocation onto plasma membrane by the activation of two parallel signaling cascades: AKT phosphorylation and Rho-family small GTPase Rac1. Our results show that in

SRP35TG mice the increased plasma membrane GLUT4 is linked to an increase of AKT_{S473} phosphorylation. The latter in turn leads to larger glycogen stores in skeletal muscle. This adaptive mechanism in SRP35TG mice is accompanied by an increase in glycogen phosphorylase (GP), the enzyme initiating the breakdown of glycogen to glucose-1-phosphate during prolonged skeletal muscle activity (7). We are confident that the longer running distance observed in SRP35TG mice is explained by the mechanism described above.

Altogether, our results unravel a novel aspect of RA signaling in skeletal muscle and raise the possibility that SRP-35 maybe targeted to affect glucose metabolism in patients with metabolic disorders.

METHODS

SRP-35 transgenic mice- The transgenic mouse line (generated in the Transgenic Animal Facility of Basel University) was constructed by inserting the mouse SRP-35 cDNA downstream the muscle specific creatine kinase promoter to target expression to skeletal muscle. Supplementary figure 1 shows a schematic representation of the construct used to create the SRP-35 over-expressing mice (SRP35TG) and a representative PCR analysis of the genomic DNA from several mouse lines generated after pronuclear injection. Mice were genotyped by PCR using genomic DNA, the following primers: 5`- GTAGCTTTTCCTGTCAATTCTGCC-3`(forward) and 5`- GAGCCCCATGGTGAAGCTT- 3`(reverse) and conditions: GoTaq G2 DNA polymerase (Promega; Madison, USA) and the following amplification protocol, 1 cycle at 95°C for 5 min followed by 38 cycles of annealing (62°C for 30 s), extension (72°C for 30 s) and denaturation (95°C for 30 s), followed by a 7 min extension cycle at 72°C. A total of three SRP35TG mouse lines expressing the transgene to different levels were obtained. Since mouse line N°5 expressed the highest SRP-35 TG levels, the experiments described in this paper were carried out on this line and confirmed in the other two lines.

mTORC2 KO (RImKO) mice: 3 months old male muscle-specific rictor knockout mice (RImKO) were obtained from Prof. M. Rüegg`s and Prof. M. Hall's laboratories (31).

Special diet- WT and SRP35TG mice were fed a Low Vitamin A Diet (LVAD; 4 UI/g; Scientific Animal food and Engineering) for 2 generations. The mice of the second generation were sacrificed at 4 months of age (35).

In vivo and in vitro assessment of muscle function- *In vivo* muscle function was assessed using the voluntary running wheel on 7 and 14 months old male mice as previously described (46). For *in vitro* assessment of muscle function, force measurements were assessed using a force transducer (MyoTonic, Heidelberg), and by measuring the force generated in response to different protocols including a single twitch (15 V pulses for 0.5 ms duration) and tetanic

frequency pulses (50, 100 and 150 Hz) in soleus (slow muscle) and (50, 100 and 200 Hz) in *extensor digitorum longus* (EDL, fast muscle). Resistance of muscle to fatigue was also measured in EDL and Soleus muscles isolated from WT and SRP35TG mice kept for 2 generations on a low Vitamin A diet; muscles were incubated in Krebs Ringer containing 100 nM insulin, and stimulated electrically using a fatigue protocol (EDL: 300 ms duration, 70 Hz and 0.33 Hz of time between stimulus (tbs); Soleus, 600 ms duration, 50 Hz frequency and 0.33 Hz of tbs) as described (Johansson et al. 2003).

Basic metabolic rate- The metabolic rate of WT and TG (7 months old) male mice was assessed by indirect calorimetry using a Comprehensive Lab Animal Monitoring System (Oxymax/CLAMS; Columbus Instruments, Columbus, OH, USA). Following an initial 48 h acclimatization, mice were monitored every 17 min for 24 h for a complete 12 h active (dark) and 12 h inactive (light) cycle. Oxygen consumption (VO_2), CO_2 production (VCO_2), physical activity, heat production and respiratory exchange ratio (RER = $V^{\cdot}CO_2$ /VO_2) were measured during 72 hours.

Histological examination, changes in muscle fiber type and glycogen content- Calculation of the minimal Feret's diameter, the closest possible distance between the two parallel tangents of an object, was determined as described (46). Images were obtained using an Olympus IX series microscope and analyzed using the CellP Software. The fiber type composition was assessed by determining the expression of different myosin heavy chain isoforms by high resolution gel electrophoresis followed by Coomassie Brilliant blue gel staining as described (47, 48).

Glycogen content was assessed enzymatically on snap frozen EDL and soleus muscles using a hexokinase-dependent, kit according to the manufacturer's instructions (GAHK-20, Sigma-Aldrich; USA). A control to measure free glucose levels in the muscle (not related to glycogen stores), was also performed.

Gel electrophoresis and western blotting- Total homogenates, sarcoplasmic reticulum (SR) and skeletal muscle subcellular fractions longitudinal sarcoplasmic reticulum (LSR) and terminal cisternae (TC), were prepared as described (25). Protein concentration was determined using a kit from BioRad (Bio-Rad, 500-0006) using bovine serum albumin as standard; proteins were separated on SDS-PAG gels, transferred onto nitrocellulose membranes and probed with commercially available antibodies. Immunopositive bands were visualized by chemiluminescence.

Signaling pathways involved in glucose uptake: AKT and AMPK phosphorylation- Isolated soleus muscles from 28 weeks old mice were used to determine the levels of AKT and AMPK phosphorylation. Muscles were homogenized in lysis buffer (10% Glycerol, 5% β-mercaptoethanol, 2.3 % SDS, 62.5 mM Tris-HCl pH 6.8 and 6 M urea, supplemented with 1 % phosphatase inhibitor cocktails 2 and 3 Sigma Aldrich) at a concentration of 10 mg of muscle/ml buffer. Subsequently, 50 µg of protein were separated on a 10% SDS PAG, transferred onto nitrocellulose (Amersham), and probed with the following primary antibodies: phospho-AMPK (Thr172), AMPK alpha, phospho- AKT (ser 473), phopho-Akt (thr 308) and AKT total from Cell Signaling and Desmin (used as housekeeping loading control) from Santa Cruz. The intensity of the immunopositive bands was determined using Image J.

Glucose Uptake- Glucose uptake by isolated EDL and soleus muscles was measured in isolated muscles incubated for 1h at room temperature in Krebs-Ringer buffer supplemented with 1 mM glucose, 10 mM sodium pyruvate and 0.5% bovine serum albumin. The medium was continuously gassed with 95% O_2 and 5% CO_2. For electrical stimulation, muscles were stimulated with a 300 ms train of action potentials of 0.5 ms duration at a frequency of 80 Hz by using a stimulator (Myotronic, Heidelberg Germany); the 300 ms trains of action potentials were delivered for a 5 min at a frequency of 0.27Hz. For insulin stimulation, muscles were

incubated in the presence or absence of insulin (100 nM; Novo Nordisk Pharma AG; Bagsværd, Denmark) for 10 min at room temperature. Contralateral non-stimulated muscles were used as controls. Stimulated or control muscles were then incubated with 0.375 µCi/ml Deoxy-D-glucose, 2-[1,2-^{3}H (N)] (2-[^{3}H]-DG (Perkin Elmer, Waltham, MA) for an additional 20 min at room temperature, flash frozen and stored in liquid nitrogen until ready for use. The amount of radioactive glucose taken up by the muscles was assessed by liquid scintillation counting, using a Packard 1900 TR liquid scintillation analyzer.

***Glucose and insulin tolerance tests*-** For the glucose tolerance test (GTT), following a 6 h fast and starting in the morning, mice were injected intraperitoneally with a glucose-containing solution (1 µg glucose/g of body weight). Glucose plasma levels were determined at different time points (0, 15, 30, 60 and 90 min) using a glucometer (Freestyle; Abbott Diabetes Care Inc., Alameda, CA; USA). Insulin plasma levels were determined at different time points (0, 15 and 30 min) using an insulin ELISA kit (Mercodia; Uppsala, Sweden) following the manufacturer's recommendations.

***Effect of all-trans-retinoic acid (atRA*)**-EDL and soleus muscles from 28 weeks old WT mice, were cleaned in a Ringer solution continuously gassed with 95% O_2 and 5% CO_2 at room temperature. The muscles were incubated in the presence or absence of 10 µM All-trans-retinoic acid (atRA, dissolved in DMSO; Sigma), control muscle were incubated with the vehicle DMSO. After 30 or 60 min of incubation, the muscles were washed and stored in liquid N_2. In some experiments insulin (100 nM) was also added to the muscles incubated with atRA and the controls. The muscles were homogenized; proteins separated by SDS/PAGE and transferred to a nitrocellulose membranes. Phosphorylation sites and total protein content of AMPK and AKT were analyzed. All experiments were performed under red light illumination.

Effect of Retinoic acid Receptor (RaR) inhibitors- EDL and soleus muscles isolated from WT mice were incubated in Ringer's solution containing one of 3 different RAR inhibitors (RARα, RARβ or RARγ inhibitors), 100 nM insulin and in presence or absence of 10 µM atRA. Muscles from the contralateral leg were taken as controls and incubated with the same RAR inhibitor as their counterpart muscles, together with100 nM insulin and DMSO. After a 30 min incubation with the RARα inhibitor Ro 41-5253 (50 nM; Sigma), RARβ inhibitor LE 135 (220 nM; Sigma) or RARϒ inhibitor Acacetin (30 uM; Sigma), insulin and atRA/DMSO, the muscles were flash frozen in liquid N_2 and subsequently analysed by western blotting for AKT and AMPK phosphorylation. All experiments were performed under red light illumination.

PIP_3 measurements- PIP_3 levels were measured in muscles of WT and SRP35TG mice fed a standard chow or a low vitamin A diet. Freshly isolated EDL muscles were flash frozen in liquid N_2 and ground using a pestle and mortar. Lipids were extracted from the powdered muscles and PIP_3 content was assessed as previously described (49) using the PIP_3 Mass ELISA kit (K-2500s, Echelon, USA).

Animal permits- All experiments were conducted according to the Swiss Veterinary Law and institutional guidelines and were approved by the Swiss authorities (Kantonal permits 1728 and 2115). All animals were housed in a temperature-controlled room with a 12 h light–12 h dark cycle and had free access to food and water.

Statistical analysis- Statistical analysis was performed using the software OriginPro 8.6.0 (OriginLab Corporation). Comparisons of two groups were performed using the Student's *t*-test, for groups of three or more comparisons were made using the ANOVA test followed by the Bonferroni post-hoc test unless otherwise stated. Means were considered statistically significant when P values were < 0.05. All figures were created using Adobe Photoshop CS6

or R Studio (version 0.99.891 or newer). For non- parametric results, the Man Whitney test was used.

Author Contributions Section:

A.R., C.B., E.D., F.Z., R.F. and S.T., performed the experiments.

C.B. drew Figure 7

A.R, F.Z. and S.T., analyzed the data and drafted the article.

C.H. and R.F. provided the CLAMS system.

A.R., C.H., J. P-S, F.Z and S.T., critically revised the manuscript.

F.Z. and S.T., supervised all the steps of the study.

Acknowledgements

This work was supported by funds from Swiss Muscle foundation, A.F.M. and the Department of Anesthesia of the Basel University Hospital. We would like to thank Prof. Markus Rüegg and Prof. Michael Hall for kindly providing the muscle-specific Rictor knockout mouse and Ms Anne-Sylvie Monnet for her expert technical assistance.

The authors declare no competing financial interests.

REFERENCES

1) Loiselle, D.S., Johnston, C.M., Han, J.C., Nielsen, P.M. & Taberner, A.J. Muscle heat: a window into the thermodynamics of a molecular machine. *Am. J. Physiol. Heart Circ. Physiol*. **310**, H311-H325 (2016).

2) Sopariwala, D.H., Pant, M., Shaikh, S.A., Goonasekera, S.A., Molkentin, J.D., Weisleder, N., Ma, J., Pan, Z. & Periasamy, M. Sarcolipin overexpression improves muscle energetics and reduces fatigue. *J. Appl. Physiol*. **118**, 1050-1058(1985).

3) Bottinelli, R. & Reggiani, C. Human skeletal muscle fibres: molecular and functional diversity. *Prog. Biophys. Mol. Biol*. **73**, 195–262 (2000).

4) Schiaffino, S. & Reggiani, C. Fiber types in mammalian skeletal muscles. *Physiol. Rev*. **91**, 1447-1531 (2011).

5) Calderón, J.C., Bolaños, P. & Caputo, C. Myosin heavy chain isoform composition and Ca^{2+} transients in fibres from enzymatically dissociated murine soleus and extensor digitorum longus muscles. J. Physiol. **588**, 267-279 (2010).

6) Chemello, F., Bean, C., Cancellara, P., Laveder, P., Reggiani, C. & Lanfranchi G. Microgenomic Analysis in Skeletal Muscle: Expression Signatures of Individual Fast and Slow Myofibers. *PLoS One* 6, e16807, doi: 10.1371/journal.pone.0016807 (2011).

7) Westerblad, H., Bruton, J. & Katz, ASkeletal muscle: energy metabolism, fiber types, fatigue and adaptability. *Exp Cell Res*. **316**, 3093-3099 (2010).

8) Zurlo, F., Larson, K., Bogardus, C. & Ravussin, E. Skeletal muscle metabolism is a major determinant of resting energy expenditure. *J. Clin. Invest*. **86**,1423–1427 (1990).

9) Jensen, J., Rustad, P., Kolnes, A.J. & Lai, Y.C. The role of skeletal muscle glycogen breakdown for regulation of insulin sensitivity by exercise. *Front. Physiol*. 2, 112. doi: 10.3389/fphys.2011.00112 (2011).

10) Douen, A.G., Ramlal, T., Rastogi, S., Bilan, P.J., Cartee, G.D., Vranic, M., Holloszy, J.O. & Klip, A. Exercise induces recruitment of the "insulin-responsive glucose transporter". Evidence for distinct intracellular insulin- and exercise-recruitable transporter pools in skeletal muscle. *J. Biol. Chem*. **265**, 13427-13430 (1990).

11) Mueckler, M. Insulin resistance and the disruption of GLUT4 trafficking in skeletal muscle. *J. Clin. Invest*. **107**, 1211-1213 (2001).

12) Hansen, P.A., Wang, W., Marshall, B.A., Holloszy, J.O. & Mueckler, M. Dissociation of GLUT4 translocation and insulin-stimulated glucose transport in transgenic mice overexpressing GLUT1 in skeletal muscle. *J. Biol. Chem*. **273**, 18173-18179 (1998).

13) Klip, A., Sun, Y., Chiu, T.T., Foley & K.P. Signal transduction meets vesicle traffic: the software and hardware of GLUT4 translocation. *Am. J. Physiol. Cell Physiol*. **306**, C879-C886 (2014).

14) Treves, S., Vukcevic, M., Maj, M., Thurnheer, R., Mosca, B. & Zorzato, F. Minor sarcoplasmic reticulum membrane components that modulate excitation-contraction coupling in striated muscles. *J. Physiol*. **587**, 3071-3079 (2009).

15) Duester, G. Involvement of alcohol dehydrogenase, short-chain dehydrogenase/reductase, aldehyde dehydrogenase, and cytochrome P450 in the control of retinoid signaling by activation of retinoic acid synthesis. *Biochemistry* **35**, 12221-12227 (1996).

16) Persson, B., Kallberg, Y., Bray, J.E., Bruford, E., Dellaporta, S. L., Favia, A.D., Duarte, R. G., Jörnvall, H., Kavanagh, K.L. & Kedishvili N. The SDR (short-chain

dehydrogenase/reductase and related enzymes) nomenclature initiative. *Chem. Biol. Interact*. **178**, 94–98 (2009).

17) Treves, S., Thurnheer, R., Mosca, B., Vukcevic, M., Bergamelli, L., Voltan, R., Oberhauser, V., Ronjat, M., Csernoch, L., Szentesi, P. & Zorzato, F. SRP-35, a newly identified protein of the skeletal muscle sarcoplasmic reticulum, is a retinol dehydrogenase. *Biochem. J*. **441**, 731-741 (2012).

18) Cunningham, T. & Duester, G. Mechanisms of retinoic acid signalling and its roles in organ and limb development. *Nat. Rev. Mol. Cell Biol*. **16**, 110-123 (2015).

19) Berry, D.C. & Noy, N. All-trans-retinoic acid represses obesity and insulin resistance by activating both peroxisome proliferation-activated receptor beta/delta and retinoic acid receptor. *Mol. Cell Biol*. **29**, 3286-3296 (2009).

20) Sugita, S., Kamei, K., Akaike, F., Suganami, T., Kanai, S., Hattori, M., Manabe, Y., Fujii, N., Takai-Igarashi, T., Tadaishi, M., Oka, J., Aburatani, H., Yamada, T., Katagiri, H., Kakehi, S., Tamura, Y., Kubo, H., Nishida, K., Miura, S., Ezaki, O. & Ogawa, Y. Increased Systemic Glucose Tolerance with Increased Muscle Glucose Uptake in Transgenic Mice Overexpressing RXRγ in Skeletal Muscle. *PLoS One*. 6, e20467, doi: 10.1371/journal.pone.0020467 (2011).

21) Lee,Y., Lee, J., Jung, J., Kim, J., Park, S., Park, J., Kim, E., Suh, P. & Kim, M.H. Retinoic acid leads to cytoskeletal rearrangement through AMPK-Rac1 and stimulates glucose uptake through AMPK-p38 MAPK in skeletal muscle cells. *J. Biol. Chem*. **283**, 33969-33974 (2008).

22) Sleeman, M., Zhou, H., Rogers, S., Wah, K. & Best, J. Retinoic acid stimulates glucose transporter expression in L6 muscle cells. *Molec. Cell Endocrinol*. **108**, 161-167 (1995).

23) Parolin, M., Chesley, A., Matsos, M., Spriet, L., Jones, N. & Heigenhauser, G. Regulation of skeletal muscle glycogen phosphorylase and PDH during maximal intermittent exercise. *Am. J. Physiol*. **277**, E890-E900 (1999).

24) Dos Santos, J.M., Benite-Ribeiro, S.A., Queiroz, G. & Duarte, J.A. The effect of age on glucose uptake and GLUT1 and GLUT4 expression in rat skeletal muscle. *Cell Biochem. Funct*. **30**,191-197 (2012).

25) Saito, A., Seiler, S., Chu, A. & Fleischer. S. Preparation and morphology of sarcoplasmic reticulum terminal cisternae from rabbit skeletal muscle. *J. Cell Biol*. **99**, 875-885 (1984).

26) Gowans, G.J. & Hardie, D.G. AMPK: a cellular energy sensor primarily regulated by AMP. *Biochem. Soc. Trans*. **42**, 71-75 (2014).

27) Muindi, J., Frankel, S.R. & Huselton C. Clinical pharmacology of oral all-trans retinoic acid in patients with acute promyelocytic leukemia. *Cancer Res*. **52**, 2138–2142 (1992).

28) Mukherjee, R., Davies, P.J., Crombie, D.L., Bischoff, E.D., Cesario, R.M., Jow, L., Hamann, L.G., Boehm, M.F., Mondon, C.E., Nadzan, A.M., Paterniti, J.R. Jr & Heyman, R.A. Sensitization of diabetic and obese mice to insulin by retinoid X receptor agonists. *Nature* **386**, 407-410 (1997).

29) Sarbassov, D.D., Guertin, D.A., Ali, S.M. & Sabatini, D.MPhosphorylation and regulation of AKT/PKB by the rictor-mTOR complex. *Science* **307**, 1098-1101 (2005).

30) Laplante, M. & Sabatini. D. mTOR signaling at a glance. *J. Cell Sci*. **122**, 3589-3594 (2009).

31) Liko, D. & Hall, M.N. mTOR in health and in sickness. *J. Mol. Med*. **93**,1061-1073 (2015).

32) Bentzinger, F., Romanino, K., Cloëtta, D., Lin, S., Mascarenhas, J., Oliveri, F., Xia, J., Casanova, E., Costa, C., Brink, M., Zorzato, F., Hall, M. & Rüegg, M. Skeletal muscle-specific ablation of raptor, but not of rictor, causes metabolic changes and results in muscle dystrophy. *Cell Metab*. **8**, 411–424 (2008).

33) Liu, P., Gan, W., Chin Y.R., Ogura, K., Guo, J., Zhang, J., Wang, B., Blenis, J., Cantley, L.C., Toker, A., Su, B. & Wei, W. PtdIns(3,4,5)P3-dependent activation of the mTORC2 kinase complex. *Cancer Discov*. **5**, 1194–1209 (2015).

34) López-Carballo, G., Moreno, L., Masiá, S., Pérez, P. & Barettino, D. Activation of the phosphatidylinositol 3-kinase/ AKT signaling pathway by retinoic acid is required for neural differentiation of SH-SY5Y human neuroblastoma cells. *J. Biol. Chem*. **277**, 25297-304 (2002).

35) Obrochta, K.M., Kane, M.A. & Napoli, J.L. Effects of diet and strain on mouse serum and tissue retinoid concentrations. PLoS One 9, e99435. doi: 10.1371/journal.pone.0099435 (2014).

36) Laplante, M. & Sabatini, D. mTOR signaling in growth control and disease. *Cell* **149**, 274-293 (2012).

37) García-Regalado, A., Vargas, M., García-Carrancá, A., Aréchaga-Ocampo, E. & González-De la Rosa, C. Activation of AKT pathway by transcription-independent mechanisms of retinoic acid promotes survival and invasion in lung cancer cells. *Mol. Cancer*. 12, 44. doi: 10.1186/1476-4598-12-44 (2013).

38) Lee, Y., Lee, J.Y. & Kim, M.H. PI3K/ AKT pathway regulates retinoic acid-induced Hox gene expression in F9 cells. *Develop. Growth Differ*. **56**, 518–525 (2014).

39) Matkovic, K., Brugnoli, F., Bertagnolo, V., Banfic, H. & Visnjic, D. The role of the nuclear AKT activation and AKT inhibitors in all-trans-retinoic acid-differentiated HL-60 cells. *Leukemia* **20**, 941–951 (2006).

40) Luo, X. & Ross, C. Physiological and receptor-selective retinoids modulate interferon γ signaling by increasing the expression, nuclear localization, and functional activity of interferon regulatory factor-1. *J. Biol. Chem.* **280**, 36228-36236 (2005).

41) Bozulic, L., Surucu, B., Hynx, D. & Hemmings, B.A. PKBalpha/ AKT1 acts downstream of DNA-PK in the DNA double-strand break response and promotes survival. *Mol Cell* **30**, 203-213 (2008).

42) Masiá, S., Alvarez, S., de Lera, A.R. & Barettino, D. Rapid, nongenomic actions of retinoic acid on phosphatidylinositol-3-kinase signaling pathway mediated by the retinoic acid receptor. *Mol. Endocrinol*. **21**, 2391-2402 (2007).

43) Qiaoa, J., Paula, P., Leea, S., Qiaoa, L., Josifia, E., Tiaoa, J. & Chung, D. PI3K/ AKT and ERK regulate retinoic acid-induced neuroblastoma cellular differentiation. *Biochem. Biophys. Res. Commun.* **424**, 421-426 (2012).

44) Lai, K.M., Gonzalez, M., Poueymirou, W.T., Kline, W.O., Na, E., Zlotchenko, E., Stitt, T.N., Economides, A.N., Yancopoulos, G.D. & Glass D.J. Conditional activation of AKT in adult skeletal muscle induces rapid hypertrophy. *Mol, Cell Biol*. **24**, 9295-9304 (2004).

45) Keni, O.J., Loennechen, J.P., Wisløff, U. & Ellingsen, Ø. Intensity-controlled treadmill running in mice: cardiac and skeletal muscle hypertrophy. *J. Appl. Physiol*. **93**, 1301-1309 (20012).

46) Briguet, A., Courdier-Fruh, I., Foster, M., Meier T. & Magyar, J.P. Histological parameters for the quantitative assessment of muscular dystrophy in the mdx-mouse. *Neuromuscul Disord*. **14**, 675-682 (2004).

47) Delbono, O., Xia, J., Treves, S., Wang, Z.M., Jimenez-Moreno, R., Payne, A., Messi, M.L., Briguet, A., Schaerer, F., Nishi, M., Takeshima, H. & Zorzato, F. Loss of skeletal muscle strength by ablation of the sarcoplasmic reticulum protein JP-45. *Proc. Natl. Acad. Sci. U.S.A.* **104**, 20108-20113 (2007).

48) Talmadge, R.J. & Roy, R.R. Electrophoretic separation of rat skeletal muscle myosin heavy chain isoforms. *J. Appl. Physiol*. **75**, 2337-2340 (1993).

49) Bachmann, C., Jungbluth, H., Muntoni, F., Manzur, A.Y., Zorzato, F. & Treves, S. Cellular, biochemical and molecular changes in muscles from patients with X-linked myotubular myopathy due to MTM1 mutations. *Hum. Mol. Genet*. ***26***, 320-332 (2017).

FIGURE LEGENDS

Figure 1: Spontaneous activity, fiber type composition, force measurements and SR protein composition of muscles from SRP35TG mice. (A) Spontaneous daily activity of WT (white symbols; n=16) and SRP35TG (black symbols; n=16) mice. Data points from 7 months (left) and 14 months (right) old mice are expressed as mean (±S.D.), ***p <0.001 Mann–Whitney test. **(B)** Dark phase speed events recorded from the 15^{th} to 20^{th} day of running (mean ±S.D., n=16). **(C)** and **(D**) Fibre type composition Minimal Ferret's diameter determined by myosin-heavy chain (MyHC) immunohistochemistry in EDL and soleus muscles of slow (MyHCI) and fast (MyHCII) fibres (mean±S.D., n= 10, *p<0.05 Student's *t* test). (**E)** Fibre size distribution of EDL and soleus muscles from WT and SRP35TG mice (mean ±S.D., n=10). **(F**) Mechanical properties of EDL and soleus muscles from WT (continuous line, representative trace of experiments carried out in 7 mice) and SRP35TG (dashed line, representative trace of experiments carried out in 13 mice) mice. Twitch force stimulated by a 15 V pulse of 0.5ms duration. Maximal tetanic force induced by a train of pulses delivered at 150 and 120 Hz for EDL and soleus, respectively. (**G)** Western blot analysis. Thirty-five µg of total SR protein were loaded per lane, separated on 6% or 10% SDS/PAGE. Bar histograms represent the mean (±S.D.) intensity of the immunoreactive band in SRP35TG fraction expressed as % of the intensity of the band in WT mice (n=6, **p<0.01 Student's *t* test).

Figure 2: Glucose uptake and plasma membrane GLUT4 levels are increased in SRP35TG mice. (A) Glucose tolerance test (ipGTT) in WT (n=8) and SRP35TG (n=8) mice, values are expressed as mean (±S.D.) blood glucose levels; *p<0.05; **p<0.01 Student's *t* test. (**B)** Circulating insulin in WT (n=8) and SRP35TG (n=8), is expressed as mean (±S.D.) pg of insulin measured after glucose injection. Values were not significantly different in WT and SRP35TG mice (Student's *t* test). **(C)** GLUT4 content of total SR and R1 fraction (tubule

T/sarcolemma membranes) of skeletal muscles from wild type (wt; n=8) and SRP3TG (tg; n=8) mice. Ten µg of protein were loaded per lane and separated on 7.5% SDS/PAGE (left); bar histograms of GLUT4 content in skeletal muscles from SRP35TG (black bars), normalized to control levels (white bars). Results are expressed as mean ±S.D., **p<0.01; ***p<0.001 Student's *t* test. **(D)** Western blot of GLUT4 in total homogenate from EDL and soleus muscles.

Figure 3: Skeletal muscle glycogen stores and RER in SRP35TG mice. (A) *In vitro* glucose uptake in EDL and soleus muscles from WT and SRP35TG. Three conditions were used: (i) no treatment (Basal; n=8); (ii) 10 min incubation with 100 nM insulin (n=6), (iii) electrical stimulation with a train of tetani (80 Hz, 300 ms duration) delivered at 0.27 Hz for 5 min (n=6). Data is expressed as mean (±S.D.); *p<0.05; **p<0.01 Student's *t* test. **(B)** Glycogen content was assessed enzymatically in total homogenates from EDL and soleus muscles. Each symbol represents the mean value of both muscles of a single mouse; the median value is represented by the horizontal black line; *p<0.05 Student's t test. **(C)** Respiratory exchange ratio (RER) was measured in CLAMS cages in WT (n=8) and SRP35TG (n=8) mice, fed a standard chow diet. Values are expressed as mean (±S.D.); *p<0.05 Student's t test. **(D)** Spontaneous locomotor activity was recorded on X, Y and Z axis, and is expressed as mean infrared beam breaks (±S.D.); n=8, *p<0.05 Student's *t* test.

Figure 4: AMPK and AKT phosphorylation levels are increased in muscles from SRP35TG mice. Western blots of total homogenates from EDL and soleus muscles. Phosphorylation of $AMPK_{T172}$ and AKT_{S473} was determined under the following experimental conditions. **(A)** and (**B**) basal conditions (n=7). **(C)** and **(D)** electrical stimulation with a train of tetani (80 Hz, 300 ms duration) delivered at 0.27 Hz for 5 min (n=6). **(E)** and **(F)** stimulation with 100 nM insulin (n=6). Representatives western blots from the three conditions are show in panels A, C and E and the Bar histograms in panels B, D and F. Fifty

µg of protein from total muscle homogenates were loaded per lane, separated on 10% SDS-PAGE and blotted onto nitrocellulose. The immunoreactivity to desmin was used to normalize protein loading. Data are presented as % (±S.D.) of WT values (control); *p<0.05 Student's *t* test.

Figure 5: atRA activates AKT_{S473} phosphorylation in WT EDL and soleus muscles. Fifty µg of protein from total muscle homogenates were loaded per lane, separated on 10% SDS-PAGE and blotted onto nitrocellulose. The immunoreactivity to desmin was used to normalize gel loading. Data are presented as % (±S.D.) of control (empty bar); * p<0.05 Student's t test. $AMPK_{T172}$, AKT_{S473} and AKT_{T308} phosphorylation levels were measured by western blotting on total homogenates from EDL and soleus with specific anti-phospho Ab. **(A)** and **(C)** Skeletal muscles isolated from WT mice were incubated with 10 µM all-*trans*-retinoic acid (atRA, bars; n=6). Control values (empty bar) were obtained by incubating the contralateral muscle in the presence of the vehicle solution (DMSO). **(B)** and **(D)** EDL and soleus muscles incubated with 100 nM insulin plus or minus 10 µM atRA. Left side: representative western blots at 30 min of incubation; right side: bar histogram plots, (n=6 *p<0.05 Student's *t* test). Control values (empty bar) for normalization were obtained by performing the experiments in the presence of 100 nM insulin plus vehicle (DMSO). **(E)** and **(F)** EDL muscles were incubated for 10 min in presence of 100 nM insulin, RARα, RARβ and RARγ inhibitors plus or minus 10 µM atRA. Control values (empty bar) were obtained in the presence of 100 nM insulin, plus the RAR inhibitor. Data are presented as mean ±S.D., n=6, *p<0.05 Student's t test.

Figure 6: SRP-35 and atRA activation of AKT_{S473} is controlled by mTORC2 and the PI3K signaling pathway. (A) and **(B)** Western blot images and bar histograms showing the phosphorylation of AKT in EDL and soleus muscles from WT (n=5) and RimKO (n=5) mice incubated with or without 10 µM atRA in presence of 100 nM insulin. Fifty µg of total

homogenate protein were loaded per lane, separated on 10% SDS/PAGE and blotted onto nitrocellulose. Anti-desmin immunoreactivity was used as loading control (bars represent the mean ±S.D., *p<0.05 Student's *t* test). **(C)** PIP_3 levels from EDL muscles isolated from WT and SRP35TG mice fed a standard chow diet (Top panel) and on a low vitamin A diet (LVA, 4 I.U/Kg, Bottom panel). Each symbol represents PIP_3 values from a single mouse; the median value of the data is shown in the box-plot; n.d= non detectable (muscles from 7 mice) *p<0.05 Mann Whitney test. **(D)** PIP_3 levels from soleus muscles isolated from WT and SRP35TG mice fed a standard chow diet (Top panel) and on a low vitamin A diet (LVA, 4 I.U/Kg, Bottom panel). Each symbol represents PIP_3 values from a single mouse; the median value of the data is shown in the box-plot; *p<0.05 Mann Whitney test. **(E)** EDL muscles from WT (closed squares) and SRP35TG (closed triangles) mice kept for 2 generations under low Vit A diet (LVA), were electrically stimulated in the presence of 100 nM insulin using a fatigue protocol (70Hz, 300 ms duration, delivered at 0.33Hz) and the force generated (% of initial force) at the indicated times was calculated. Each point represents the mean (±S.D.; n= 5 WT and 5 SRP35TG) force; P<0.05 Mann Whitney. **(F)** Soleus muscles from WT (closed squares) and SRP35TG (closed triangles) mice kept for 2 generations under low Vit A diet (LVA), were electrically stimulated in the presence of 100 nM insulin using a fatigue protocol (50Hz, 600 ms duration, delivered at 0.33Hz) and the force generated (% of initial force) at the indicated times was calculated. Each point represents the mean (±S.D.; n= 5 WT and 5 SRP35TG) force; P<0.05 Mann Whitney. **(G)** Glycogen content was assessed enzymatically in total homogenates from EDL muscles at the end of the fatigue protocol. Each symbol represents the value from a single mouse; the median value of the data is shown in the box-plot; *p<0.05 Mann Whitney test. **(H)** Glycogen content was assessed enzymatically in total homogenates from soleus muscles at the end of the fatigue protocol. Each symbol represents the value from a single mouse; the median value of the data is shown in the box-plot; *p<0.05 Mann Whitney test.

<u>Figure 7:</u> Schematic representation of the SRP-35 pathway and its effect on glucose metabolism. SRP-35 transforms retinol to retinal and the latter is converted to retinoic acid. In the presence of insulin, retinoic acid activates the Retinoic Acid Receptor α and γ (RARα and RARγ)/ Phosphoinositide 3-kinase (PI3K)/ mTOR Complex 2 (mTORC2)/ AKT_{S473}. Activation of AKT induces the downstream translocation of GLUT4 onto the sarcolemma leading to higher glucose uptake by muscles which in turn leads to greater glycogen stores giving the skeletal muscle machinery a higher energy source.

Figure 1

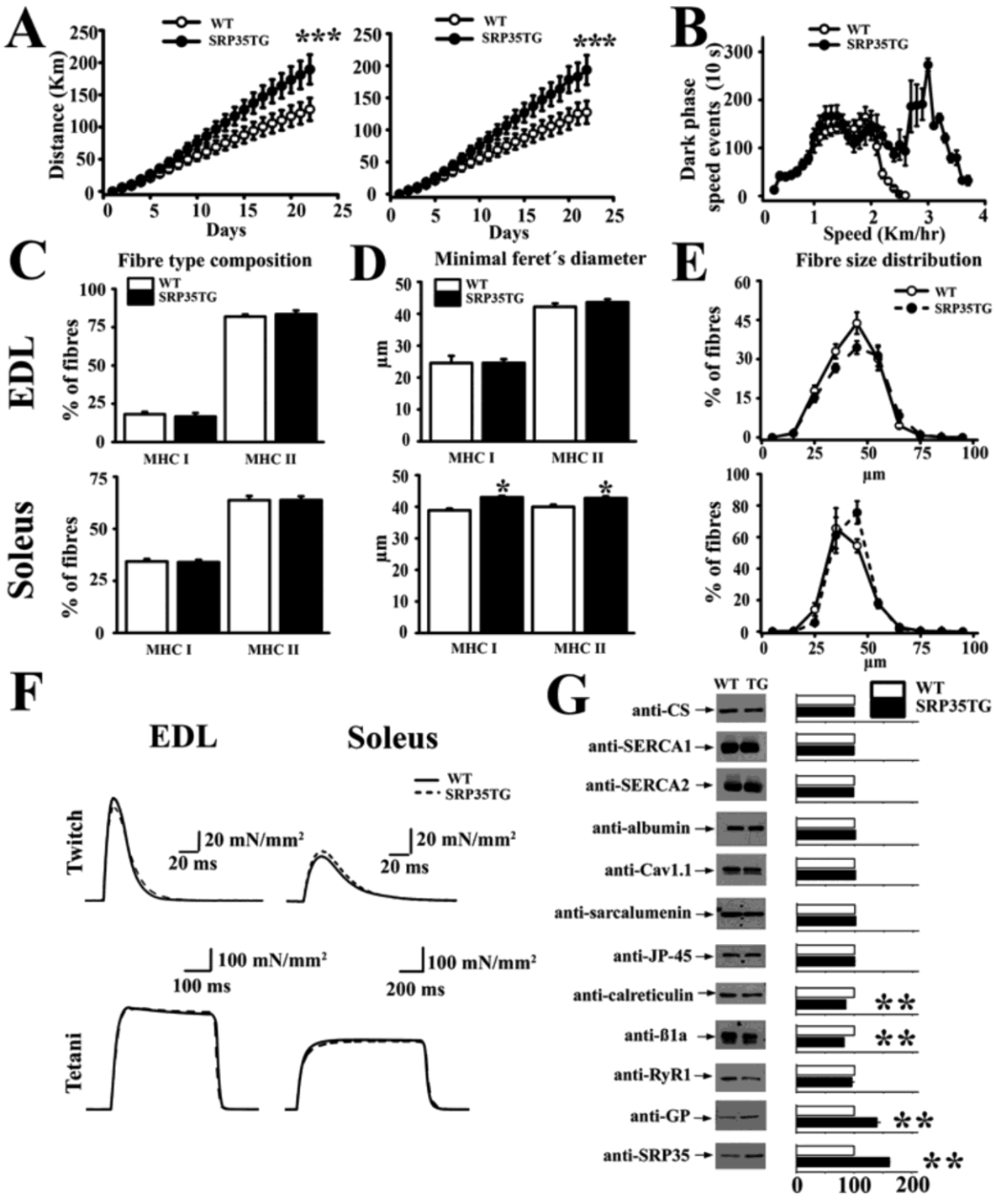
A
WT
SRP35TG
***
Distance (Km)
Days
B
Dark phase speed events (10 s)
Speed (Km/hr)
C
Fibre type composition
EDL
Soleus
% of fibres
MHC I
MHC II
D
Minimal feret´s diameter
µm
E
Fibre size distribution
F
EDL
Soleus
Twitch
Tetani
20 mN/mm²
20 ms
100 mN/mm²
100 ms
200 ms
G
WT TG
anti-CS
anti-SERCA1
anti-SERCA2
anti-albumin
anti-Cav1.1
anti-sarcalumenin
anti-JP-45
anti-calreticulin
anti-ß1a
anti-RyR1
anti-GP
anti-SRP35

Figure 2

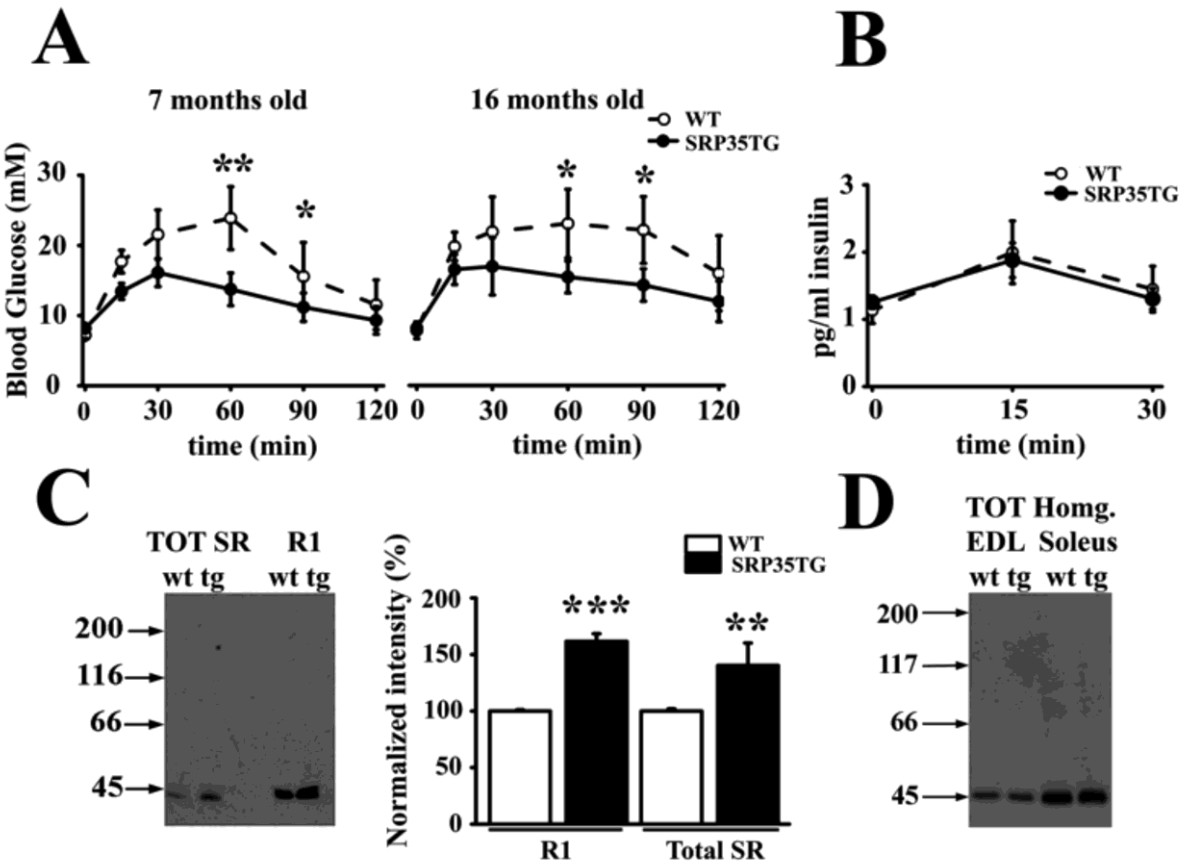
A
7 months old
16 months old
WT
SRP35TG
Blood Glucose (mM)
time (min)
B
pg/ml insulin
time (min)
C
TOT SR
R1
wt tg
wt tg
200
116
66
45
Normalized intensity (%)
R1
Total SR
D
TOT Homg.
EDL Soleus
wt tg wt tg
200
117
66
45

Figure 3

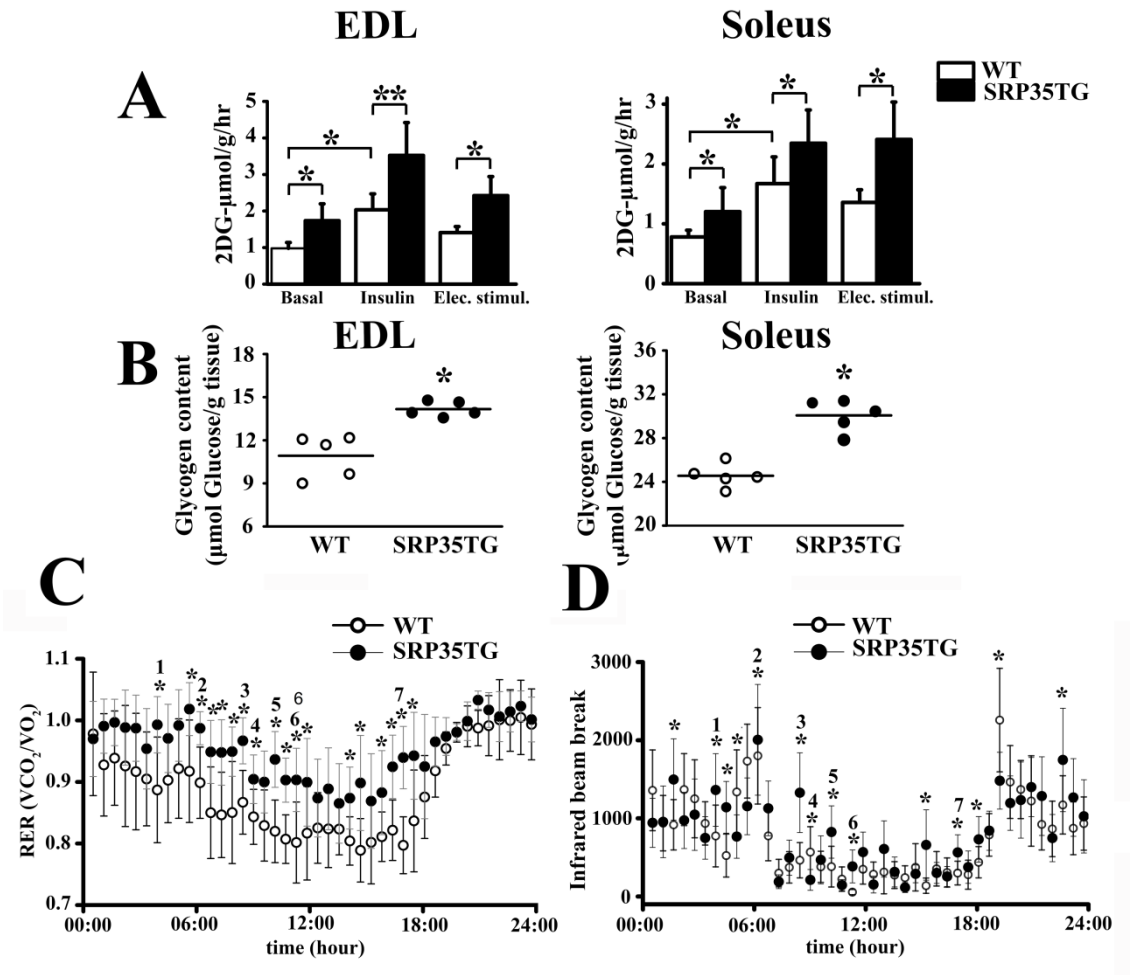
EDL
Soleus
A
WT
SRP35TG
2DG-µmol/g/hr
Basal
Insulin
Elec. stimul.
B
Glycogen content
(µmol Glucose/g tissue)
WT
SRP35TG
C
D
RER (VCO2/VO2)
Infrared beam break
time (hour)
00:00
06:00
12:00
18:00
24:00

Figure 4

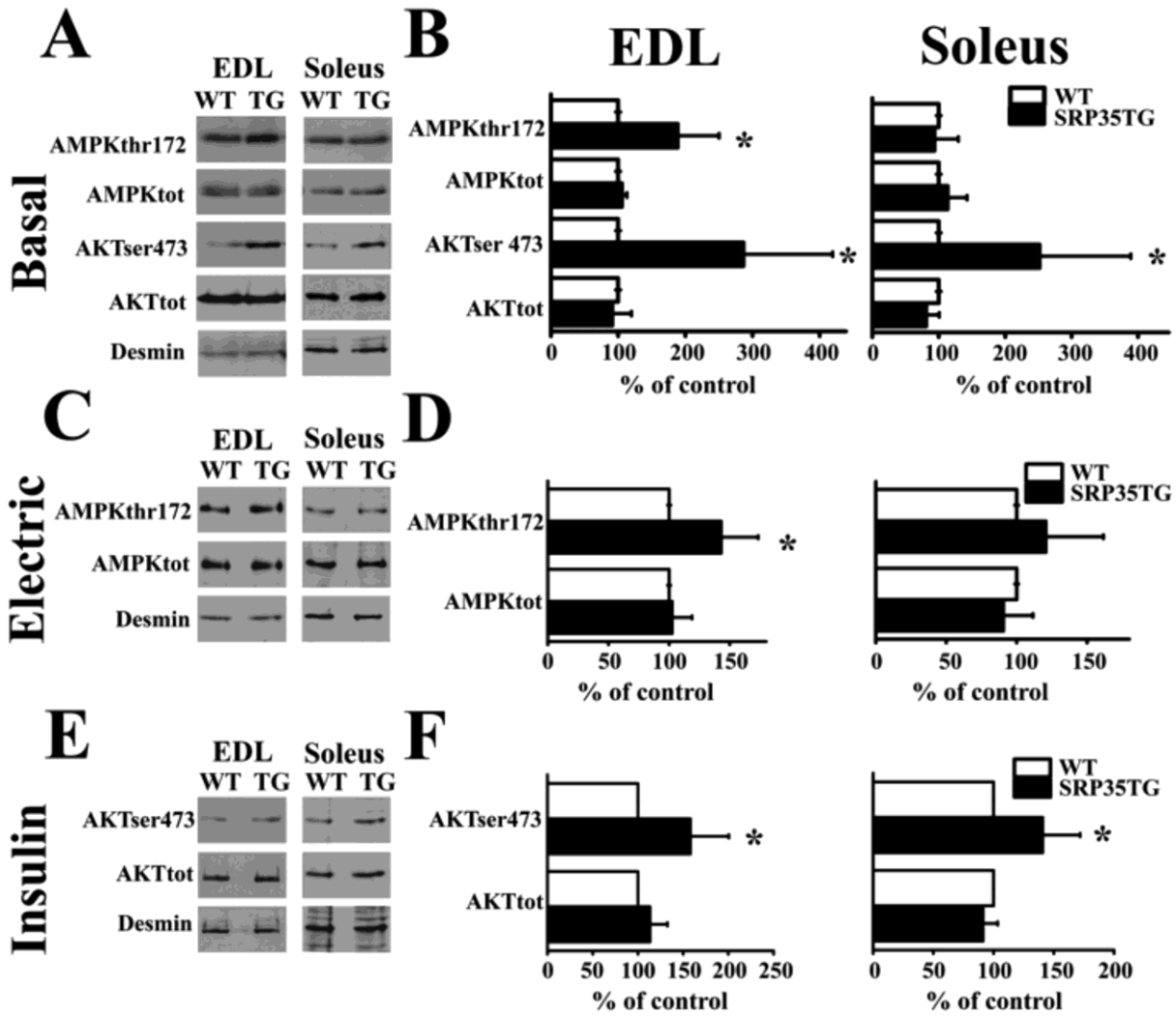
A
EDL
Soleus
WT TG WT TG
Basal
AMPKthr172
AMPKtot
AKTser473
AKTtot
Desmin
B
EDL
Soleus
WT
SRP35TG
AMPKthr172
AMPKtot
AKTser 473
AKTtot
0 100 200 300 400
% of control
C
Electric
D
0 50 100 150
E
Insulin
F
0 50 100 150 200 250
0 50 100 150 200

Figure 5

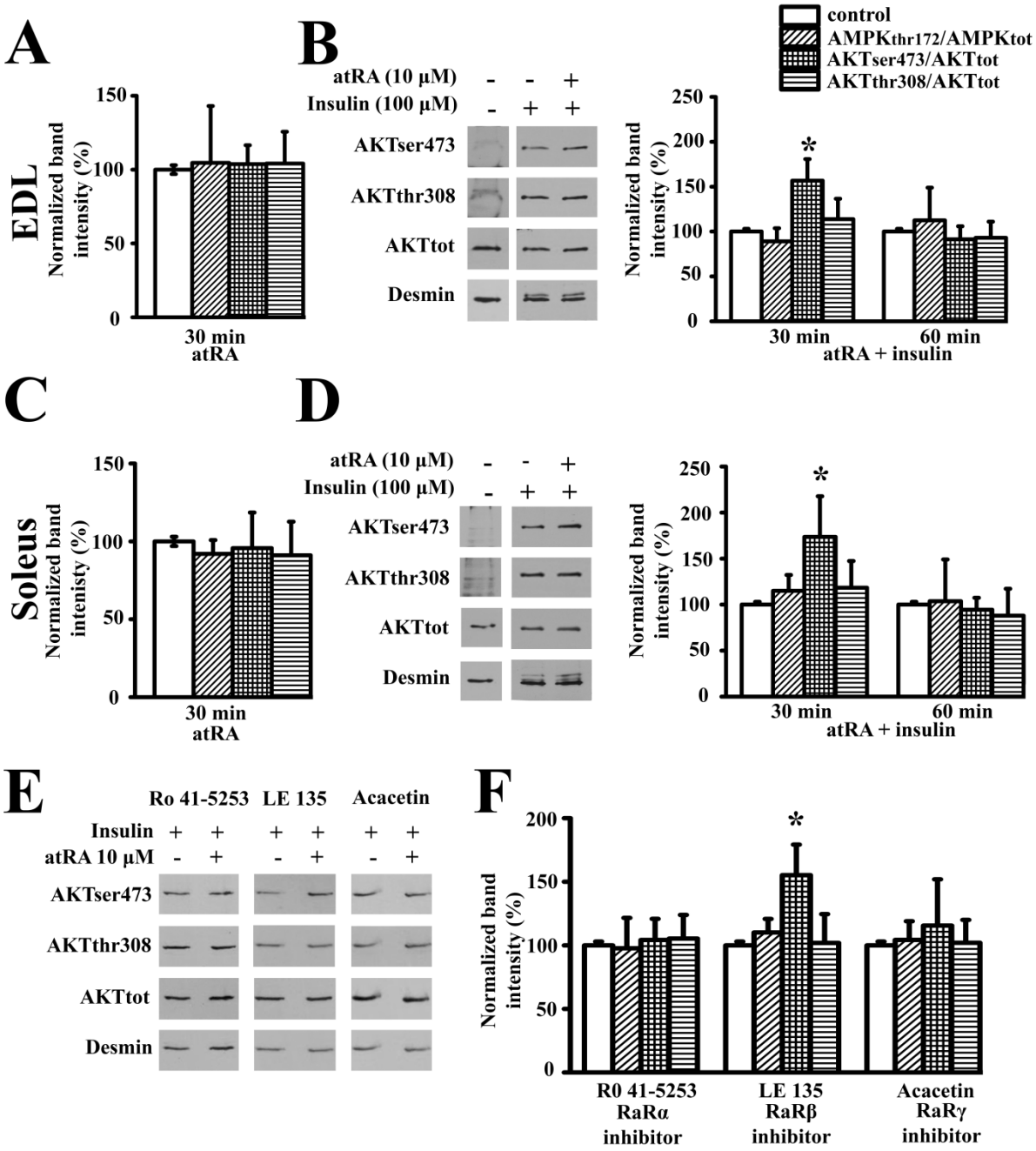
A
EDL
Normalized band intensity (%)
150
100
50
0
30 min atRA
B
atRA (10 µM) - - +
Insulin (100 µM) - + +
AKTser473
AKTthr308
AKTtot
Desmin
control
AMPKthr172/AMPKtot
AKTser473/AKTtot
AKTthr308/AKTtot
Normalized band intensity (%)
250
200
150
100
50
0
*
30 min
60 min
atRA + insulin
C
Soleus
Normalized band intensity (%)
150
100
50
0
30 min atRA
D
atRA (10 µM) - - +
Insulin (100 µM) - + +
AKTser473
AKTthr308
AKTtot
Desmin
Normalized band intensity (%)
250
200
150
100
50
0
*
30 min
60 min
atRA + insulin
E
Ro 41-5253 LE 135 Acacetin
Insulin + + + + + +
atRA 10 µM - + - + - +
AKTser473
AKTthr308
AKTtot
Desmin
F
Normalized band intensity (%)
200
150
100
50
0
*
R0 41-5253 RaRα inhibitor
LE 135 RaRβ inhibitor
Acacetin RaRγ inhibitor

Figure 6

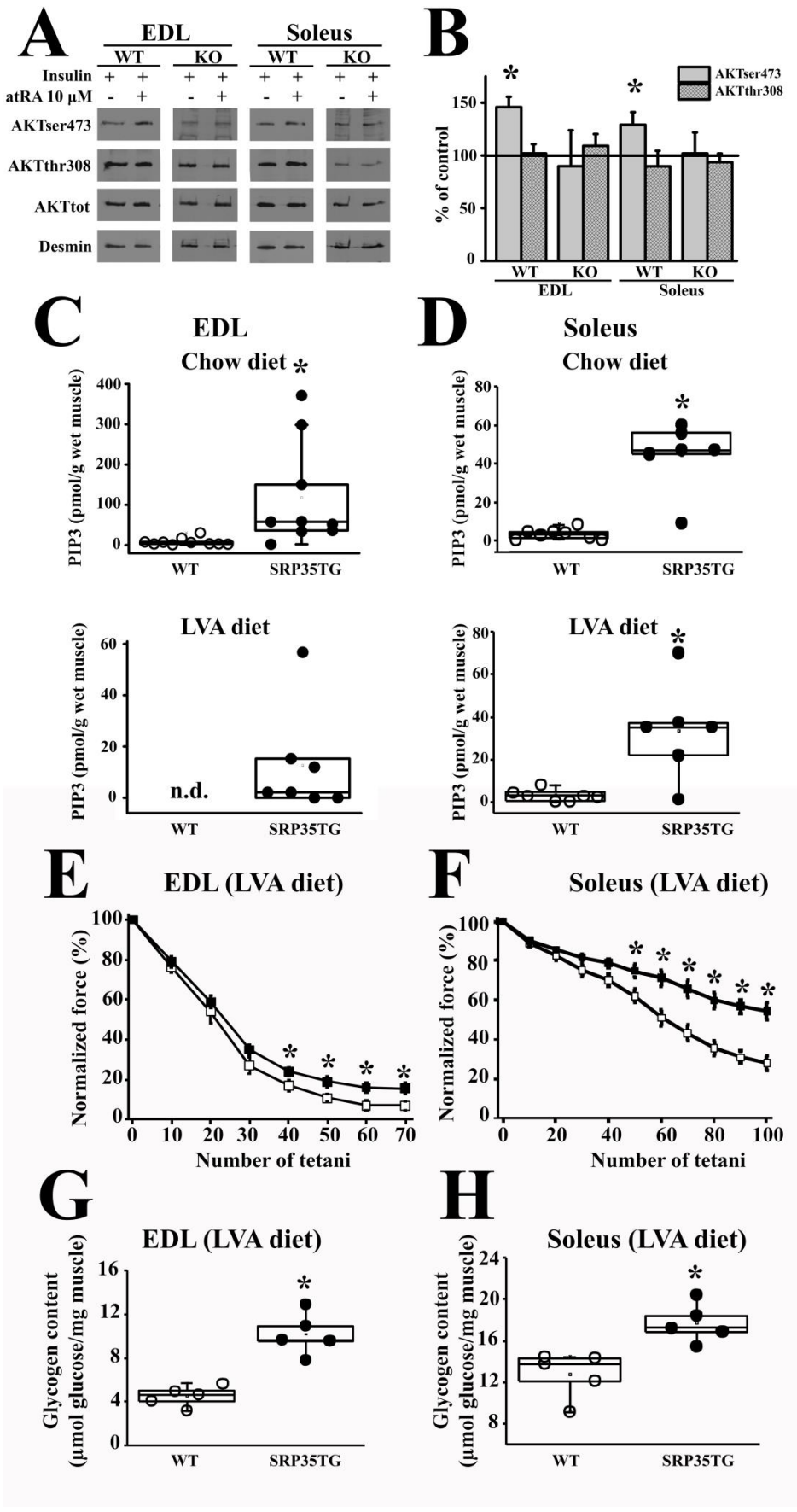
A
EDL
Soleus
WT
KO
WT
KO
Insulin + + + + + + + +
atRA 10 µM - + - + - + - +
AKTser473
AKTthr308
AKTtot
Desmin
B
AKTser473
AKTthr308
% of control
150
100
50
0
WT
KO
WT
KO
EDL
Soleus
C
EDL
Chow diet
PIP3 (pmol/g wet muscle)
400
300
200
100
0
WT
SRP35TG
LVA diet
n.d.
D
Soleus
Chow diet
80
60
40
20
0
LVA diet
E
EDL (LVA diet)
Normalized force (%)
100
80
60
40
20
0
0 10 20 30 40 50 60 70
Number of tetani
F
Soleus (LVA diet)
0 20 40 60 80 100
G
EDL (LVA diet)
Glycogen content
(µmol glucose/mg muscle)
16
12
8
4
0
H
Soleus (LVA diet)
24
20
16
12
8

Figure 7

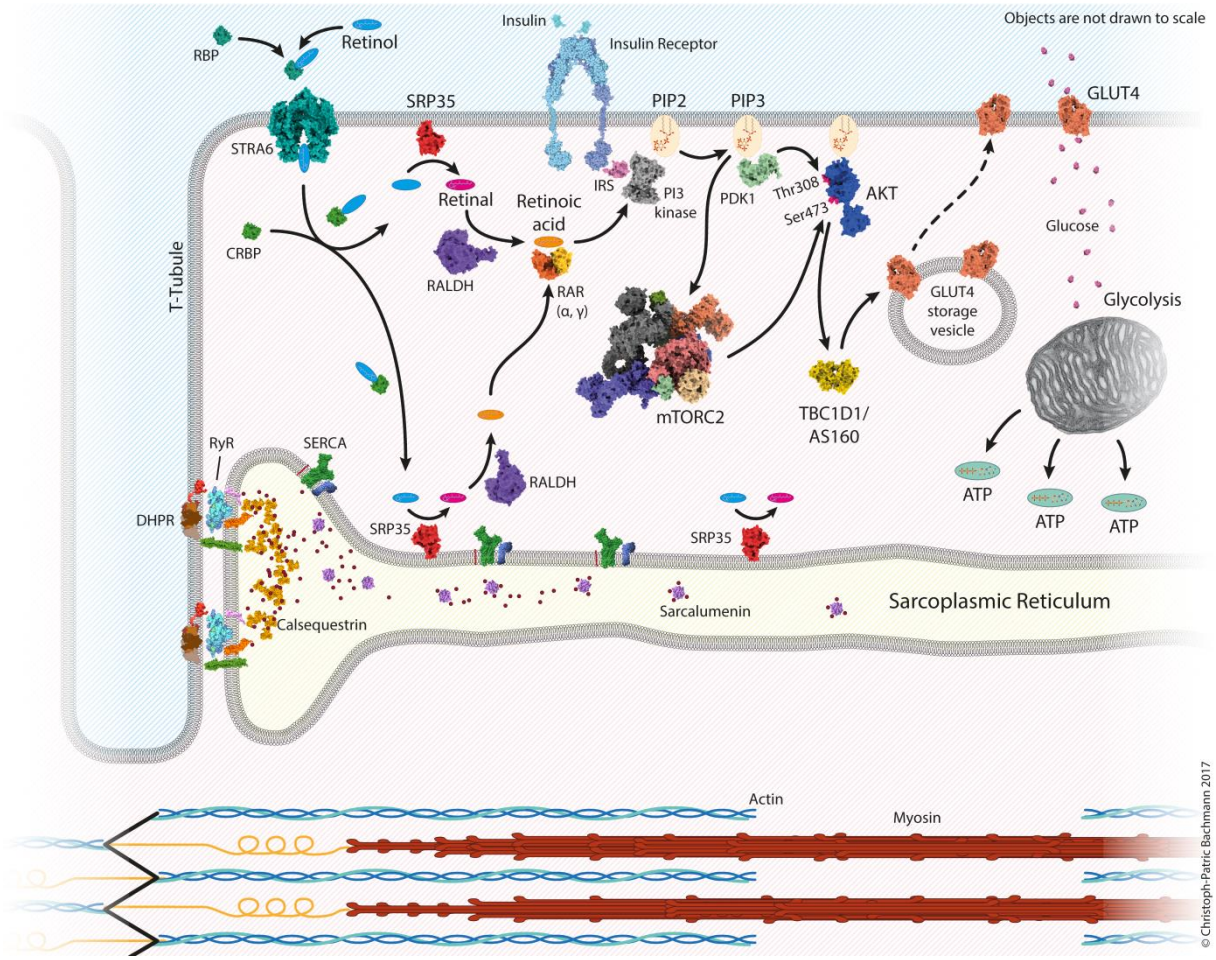
Objects are not drawn to scale
RBP
Retinol
Insulin
Insulin Receptor
SRP35
PIP2
PIP3
GLUT4
STRA6
IRS
PI3 kinase
PDK1
Thr308
Ser473
AKT
Retinal
Retinoic acid
Glucose
CRBP
RALDH
RAR (α, γ)
GLUT4 storage vesicle
Glycolysis
T-Tubule
mTORC2
TBC1D1/ AS160
RyR
SERCA
RALDH
ATP
ATP
ATP
DHPR
SRP35
SRP35
Sarcalumenin
Sarcoplasmic Reticulum
Calsequestrin
Actin
Myosin
© Christoph-Patric Bachmann 2017

2.2 Additional Unpublished Data

Effect of insulin and low vitamin A diet on glycogen content and fatigue resistance of muscles from SRP35TG mice.

Vitamin A (retinol) is a fat-soluble vitamin made up of a 20 carbon structure with a methyl substituted cyclohexenyl ring (beta-ionone ring) which is essential for vision, gene expression, reproduction, embryonic development, growth, and immune functions. Humans need to take in retinol with their diet by consuming fish, meat, colored fruits, yellow tubers and dark green leafy vegetables (O'Byrne and Blaner, 2013). The effect of vitamin A dietary concentrations have a big impact on retinoic acid production in mammals. Experiments carried out in different mice strains in which animals were fed with diet containing two different Vitamin A concentrations for 3 generations, show that the concentration of several retinoids, including retinoic acid (RA), varies depending on the dietary Vitamin A concentration (Obrochta et al., 2014). Mice fed with Low Vitamin A diet (4 IU vitamin A, LVAD) present a lower RA concentration in several tissues including liver, kidney, testis, white adiposity tissue and serum compared with mice fed with standard Chow diet (12 to >20 IU vitamin A) (Obrochta et al., 2014).

Additionally, several groups have shown that the diet is able to mask the phenotype of genetically modified animals, specifically, Chow diets containing a higher concentration of vitamin A, prevent the manifestation of specific phenotypes which would result from ablation of genes that modulate retinoid homeostasis (Obrochta et al., 2014). Experiments with retinol-binding protein (RBP) knockout mice ($RBP^{-/-}$) fed with a Chow diet presented no dramatic phenotype changes compared to wild type littermates, but $RBP^{-/-}$ mice fed with LVA diet showed clear developmental and reproduction problems (Quadro et al. 1999). Similar results were found in Cellular retinol-binding protein II-null (CRBP II −/−) mice fed with Chow diet;

such mice had no overt phenotype, however under LVA diet the CRBP II −/− mice had a 100% mortality/litter within 24 h after birth (E et al., 2002). Another interesting result was reported in retinol dehydrogenase 1 (rdh1)-null mice. Such mice fed with a normal diet did not exhibit any significant changes compared to their WT littermates, however th KO mice fed with LVA diet showed higher body weight and adipocytes (Zhang et al., 2007).

In order to test the impact of dietary Vitamin A concentrations on the phenotype of SRP35TG mice, we fed these mice for 2 generations with a LVA diet. Muscles isolated from SRP35TG mice under Chow or LVA diets were compared for various parameters, including their resistance to fatigue and glycogen content. The results of these studies will be illustrated in the next sections of my thesis.

Effect of LVA diet and insulin on the fatigue resistance of EDL and Soleus muscles from SRP35TG mice.

In the present section we describe the effects of two different concentrations of dietary vitamin A in the presence or absence of insulin on the fatigue resistance and glycogen content of EDL and soleus muscles from SRP35TG and WT mice. In addition to the *in vitro* fatigue resistance test and glycogen content performed on EDL and soleus muscles from SRP35TG and WT mice (fed for 2 generations with LVA diet), we also tested fatigue resistance and glycogen content of muscles isolated from mice under standard Chow diet. It is important to keep in mind that the aim of feeding the mice with the LVA diet is based on the hypothesis that at any given intracellular retinol concentration, muscle fibres over-expressing SRP-35 would generate greater amounts of all-trans-retinaldehyde (precursor of atRA formation). Therefore, SRP35TG mice fed with a LVA diet should be able to generate more atRA compared to WT littermates and enhance even more PI3K activity. This enhanced enzymatic activity should enhance mTORC2/AKT signaling which in turn may lead to higher glucose uptake and increased glycogen stores, leading to better muscle performance compared to WT mice. The experiments were conducted on muscles incubated with insulin (100 nM) because in our previous observations (presented in the paper) we showed that insulin is necessary to induce the non-genomic effect of RA on AKT_{S473} phosphorylation.

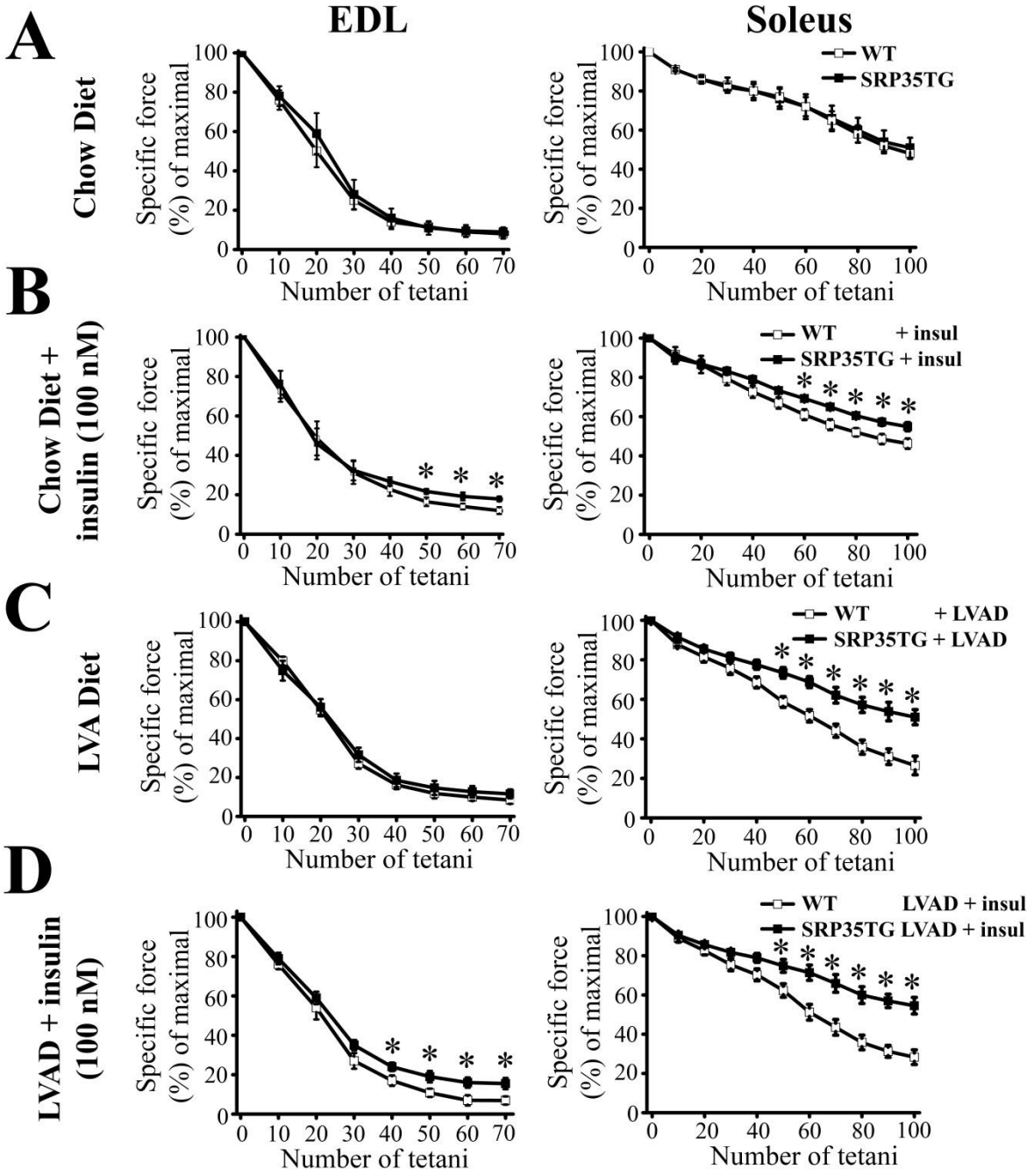

Figure R3.1- Fatigue resistance in muscles from SRP35TG mice maintained on a LVA diet. EDL and Soleus muscles from WT (open squares) and SRP35TG (closed squares) mice were stimulated with a train of tetanic stimulation (EDL: 70 Hz, 300 ms duration; Soleus 50 Hz, 600 ms duration) delivered at 0.33 Hz. Maximal specific force (mN/mm2) of the first tetanic contracture is expressed as 100%. Four different conditions were tested: Muscle from SRP35TG and WT mice **(A)** under Chow diet; **(B)** under Chow diet and incubated with insulin (100 nM); **(C)** under LVA diet; **(D)** and under LVA diet and in the presence of

insulin (100 nM). Each point represents the mean ± S.D.; n = 5 WT and 5 SRP35TG; *p < 0.05 Mann-Whitney.

As demonstrated by Quadro et al. and Zhang et al., in genetically modified mice fed with different amounts of Vitamin A (Quadro et al., 1999; Zhang et al., 2007; Obrochta et al., 2014), the effect of the LVA diet on the mouse`s phenotype is dramatic. The results depicted in Figure R3 show that under a Chow diet no significant difference in force generated by muscles from WT and SRP35TG mice were observed. However, under LVA diet, the soleus muscles of SRP35TG mice exhibited a higher resistance to fatigue compared to WT littermates (Figure R3.1 panel A and C). Interestingly, EDL muscles did not show any significant difference in their fatigue resistance in WT and SRP35TG mice under Chow diet. This effect could be related to the fibre type composition; in fact EDL (Fast-twitch) muscles express a higher proportion of fast speed fibre types (MyHC type I: 0.4 %; type IIA, type IIDB 21.4 %; and type IIB 66.0 %), compared to soleus (slow-twitch) muscles, which contain a mixute of slow and fast fibre types (MyHC type I: 37.4 %; type IIA: 38.6; type IIAD: 18.7 %) (Augusto et al., 2004). This difference in fibre type composition is very important in muscle performance, due to the specific protein expression characteristics of each MyHC type. Firstly, MyHC type I fibres show a slower rate of cross-bridge cycling and ATP consumption compared to MyHC type II. Secondly, MyHC I fibres express the SERCA type 2 isoform to a lower density compared to MyHC II fibers, where SERCA 1 is highly expressed. Thirdly, the protein parvalbumin is almost exclusively expressed in MyHC II fibres, but is almost undetectable in MyHC I fibres. (Füchtbauer et al., 1991; Biral et al., 1992; Bottinelli and Reggiani, 2000; Calderon et al., 2014). Finally, the fast type II fibres (with a higher ATP consumption) are endowed with a higher anaerobic metabolism and lower oxidative capacity that allows them to have short explosive movements, but with a low resistance to fatigue (Westerblad et al., 2010; Argilés et al., 2016). Thus, in order to clarify

the mechanism leading to the different fatigue responses between EDL and Soleus muscles from SRP35TG mice under LVA diet more detailed investigations are required and these could be the aim of future studies.

While performing the experiments included in my thesis we also discovered that the presence of insulin is a necessary requirement to observe a non-genomic effect of RA. Skeletal muscle from SRP35TG mice under Chow diet did not present any significant change in fatigue resistance, however EDL and soleus muscles obtained from SRP35TG mice kept under a Chow diet, and incubated with insulin (100 nM) during the experimental procedure, exhibited a slightly better performance compared to muscles from WT mice (figure R31. Panel B). Interestingly, muscles from SRP35TG mice under LVAD and in the presence of insulin (100 nM) showed the largest difference in fatigue resistance for both EDL and soleus muscles compared to muscles from WT mice also fed wit LVA diet (figure R3.1 panel D).

As mentioned previously glycogen storage is a very important role played by skeletal muscle; indeed glycogen is a form of stored, energy which allows the muscle to respond rapidly to any environmental signal when glucose is not available, making this tissue an important player for whole body metabolism (Argilés et al., 2016). Figure R3.2 panel A and C show that the levels of glycogen stores in mice fed with the LVA diet, decreased significantly both in WT mice and SRP35TG mice. However, SRP35TG mice still exhibit higher glycogen stores under all tested conditions (Figure R3.2). These results indicate that SRP-35 is directly involved in the regulation of glycogen stores in skeletal muscle. In line with this result it should be remember that EDL and soleus muscles from SRP35TG mice exhibit higher glucose uptake which in turn would facilitate the maintenance of larger glycogen stores in muscles from SRP35TG mice compared to WT mice.

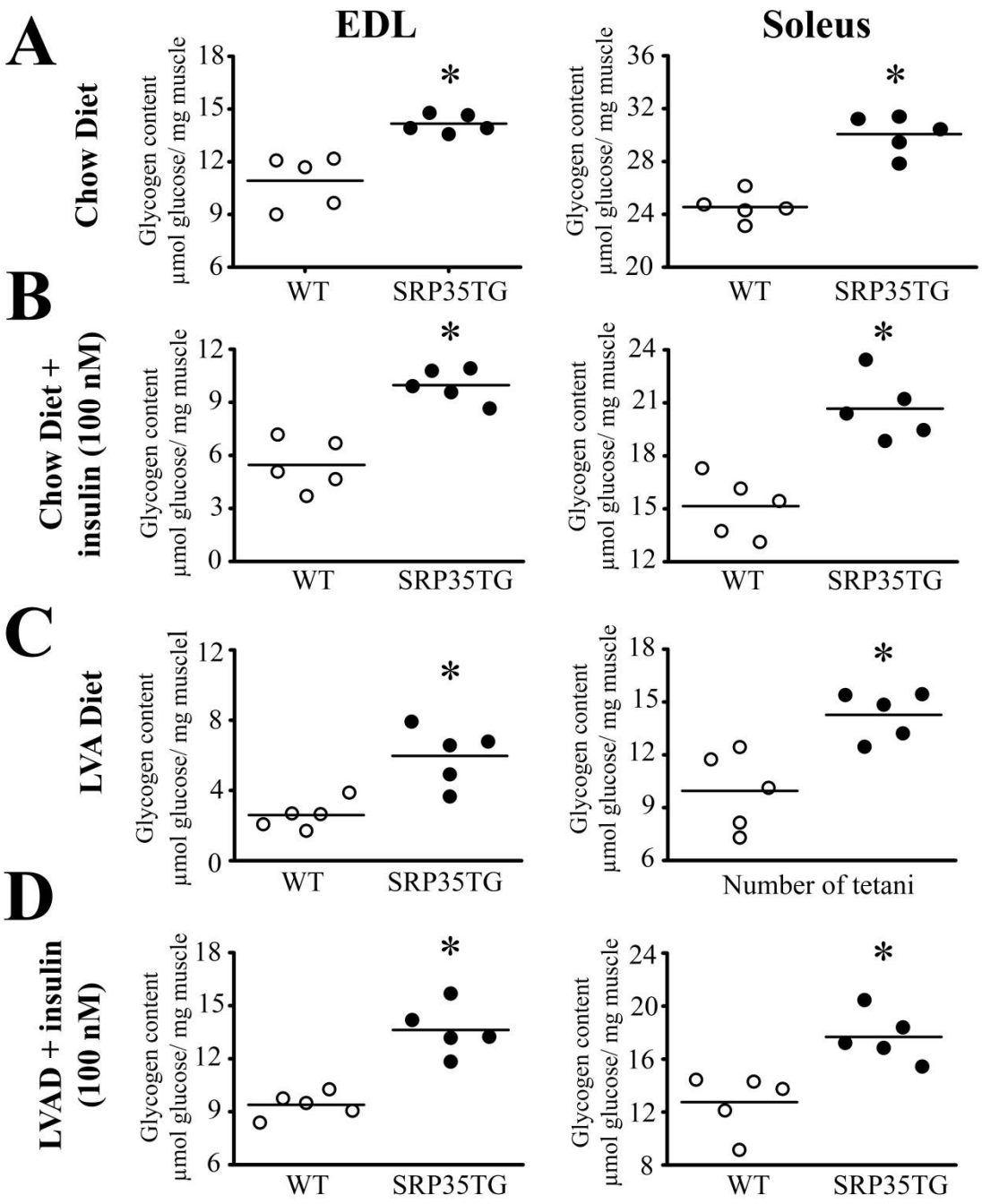

Figure R3.2- Glycogen content. EDL and Soleus muscles from WT (open squares) and SRP35TG (closed squares) mice were stimulated with a train of tetanic stimulation (EDL: 70 Hz, 300 ms duration; Soleus 50 Hz, 600 ms duration) delivered at 0.33 Hz. Glycogen content was assessed enzymatically in muscle total homogenate. Four different conditions were tested: Muscle from SRP35TG and WT mice **(A)** under chow diet; **(B)** under Chow diet and incubated with insulin (100 nM); **(C)** under LVA diet; **(D)** and under LVA diet and in presence of insulin (100 nM). The median value of the data is shown in the box-plot; *$p < 0.05$ Mann-Whitney test.

In conclusion, our results show that the higher vitamin A levels of Chow diet might mask the phenotype of SRP-35 overexpression in skeletal muscle. However, our results unambiguously show that SRP35TG mice fed with a LVA diet exhibit a higher fatigue resistance compared to WT littermates mice and the presence of insulin in the solution bathing the isolated skeletal muscles further increased the difference between these two groups of mice. The lack of a significant differences between WT and SRP35TG mice fed with Chow diet could be due to the fact that large amount of dietary vitamin A may allow the synthesis of atRA by pathways independent of retinoid-chaperoning proteins (Obrochta et al. 2014), and thereby would mask the functions of proteins such as SRP-35, that evolved to increase the efficiency of vitamin A use.

CHAPTER 3 – GENERAL CONCLUSION AND PERSPECTIVES

Diabetes and others metabolic diseases are linked to negative effects of skeletal muscle metabolism. The incidence of metabolic diseases is rising rapidly. Type 2 diabetes (mellitus) alone currently affects 190 million people worldwide and is predicted to increase to 300 million by 2025. The effect of metabolic disease affecting skeletal muscle metabolism are very dramatic for the whole organism because of the important role played by muscle in removing 70-75 % of circulating glucose in an insulin-dependent manner. The skeletal muscle presents a complex machinery that induces muscle contraction and requires a high amount of energy consumed in form of ATP,; this triggers the AMPK pathway that induces glucose uptake into the cell and increasing the insulin sensitivity. The proper functioning of the skeletal muscle machinery during Excitation Contraction Coupling (ECC) affects the whole body energy consumption, by affecting AMPK and insulin.

In the past few years our lab has focused on proteins relating to ECC, discovering new proteins involved in this process, or related to muscle function or metabolism. SRP-35, a protein present in the longitudinal sarcoplasmic reticulum, was discovered by our group several years ago; the present investigation reveals the role of SRP-35 in skeletal muscle metabolism. Transgenic mice overexpressing SRP-35 in their skeletal muscles were characterized biochemically and physiologically. The first important result obtained was the higher running capacity exhibited by the transgenic mice. This effect was not related to changes in fiber type composition or muscle force. Our results also show that SRP-35 is not directly involved in the ECC mechanism. This observation promoted us to further investigate the role of SRP-35 in skeletal muscle physiology. We thus discovered that the enhanced running capacity of SRP35TG mice was due to a metabolic effect on skeletal muscle, which

triggered the translocation of Glut4 to the sarcolemma and thus increased glucose uptake into the muscle, via the phosphorylation of AKT_{S473}.

This result was novel and exciting exposing the relationship between SRP-35 and muscle metabolism. After discovering the enhanced Glut4 translocation in muscles from SRP35TG mice, we discovered that this effect was mediated by a non-genomic effect of RARα and RARγ, inducing the stronger activation of PI3K and of mammalian target of rapamycin complex 2 (mTORC2) signaling pathways, which trigger the phosphorylation of AKT_{S473}. Curiously, RA had been previously reported to activate in a non-genomic manner, the RARα and RARγ, triggering the activation of Ribosomal protein S6 kinase 3 (RSK2) and Mitogen- and stress-activated kinase 1 (MSK1) proteins, respectively (Tanoury et al., 2013), but a direct effect on mTORC2 pathway had not been clearly exposed..

The signaling pathway downstream SRP-35 was elucidated in this study, showing that non-genomic effects of atRA induce the activation of mTORC2 and finally the translocation of Glut4 to the sarcolemma. However, an important question still remains unanswered: how is SRP-35 activated physiologically? Which processes modulate the activation or inhibition of this enzyme? A hint to solve this question could be the observed synergetic effects between SRP-35/RA and insulin on AKT_{S473} phosphorylation. The fact that SRP-35 in the skeletal muscle is able to induce a higher glucose uptake on top of that induced by insulin alone exposes the possibility that SRP-35 could be under the control of an insulin-related pathway. Nevertheless, this theory needs to be confirmed by a deeper investigation on the upstream pathway leading to the activation of SRP-35.

One important point to be considered for possible futures clinical treatments are the possible collateral effects of RA administration to the whole organism. For decades the teratogenic effect of RA on women of child-bearing potential had been known (David et al., 1988), and more recently a connection between RA and allergy development has been established

(Babina et al., 2017). On the other hand, overexpression of SRP-35 could offer an advantage over RA administration. We believe that due to the location of SRP-35 on the plasma membrane (same region of PI3K) of skeletal muscle, it is possible to form micro-domains where the RA concentration is higher and the effect on RARα/β and PI3K more specific. Increasing the levels of SRP-35 and skeletal muscle RA offers the advantage of increasing the sensitivity to insulin and avoids the collateral effects of the high concentration of pharmacological doses of RA, which cause unspecific and adverse effects for the whole organism.

In conclusion SRP-35 may be a novel target for the treatment of metabolic syndromes characterized by a decreased sensitivity to insulin and decreased Glut4 translocation onto the plasma membrane. In order to evaluate if the higher expression of SRP-35 can rescue the phenotype of mice with type 2 diabetes futures studies based on crosses between SRP35TG mice and $Lep^{ob/ob}$ mice could be envisaged. These latter Lep negative mice are a commonly used model for obesity and emulate type 2 diabetes because of their obesity-induced hyperglycaemia. The results could give a hint as to the role of SRP-35 on the whole body metabolism; if this enzyme is able to rescue the phenotype of type 2 diabetes it would be a basic and important step for the future treatment of humans affected by metabolic disorders.

REFERENCES

Abel E., Peroni, O., Kim J., Kim Y., Boss O., Hadro E., Minnemann, T., Shulman, G., and Kahn, B. (2001). Adipose-selective targeting of the GLUT4 gene impairs insulin action in muscle and liver. Nature 409, 729–733.

Adeva-Andany M., González-Lucán M., Donapetry-García C., Fernández-Fernández C. and Ameneiros-Rodríguez E. (2016). Glycogen metabolism in humans. BBA Clin. 2016 Jun; 5: 85–100.

Augustin R. (2010). The protein family of glucose transport facilitators: It's not only about glucose after all. IUBMB Life. 62(5):315-33.

Altucci L., Rossin A., Raffelsberger W., Reitmair A., Chomienne C., and Gronemeyer H.(2001). Retinoic acid-induced apoptosis in leukemia cells is mediated by paracrine action of tumor-selective death ligand TRAIL. Nat. Med. 7, 680-686

Anderson A., Treves S., Biral D., Betto R., Sandonà D., Ronjat M., Zorzato F. (2003). The novel skeletal muscle sarcoplasmic reticulum JP-45 protein. Molecular cloning, tissue distribution, developmental expression, and interaction with alpha 1.1 subunit of the voltage-gated calcium channel. J Biol Chem. 278(41):39987-92.

Argilés J,. Campos N., Lopez-Pedrosa J., Rueda R., Rodriguez-Mañas L. (2016) Skeletal Muscle Regulates Metabolism via Interorgan Crosstalk: Roles in Health and Disease. J Am Med Dir Assoc. 17, 9,: 789–796.

Ashrafian H., McKenna W., Watkins H., and Robbins J. (2011). Disease Pathways and Novel Therapeutic Targets in Hypertrophic Cardiomyopathy. Circulation Research. 109:86-96.

Baker J., McCormick M. and Robergs R. (2010). Interaction among Skeletal Muscle Metabolic Energy Systems during Intense Exercise. J Nutr Metab. 2010; 2010: 905612.

Bakker W., Harris I. and Mak T. (2007). FOXO3a is activated in response to hypoxic stress and inhibits HIF1-induced apoptosis via regulation of CITED2. Mol Cell. 28: 941–953.

Bannister, A. & Beam, G. (2013). CaV1.1: The atypical prototypical voltage-gated Ca^{2+} channel. Biochim. Biophys. Acta 1828, 1587–1597.

Barnes B., Marklund S., Steiler T., Walter M., Hjälm G., Amarger V., Mahlapuu M., Leng Y., Johansson C., Galuska D., Lindgren K., Abrink M., Stapleton D., Zierath JR. and Andersson L. (2004). The 5'-AMP-activated protein kinase gamma3 isoform has a key role in carbohydrate and lipid metabolism in glycolytic skeletal muscle. J Biol Chem. 279(37):38441-7.

Barré L., Richardson C., Hirshman M., Brozinick J., Fiering S., Kemp B., Goodyear L. and Witters L. (2007). Genetic model for the chronic activation of skeletal muscle AMP-activated

protein kinase leads to glycogen accumulation. Am J Physiol Endocrinol Metab. 292(3):E802-11.

Baylor S. and Hollingworth S., (2011). Calcium indicators and calcium signalling in skeletal muscle fibres during excitation–contraction coupling. Progress in Biophysics and Molecular Biology. 105, 3, 162-179.

Berry D., and Noy N., (2009). All-trans-Retinoic Acid Represses Obesity and Insulin Resistance by Activating both Peroxisome Proliferation-Activated Receptor β/δ and Retinoic Acid Receptor. Molecular and cellular biology. 29, 12, 3286-3296.

Bers D., (2002). Cardiac excitation-contraction coupling. Nature 415: 198–205.

Bleunven C., Treves S., Jinyu X., Leo E., Ronjat M., De Waard M, Kern G., Flucher B., Zorzato F. (2008). SRP-27 is a novel component of the supramolecular signalling complex involved in skeletal muscle excitation-contraction coupling. Biochem J. 411(2):343-9.

Biral D., Volpe P., Damiani E. and Margreth A. (1992). Coexistence of two calsequestrin isoforms in rabbit slow-twitch skeletal muscle fibres. FEBS Lett. 299(2):175-8.

Block B., Imagawa T., Campbell K. and Franzini-Armstrong C. (1988). Structural evidence for direct interaction between the molecular components of the transverse tubule/sarcoplasmic reticulum junction in skeletal muscle. J Cell Biol. 107(6), 2:2587-600.

Bottinelli R., and Reggiani C. (2000). Human skeletal muscle fibres: molecular and functional diversity. Prog Biophys Mol Biol. 73(2-4):195-262.

Brian R. MacIntosh, Robert J. Holash, Jean-Marc Renaud. (2012). Skeletal muscle fatigue – regulation of excitation–contraction coupling to avoid metabolic catastrophe. J Cell Sci. 125: 2105-2114.

Bruck N., Vitoux D., Ferry C., Duong V., Bauer A., de The H. and Rochette-Egly C. (2009). A coordinated phosphorylation cascade initiated by p38MAPK/MSK1 directs RARalpha to target promoters. EMBO J. 28: 34–47.

Bunner A., Chandrasekera P. and Barnard N. (2014). Knockout mouse models of insulin signaling: Relevance past and future. World J Diabetes. 5(2): 146–159.

Burkholder T., Fingado B., Baron S. and Lieber R. (1994). Relationship between muscle fibre types and sizes and muscle architectural properties in the mouse hindlimb.J Morphol. 221(2):177-90.

Calderón J., Bolaños P. and Caputo C. (2014). The excitation-contraction coupling mechanism in skeletal muscle. Biophys Rev. 6(1):133-160.

Carretero G., Ribera M., Belinchón I., Carrascosa J., Puig L., Ferrandiz C., Dehesa L. Vidal D., Peral F., Jorquera E., Gonzalez-Quesada A., Muñoz C., Notario F. and Vanaclocha F., Moreno J. (2013). Guidelines for the Use of Acitretin in Psoriasis Acitretina. Actas Dermosifiliogr. 104, 7 :598-616.

Carruthers A., DeZutter J., Ganguly A. and Devaskar S. (2009). Will the original glucose transporter isoform please stand up!. Am J Physiol Endocrinol Metab. 297(4):E836-48.

Chan L. and Wells R. (2009). Cross-Talk between PPARs and the Partners of RXR: A Molecular Perspective. PPAR Res. 2009:925309.

Chasiotis D. (1983). The regulation of glycogen phosphorylase and glycogen breakdown in human skeletal muscle. Acta Physiol Scand Suppl. 1983;518:1-68.

Cheung Y., Lau W., Yu M., Lai C., Yeung S., So K. and Chang R. (2009). Effects of all-trans-retinoic acid on human SH-SY5Y neuroblastoma as in vitro model in neurotoxicity research. Neurotoxicology. 30: 127–135.

Chivot M1. (2005). Retinoid therapy for acne. A comparative review. Am J Clin Dermatol. 6(1):13-9.

Cooper GM. The Cell: A Molecular Approach. 2nd edition. Sunderland (MA): Sinauer Associates; 2000. Actin, Myosin, and Cell Movement.

D'Adamo MC, Sforna L, Visentin S, Grottesi A, Servettini l, Guglielmi L, et al. (2016) A Calsequestrin-1 Mutation Associated with a Skeletal Muscle Disease Alters Sarcoplasmic Ca2+ Release. PLoS ONE 11(5): e0155516.

David M., Hodak E. and Lowe N. (1988). Adverse effects of retinoids. Med Toxicol Adverse Drug Exp. 3(4):273-88.

Desaia T, Chena F., Lüa J., Qiana J., Niederreitherc K., Dolléb P., Chambonb P., Cardoso W., (2006). Distinct roles for retinoic acid receptors alpha and beta in early lung morphogenesis. Developmental Biology. 291,1 12–24.

Dollé P, Ruberte E, Kastner P, Petkovich M, Stoner CM, Gudas LJ, Chambon P. (1989). Differential expression of genes encoding alpha, beta and gamma retinoic acid receptors and CRABP in the developing limbs of the mouse. Nature. 342(6250):702-5.

Donato L. and Noy N. (2005). Suppression of mammary carcinoma growth by retinoic acid: proapoptotic genes are targets for retinoic acid receptor and cellular retinoic acid-binding protein II signaling. Cancer Res., 65 (2005), pp. 8193-8199

Dos Santos J., Benite-Ribeiro S., Queiroz G and Duarte J. (2012). The effect of age on glucose uptake and GLUT1 and GLUT4 expression in rat skeletal muscle. Cell Biochem Funct.191-7.

Dowling R., Topisirovic I., Alain T., Bidinosti M., Fonseca B., Petroulakis E. et al. (2010). mTORC1-mediated cell proliferation, but not cell growth, controlled by the 4E-BPs. Science 328: 1172–1176.

Drum S., Weatherwax R., Dixon J. (2016) Physiology of Skeletal Muscle. In: Dixon J. (eds) Muscular Injuries in the Posterior Leg. Springer, Boston, MA.

E X., Zhang L., Lu J., Tso P., Blaner W., Levin M.,and Li E. (2002) Increased neonatal mortality in mice lacking cellular retinol-binding protein II. J Biol Chem 277: 36617–36623.

Filippi B., Abraham M., Yue J. and Lam T. (2013). Insulin and glucagon signaling in the central nervous system. Rev Endocr Metab Disord. 14:365–375.

Franzini-Armstrong C. and Nunzi G. (1983). Junctional feet and particles in the triads of a fast-twitch muscle fibre. J Muscle Res Cell Motil. 4(2):233-52.

Franzini-Armstrong C, Protasi F, Ramesh V. (1998). Comparative ultrastructure of Ca2+ release units in skeletal and cardiac muscle.Ann N Y Acad Sci. 16; 853():20-30.

Franzini-Armstrong C. (1999). The sarcoplasmic reticulum and the control of muscle contraction. FASEB J. 13 (2):266-70.

Frontera, W. and Ochala, J. (2015). Skeletal Muscle: A Brief Review of Structure and Function Calcif Tissue Int. 96: 183.

Füchtbauer E., Rowlerson A., Götz K., Friedrich G., Mabuchi K., Gergely J., Jockusch H. (1991). Direct correlation of parvalbumin levels with myosin isoforms and succinate dehydrogenase activity on frozen sections of rodent muscle. J Histochem Cytochem. 39(3):355-61.

Giannini G, Conti A, Mammarella S, Scrobogna M, Sorrentino V. (1995). The ryanodine receptor/calcium channel genes are widely and differentially expressed in murine brain and peripheral tissues. J Cell Biol. 128(5):893-904.

Halevy O. and Lerman O. (1993). Retinoic acid induces adult muscle cell differentiation mediated by the retinoic acid receptor-alpha. J Cell Physiol. 154(3):566-72.

Halse R., Bonavaud S., Armstrong J., McCormack J and Yeaman S. (2001). Control of glycogen synthesis by glucose, glycogen, and insulin in cultured human muscle cells. Diabetes. 50(4):720-6.

Harris A, Duxson M., Butler J., Hodges P., Taylor J. and Gandevia S. (2005). Muscle Fibre and Motor Unit Behavior in the Longest Human Skeletal Muscle. JNeurosci. 25 (37) 8528-8533.

Hegarty P. and Hooper A. (1971). Sarcomere length and fibre diameter distributions in four different mouse skeletal muscles. J Anat. 110(Pt 2): 249–257.

Herzig S. and Shaw R. (2017). AMPK: guardian of metabolism and mitochondrial homeostasis. Nat Rev Mol Cell Biol.

Heilig C., Saunders T., Brosius F., Moley K., Heilig K., Baggs R., Guo L. and Conner D.. (2003). Glucose transporter-1-deficient mice exhibit impaired development and deformities that are similar to diabetic embryopathy. Proc Natl Acad Sci U S A. 100(26):15613-8.

Helgerson A. and Carruthers A. (1987). Equilibrium ligand binding to the human erythrocyte sugar transporter. Evidence for two sugar-binding sites per carrier. J Biol Chem. 262(12):5464-75.

Holloszy J. and Kohrt W. (1996). Regulation of carbohydrate and fat metabolism during and after exercise. Annu Rev Nutr. 16():121-38.

Hopkins P., (2006). Skeletal muscle physiology. Continuing Education in Anaesthesia Critical Care & Pain. 6 (1): 1–6.

Horowicz P. (1961). Influence of ions on the membrane potential of muscle fibres. In: Shanes A, editor. Biophysics of physiological and pharmacological actions. American Association for the Advancement of Science: Washington. pp. 217–234.

Huang P., Chandra V. and Rastinejad F. (2014). Retinoic Acid Actions Through Mammalian Nuclear Receptors. Chem Rev. 114(1): 233–254.

Huang S. and Czech M. (2007). The GLUT4 Glucose Transporter. Cell Metabolism. 5, 4, 237-252.

Jacobs S, Lie D., DeCicco K., Shi Y., DeLuca L., Gage F, Evans R. (2006). Retinoic acid is required early during adult neurogenesis in the dentate gyrus. Proc. Natl. Acad. Sci. USA, 103, 3902-3907

Inoki K., Zhu T., Guan K.. (2003). TSC2 mediates cellular energy response to control cell growth and survival. Cell. 115: 577–590.

Jensen T. And Richter E. (2012). Regulation of glucose and glycogen metabolism during and after exercise. Jphysiol, 590, 5, 1069–1076.

Joost H., Bell G., Best J., Birnbaum M., Charron M., Chen Y., Doege H., James D., Lodish H., Moley K., Moley J., Mueckler M., Rogers S., Schürmann A., Seino S. and Thorens B. (2002). Nomenclature of the GLUT/SLC2A family of sugar/polyol transport facilitators. Am J Physiol Endocrinol Metab. 282(4):E974-6.

Kastner P., Mark M., Leid M., Gansmuller A., Chin W., Grondona J., Décimo D., Krezel W., Dierich A. and Chambon P. (1996). Abnormal spermatogenesis in RXR beta mutant mice. Genes Dev. Jan 1;10(1):80-92.

Kennedy K., Porter T., Mehta V., Ryan S., Price F, Peshdary V., Karamboulas C., Savage J., Drysdale T., Li S., Bennett S. and Skerjanc I. (2009). Retinoic acid enhances skeletal muscle progenitor formation and bypasses inhibition by bone morphogenetic protein 4 but not dominant negative beta-catenin. BMC Biol. 8;7:67.

Kim M., Hunter RW., Garcia-Menendez L., Gong G., Yang Y., Kolwicz S., Xu J., Sakamoto K., Wang W. and Tian R. (2014). Mutation in the γ2-subunit of AMPK Stimulates Cardiomyocyte Proliferation and Hypertrophy Independent of Glycogen Storage. Circ Res. 114(6): 966–975.

Kim L., Cook R. and Chen J. (2017). mTORC1 and mTORC2 in cancer and the tumor microenvironment. Oncogene. 2017 Apr 20;36(16):2191-2201.

Kraegen, E., Sowden J., Halstead M., Clark P., Rodnick K., Chisolm D. And James D. (1993). Glucose transporters and in vivo glucose uptake in skeletal and cardiac muscle: fasting, insulin stimulation and immunoisolation studies of GLUT1 and GLUT4. Biochem. J. 295, 287-293.

Krezel W., Dupé V, Mark M, Dierich A, Kastner P, Chambon P,. (1996). RXR gamma null mice are apparently normal and compound RXR alpha +/-/RXR beta -/-/RXR gamma -/- mutant mice are viable. Proc Natl Acad Sci U S A. 1996 Aug 20; 93(17):9010-4.

Krezel W., Kastner P., Chambon P., (1999). Differential expression of retinoid receptors in the adult mouse central nervous system. Neuroscience. 1999;89(4):1291-300.

Lai FA, Erickson HP, Rousseau E, Liu QY, Meissner G (1988). Purification and reconstitution of the calcium release channel from skeletal muscle. Nature. 331(6154):315-9.

Lanner J., Georgiou D., Joshi A., and Hamilton S. (2010). Ryanodine Receptors: Structure, Expression, Molecular Details, and Function in Calcium Release. Cold Spring Harb Perspect Biol. 2(11): a003996.

Larange A., and Cheroutre H., (2016). Retinoic Acid and Retinoic Acid Receptors as Pleiotropic Modulators of the Immune System. Annual Review of Immunology. 34:369-394.

Leney S. and Tavare J. (2009). The molecular basis of insulin-stimulated glucose uptake: signalling, trafficking and potential drug targets. J Endocrinol.203(1):1-18.

Le Maire A., Alvarez S., Shankaranarayanan P., Lera A., Bourguet W. and Gronemeyer H. (2012). Retinoid receptors and therapeutic applications of RAR/RXR modulators. Curr Top Med Chem. 2012;12(6):505-27.

Leto D., and Saltiel R., (2012). Regulation of glucose transport by insulin: traffic control of GLUT4. Nature Reviews Molecular Cell Biology 13, 383-396.

Li M., Indra A., Warot X, et al., (2000). “Skin abnormalities generated by temporally controlled RXRα mutations inmouse epidermis,” Nature, vol. 407, no. 6804, pp. 633–636.

Lohnes D1, Kastner P, Dierich A, Mark M, LeMeur M, Chambon P. Function of retinoic acid receptor gamma in the mouse. (1993). Cell. 21;73(4):643-58.

Lösel R. and Wehling M. (2003). Nongenomic actions of steroid hormones. Nat. Rev. Mol. Cell Biol. 4: 46–56. The cDNA sequence encodes a protein of 367 residues plus a 28 residue amino-terminal signal sequence

MacLennan DH, Wong P. (1971). Isolation of a calcium-sequestering protein from sarcoplasmic reticulum. Proc Natl Acad Sci USA. 68(6):1231-5

Maclennan D. (2004). Interactions of the calcium ATPase with phospholamban and sarcolipin: structure, physiology and pathophysiology. J Muscle Res Cell Motil. 25(8):600-1.

Manno C,. Figueroa L., Gillespie D., Fitts R., Kang C., Franzini-Armstrong C. and Rios E. (2017). Calsequestrin depolymerizes when calcium is depleted in the sarcoplasmic reticulum of working muscle. Proc Natl Acad Sci USA. 114(4): 638–647.

Marini M. and Veicsteinas A. (2010). The exercised skeletal muscle: a review. Eur J Transl Myol. 20 (3): 105-120.

Mark M, Ghyselinck NB, Chambon P. (2009). Function of retinoic acid receptors during embryonic development. Nucl Recept Signal 7():e002.

Marty I,. Fauré J., Fourest-Lieuvin A., Vassilopoulos S., Oddoux S. and Brocard J. (2009). Triadin: what possible function 20 years later? J Physiol. 587(Pt 13):3117-21.

Marty I. (2015). Triadin regulation of the ryanodine receptor complex. J Physiol. 593(15): 3261–3266.

Mascrez B, Mark M, Krezel W, Dupé V, LeMeur M, Ghyselinck NB, Chambon P. (2001). Differential contributions of AF-1 and AF-2 activities to the developmental functions of RXR alpha. Development. 128(11):2049-62.

Meissner G, Darling E, Eveleth J. (1986). Kinetics of rapid Ca^{2+} release by sarcoplasmic reticulum. Effects of Ca^{2+}, Mg^{2+}, and adenine nucleotides. Biochemistry. 1986 Jan 14; 25(1):236-44.

Mosca B., Delbono O., Laura Messi M., Bergamelli L., Wang Z., Vukcevic M., Lopez R., Treves S., Nishi M., Takeshima H., Paolini C., Martini M., Rispoli G., Protasi F. and Zorzato F. (2013). Enhanced dihydropyridine receptor calcium channel activity restores muscle strength in JP45/CASQ1 double knockout mice. Nat Commun. 4:1541.

Nedumpully-Govindan P. and Ding F. (2015). Inhibition of IAPP aggregation by insulin depends on the insulin oligomeric state regulated by zinc ion concentration. Sci Rep. 5:8240.

Obrochta K., Kane M., and Napoli J. (2014). Effects of Diet and Strain on Mouse Serum and Tissue Retinoid Concentrations. PLoS ONE 9(6): e99435.

O'Byrne S., and Blaner W. (2013). Retinol and retinyl esters: biochemistry and physiology Thematic Review Series: Fat-Soluble Vitamins: Vitamin A. J Lipid Res. 2013 Jul; 54(7): 1731–1743.

Odermatt A., Taschner P., Khanna V., Busch H., Karpati G., Jablecki C., Breuning M., MacLennan D.. (1996). Mutations in the gene-encoding SERCA1, the fast-twitch skeletal muscle sarcoplasmic reticulum Ca2+ ATPase, are associated with Brody disease. Nat Genet. 14(2):191-4.

O'Neill H., Maarbjerg S., Crane J., Jeppesen J., Jørgensen S., Schertzer J., Shyroka O., Kiens B., van Denderen B., Tarnopolsky M., Kemp B., Richter E., and Steinberg G. (2011). AMP-

activated protein kinase (AMPK) beta1beta2 muscle null mice reveal an essential role for AMPK in maintaining mitochondrial content and glucose uptake during exercise. Proc Natl Acad Sci U S A. 108(38):16092-7.

O'Neill H., Holloway G., Steinberg G.. (2013). AMPK regulation of fatty acid metabolism and mitochondrial biogenesis: implications for obesity. Mol Cell Endocrinol. 366(2):135-51.

Otsu K., Willard H., Khanna V., Zorzato F., Green N., MacLennan D. (1990). Molecular cloning of cDNA encoding the Ca2+ release channel (ryanodine receptor) of rabbit cardiac muscle sarcoplasmic reticulum. J Biol Chem. 1990 Aug 15; 265(23):13472-83.

Ottini L, Marziali G, Conti A, Charlesworth A, Sorrentino V. (1996). Alpha and beta isoforms of ryanodine receptor from chicken skeletal muscle are the homologues of mammalian RyR1 and RyR3. Biochem J. 315 (Pt 1)():207-16.

Owerbach D., Bell G., Rutter W., Brown J., and Shows T. (1981). The Insulin Gene Is Located on the Short Arm of Chromosome 11 in Humans. Diabetes 1981 Mar; 30(3): 267-270

Pan Y., Zvaritch E., Tupling A., Rice W., de Leon S., Rudnicki M., McKerlie C., Banwell B., MacLennan D. (2003). Targeted disruption of the ATP2A1 gene encoding the sarco(endo)plasmic reticulum Ca2+ ATPase isoform 1 (SERCA1) impairs diaphragm function and is lethal in neonatal mice. J. Biol. Chem. 278, 13367-13375.

Pencek R., Fueger P., Camacho R., Wasserman D., (2005). Mobilization of glucose from the liver during exercise and replenishment afterward. Can J Appl Physiol. 30(3):292-303.

Periasamy M. and Kalyanasundaram A. (2007). SERCA pump isoforms: their role in calcium transport and disease. Muscle Nerve. 35(4):430-42.

Periasamy M., Maurya S., Sahoo S., Singh S., Sahoo S., Reis F., Bal N. (2017). Role of SERCA pump in muscle thermogenesis and metabolism. Compr Physiol.7(3):879-890.

Persaud S., Park S., Ishigami-Yuasa M., Koyano-Nakagawa N., Kagechika H. and Wei L., (2016). All trans-retinoic acid analogs promote cancer cell apoptosis through non-genomic Crabp1 mediating ERK1/2 phosphorylation. Scientific Reports 6, 22396.

Pino-Lagos K., Guo Y. and Noelle R. (2010). Retinoic acid: A key player in immunity. BioFactors Oxf Engl 36: 430–436.

Prasada V., Okunadea G., Millerb M., and Shulla G. (2004). Phenotypes of SERCA and PMCA knockout mice. Biochem. Biophys. Res. Commun. 322 (4),1192-1203.

Priori S. and Napolitano C. (2005). Cardiac and skeletal muscle disorders caused by mutations in the intracellular Ca2+ release channels. J Clin Invest. 115(8): 2033–2038.

Protasi F. (2002). Structural interaction between RYRs and DHPRs in calcium release units of cardiac and skeletal muscle cells. Front Biosci. 7:650-8.

Quadro L, Blaner WS, Salchow DJ, Vogel S, Piantedosi R, et al. (1999) Impaired retinal function and vitamin A availability in mice lacking retinol-binding protein. EMBO J 18: 4633–4644.

Racay P., Gregory P., Schwaller B.. (2006). Parvalbumin deficiency in fast-twitch muscles leads to increased 'slow-twitch type' mitochondria, but does not affect the expression of fibre specific proteins. FEBS J. 273(1):96-108.

Ralston E. and Ploug T. (1996). GLUT4 in cultured skeletal myotubes is segregated from the transferrin receptor and stored in vesicles associated with TGN. Journal of Cell Science 109 2967–2978.

Raymackers J., Gailly P., Colson-Van Schoor M., Pette D., Schwaller B., Hunziker W., Celio M., and Gillis J. (2000). Tetanus relaxation of fast skeletal muscles of the mouse made parvalbumin deficient by gene inactivation. J Physiol. 527(Pt 2): 355–364.

Reyskens K. and Arthur J., (2016). Emerging Roles of the Mitogen and Stress Activated Kinases MSK1 and MSK2. Front Cell Dev Biol. 4:56. 1-8.

Rice A., Holtz K., Karp J., Rollins S. and Sartorelli A., (2004). Analysis of the relationship between Scl transcription factor complex protein expression patterns and the effects of LiCl on ATRA-induced differentiation in blast cells from patients with acute myeloid leukemia. Leukemia research. 28(11):1227–37.

Ríos, E. and Brum, G. (1987) Involvement of dihydropyridine receptors in excitation-contraction coupling. Nature 325, 717–720.

Ríos E. and Pizarro G. (1991). Voltage sensor of excitation-contraction coupling in skeletal muscle. Physiol Rev. 71(3):849-908.

Röckl K., Witczak C. and Goodyear L. (2008). Signaling mechanisms in skeletal muscle: acute responses and chronic adaptations to exercise. IUBMB Life. 60(3):145-53.

Röder P., Wu B., Liu Y. and Han W. (2016). Pancreatic regulation of glucose homeostasis. Exp Mol Med. 48(3): 219.

Sanchez E., Lewis K., Danna B. and Kang C (2012). High-capacity Ca2+ Binding of Human Skeletal Calsequestrin. jpg J Biol Chem. 287(14): 11592–11601.

Sarbassov D., Ali S., Kim D., Guertin D., Latek R., Erdjument-Bromage H. et al. (2004) Rictor, a novel binding partner of mTOR, defines a rapamycin-insensitive and raptor-independent pathway that regulates the cytoskeleton. Curr Biol 14: 1296–1302.

Sekulic-Jablanovic M., Palmowski-Wolfe A., Zorzato F., and Treves S. (2015). Characterization of excitation-contraction coupling components in human extraocular muscles. Biochem. J. 466:29–36.

Schug T., Berry D., Shaw N., Travis S. and Noy N. (2007). Dual transcriptional activities underlie opposing effects of retinoic acid on cell survival. Cell. 129(4): 723–733.

Schwaller B., Dick J., Dhoot G., Carroll S., Vrbova G., Nicotera P., Pette D., Wyss A., Bluethmann H., Hunziker W., and Celio M., (1999). Prolonged contraction-relaxation cycle of fast-twitch muscles in parvalbumin knockout mice. Am J Physiol. 1999 Feb;276(2 Pt 1):C395-403.

Scribner K., Odom D., McGrane M., (2007). Nuclear receptor binding to the retinoic acid response elements of the phosphoenolpyruvate carboxykinase gene in vivo: effects of vitamin A deficiency. J Nutr Biochem. 2007 Mar; 18(3):206-14.

Stenbit, A., Tsao S., Li J., Burcelin R., Geenen, D. L., Factor S., Houseknecht K., Katz, E., and Charron, M. (1997). GLUT4 heterozygous knockout mice develop muscle insulin resistance and diabetes.Nat. Med. 3, 1096–1101.

Su M., Alonso S., Jones J., Yu J., Kane M., Jones R., and Ghiaur G. (2015). All-Trans Retinoic Acid Activity in Acute Myeloid Leukemia: Role of Cytochrome P450 Enzyme Expression by the Microenvironment. PLoS One. 10(6): e0127790.

Takeshima H., Komazaki S., Nishi M., Iino M. and Kangawa K. (2000). Junctophilins: a novel family of junctional membrane complex proteins. Mol Cell 6, 11–22.

Tanoury Z., Piskunov A. and Rochette-Egly C. (2013). Vitamin A and retinoid signaling: genomic and nongenomic effects. Thematic Review Series: Fat-Soluble Vitamins: Vitamin A. J. Lipid Res 54, 7 1761-1775.

Taylor C., Tovey S., Rossi A., Lopez Sanjurjo C., Prole D. and Rahman T. (2014). Structural organization of signalling to and from IP3 receptors. Biochem Soc Trans. 42(1):63-70.

Theodosiou M, Laudet V, Schubert M. (2010). From carrot to clinic: an overview of the retinoic acid signaling pathway. Cell Mol Life Sci. 67(9):1423-45.

Thorens B. and Mueckler M. (2010). Glucose transporters in the 21st Century. Am J Physiol Endocrinol Metab. 298(2): E141–E145.

Treves S., Chiozzi P., and Zorzato F. (1993). Identification of the domain recognized by anti-(ryanodine receptor) antibodies which affect Ca(2+)-induced Ca2+ release. Biochem J. 291(Pt 3): 757–763.

Treves F., Vukcevic M., Maj M., Thurnheer R., Mosca B., and Zorzato F. (2009). Minor sarcoplasmic reticulum membrane components that modulate excitation–contraction coupling in striated muscles

Treves S., Jungbluth H., Voermans N., Muntoni F. and Zorzato F.. (2017). Ca2+ handling abnormalities in early-onset muscle diseases: Novel concepts and perspectives. Semin Cell Dev Biol. 64:201-212.

Vassilopoulos S., Thevenon D,, Rezgui S., Brocard J., Chapel A., Lacampagne A., Lunardi J., Dewaard M. and Marty I. (2005). Triadins are not triad-specific proteins: two new skeletal muscle triadins possibly involved in the architecture of sarcoplasmic reticulum. J Biol Chem. 280(31):28601-9.

Verma A., Conrad E., and Boutwell R. (1982). Differential effects of retinoic acid and 7,8-benzoflavone on the induction of mouse skin tumors by the complete carcinogenesis process and by the initiation-promotion regimen. Cancer Res. 42, 3519-3525

Viollet B., Andreelli F., Jørgensen S., Perrin C., Flamez D., Mu J., Wojtaszewski J., Schuit F., Birnbaum M., Richter E., Burcelin R. and Vaulont S. (2003a). Physiological role of AMP-activated protein kinase (AMPK): insights from knockout mouse models. Biochem Soc Trans. 31(1):216-9.

Viollet B., Andreelli F., Jørgensen S., Perrin C., Geloen A., Flamez D., Mu J., Lenzner C., Baud O., Bennoun M., Gomas E., Nicolas G., Wojtaszewski J., Kahn A., Carling D., Schuit F., Birnbaum M., Richter E., Burcelin R. and Vaulont S. (2003b). The AMP-activated protein kinase alpha2 catalytic subunit controls whole-body insulin sensitivity. J Clin Invest. 111(1):91-8.

Wang J., Ye C., Chen C., Xiong H., Xie B., Zhou J., Chen Y., Zheng S. and Wang L. (2017). Glucose transporter GLUT1 expression and clinical outcome in solid tumors: a systematic review and meta-analysis. Oncotarget. 8(10): 16875–16886.

Wei R., et al., Structural insights into Ca^{2+}-activated long-range allosteric channel gating of RyR1. Cell Research 26, 977–994

Willows R., Navaratnam N., Lima A., Read J. and Carling D. (2017). Effect of different γ-subunit isoforms on the regulation of AMPK. Biochem J. 474(10):1741-1754.

Wu J., Yan Z., Li Z., Yan C., Lu S., Dong M. and Yan N. (2015). Structure of the voltage-gated calcium channel Cav1.1 complex. Science. 350(6267):aad2395.

Wu Y.,, Zhang X., Bardag-Gorce, F. et al., (2004). "Retinoid X receptor α regulates glutathione homeostasis and xenobiotic detoxification processes in mouse liver, Mol Pharm, 65 (3) 550–557.

Wuytack F., Raeymaekers L., Missiaen L., (2002). Molecular physiology of the SERCA and SPCA pumps. Cell Calcium. 32, 5, 279-305.

Xiao B., Sanders M., Underwood E., Heath R., Mayer F., Carmena D., Jing C., Walker P., Eccleston J., Haire L., Saiu P., Howell S., Aasland R., Martin S., Carling D. and Gamblin S. (2011). Structure of mammalian AMPK and its regulation by ADP. Nature. 472(7342):230-3.

Yang G., Murashige D., Humphrey S., James D., (2015). A Positive Feedback Loop between AKT and mTORC2 via SIN1 Phosphorylation. Cell Rep. 12(6):937-43.

Yavari A., et at., (2017). Mammalian γ2 AMPK regulates intrinsic heart rate. Nat Commun. 8(1):1258.

Zarain-Herzberg A1, Fliegel L, MacLennan DH. (1988). Structure of the rabbit fast-twitch skeletal muscle calsequestrin gene. J Biol Chem. 263(10):4807-12.

Zarogoulidis P., Lampaki S., Turner J., Huang H., Kakolyris S., Syrigos K., Zarogoulidis K.. (2014). mTOR pathway: A current, up-to-date mini-review (Review). Oncol Lett. 8(6):2367-2370.

Zhang K., Quan C., Huang H., Taulier N., and Wu X. (2004). On the stability of insulin delivered through a new glucose-responsive polymeric composite membrane. J Pharm Pharmacol. 56(5):611-20.

Zhang L., Kelley J., Schmeisser G., Kobayashi Y., and Jones L. (1997). Complex formation between junctin, triadin, calsequestrin, and the ryanodine receptor. Proteins of the cardiac junctional sarcoplasmic reticulum membrane. J Biol Chem. 12;272(37):23389-97.

Zhang M., Hu P., Krois C., Kane M. and Napoli J. (2007) Altered vitamin A homeostasis and increased size and adiposity in the rdh1-null mouse. FASEB J Off Publ Fed Am Soc Exp Biol 21: 2886–2896.

Zhang R., Wang Y., Li R., and Chen G., (2015). Transcriptional Factors Mediating Retinoic Acid Signals in the Control of Energy Metabolism. Int J Mol Sci. 16(6): 14210–14244.

Zinzalla V., Stracka D., Oppliger W. and Hall M. (2011). Activation of mTORC2 by association with the ribosome. Cell 2011; 144: 757–768.

Zisman A., Peroni O., Abel E., Michael M., Mauvais-Jarvis F., Lowell B., Wojtaszewski J., Hirshman M., Virkamaki A., Goodyear L. (2000). Targeted disruption of the glucose transporter 4 selectively in muscle causes insulin resistance and glucose intolerance. Nat. Med., 6, 924-928.

Zorzato F, Fujii J, Otsu K, Phillips M, Green NM, Lai FA, Meissner G, MacLennan DH (1990). Molecular cloning of cDNA encoding human and rabbit forms of the Ca2+ release channel (ryanodine receptor) of skeletal muscle sarcoplasmic reticulum. J Biol Chem. 265(4):2244-56.

Zorzato F., Anderson A. A., Ohlendieck K., Froemming G., Guerrini R., and Treves S. (2000) Identification of a novel 45-kDa protein (JP-45) from rabbit sarcoplasmic-reticulum junctional-face membrane. Biochem. J. 351, 537–543.

Curriculum vitae
(February 13th 2018)

Personal data

Name (First, middle, family):	Alexis Jesus Ruiz Velez
Place and date of birth:	La Guaira, Venezuela/ 03-05-1988
Nationality:	Venezuelan
Telephone(s): 061-2652372	Mobile: 076-6208805
E-mail:	alexis.ruiz@unibas.ch or alejrv41@hotmail.com
Address:	Hegenheimerstrasse 151, Basel, 4055

Education:

2013-2018	PhD student/Cell Biology/: Perioperative Patient Safety Group, Department of Biomedicine, University Hospital Basel University of Basel
2006- 2013	Licentiate in Biology (five years course of studies with a research thesis)/University Simón Bolivar (USB), Venezuela.
1999-2005	High School final certificate/ Liceo Armando Reveron, Catia la mar, Venezuela.

Research training:

Training student at Venezuelan Institute for Scientific Research (IVIC), in the laboratory of Muscle Physiology under the supervision of Drs. Carlo Caputo and Pura Bolaños, 2012.

Thesis student at Venezuelan Institute for Scientific Research (IVIC), in the laboratory of Muscle Physiology under the supervision of Drs. Carlo Caputo and Pura Bolaños, 2012.

Training Professional at Venezuelan Institute for Scientific Research (IVIC), in the laboratory of Muscle Physiology under the supervision of Drs. Carlo Caputo and Pura Bolaños, 2013.

Courses.

Polish your English. English for academic purposes: speaking, listening, reading, and writing. Sprachenzentrum der Universität Basel. Basel, October –December 2013.

LTK Module 1: Introductory Course in Laboratory Animal Science. Couse for Persons Conducting Animal Experiments (Minimum 40 hours, Mice/Rats) and accredited as FELASA category B Course 027/08 by T&T FELASA board. Basel, April 2014.

Languages

Spanish (mother tongue), English.

Publications.

Over-expression of a retinol dehydrogenase (SRP35/DHRS7C) in skeletal muscle activates mTORC2, enhances glucose metabolism and muscle performance. (2018). Ruiz A., Dror E., Handschin C., Furrer R., Perez-Schindler J., Bachmann C., Treves S. and Zorzato F. Sci Rep. 8: 636.

Persons that can be contacted for further information:

Prof. Dr. Susan Treves	susan.treves@unibas.ch (Professor and Researcher).
Prof. Dr. Francesco Zorzato	fzorzato@uhbs.ch (Professor and Researcher).
Prof. Dr. Carlo Caputo	ccaputofra@gmail.com (Professor and Researcher).